İ.AKDAĞ

IZMIR KATIP CELEBI UNIVERSITY

2021

IZMIR KATIP CELEBI UNIVERSITY

GRADUATE SCHOOL OF NATURAL AND APPLIED SCIENCES

INTEGRATION AND TESTING OF THE RFID-ENABLED SMART FACTORY

M.Sc. THESIS

İsmail AKDAĞ

Department of Electrical and Electronics Engineering

Thesis Advisor: Prof. Dr. Adnan KAYA

JANUARY 2021

IZMIR KATIP CELEBI UNIVERSITY
GRADUATE SCHOOL OF NATURAL AND APPLIED SCIENCES

INTEGRATION AND TESTING OF THE RFID-ENABLED SMART FACTORY

M.Sc. THESIS

İsmail AKDAĞ
(Y180207001)

ORCID NO: 0000-0001-6470-5892

Department of Electrical and Electronics Engineering

Thesis Advisor: Prof. Dr. Adnan KAYA

JANUARY 2021

İZMİR KATİP ÇELEBİ ÜNİVERSİTESİ
FEN BİLİMLERİ ENSTİTÜSÜ

RFID-ETKİN AKILLI FABRİKANIN ENTEGRASYONU VE TEST EDİLMESİ

YÜKSEK LİSANS TEZİ

İsmail AKDAĞ
(Y180207001)

ORCID NO: 0000-0001-6470-5892

Elektrik-Elektronik Mühendisliği Ana Bilim Dalı

Tez Danışmanı: Prof. Dr. Adnan KAYA

OCAK 2021

İsmail Akdağ, a **M.Sc.** student of **IKCU Graduate School Of Natural And Applied Sciences**, successfully defended the thesis entitled "**Integration and Testing of the RFID-enabled Smart Factory**", which he prepared after fulfilling the requirements specified in the associated legislations, before the jury whose signatures are below.

Thesis Advisor :

Prof. Dr. Adnan KAYA .....
İzmir Kâtip Çelebi University

Jury Members :

Prof. Dr. Adnan KAYA .....
İzmir Kâtip Çelebi University

Assoc. Prof. Dr. Merih PALANDÖKEN .....
İzmir Kâtip Çelebi University

Asst. Prof. Dr. Yavuz ÖZTÜRK .....
Ege University

Date of Defense : 11.01.2021

To my family

FOREWORD

First and foremost, I would like to thank my advisor, Prof. Dr. Adnan KAYA for his guidance and support throughout the study. It is an honor for me to work with him and benefit from his vast knowledge. Whenever I needed something throughout the study, his door was open for me. In addition, I would not have been able to complete this work properly without Assoc. Prof. Merih Palandöken's guidance, both academically and personally, throughout the study. My dear professor has always sincerely provided me with his precious knowledge and experience. He always encouraged me and showed his support. Therefore, I would like to express my special gratitude to him. I would like to thank my friend, Research Assistant Cem Göçen, with whom we shared the same work environment, who helped me in my studies. His support was valuable to me. I would also like to thank "Kur Mermer Granit A.Ş.", "İBİA Teknoloji Makina Ar-Ge Danışmanlık Sanayi ve Ticaret LTD. ŞTİ.", companies for their contributions in the project process and spesifically İhsan Kaya for his assistance and support. I sincerely thank my family, which is the most precious thing in life, for always supporting me, encouraging me, and always being by my side. I would never have been able to accomplish this work without my family.

January 2021

İsmail AKDAĞ

TABLE OF CONTENTS

Page

LIST OF TABLES

Page

LIST OF FIGURES

Page

ABBREVIATIONS

RFID : Radio Frequency Identification

UHF : Ultra High Frequency

EIRP : Effective Isotropic Radiated Power

Wi-Fi : Wireless Fidelity

RF : Radio Frequency

dB : Decibel

dBi : Decibel Isotropic

dBiC : Decibel Isotropic Circular

LF : Low Frequency

HF : High Frequency

Hz : Hertz

FCC : Federal Communications Commission

CST : Computer Simulation Technology

HFSS : High-frequency Structure Simulator

LAN : Local Area Network

EM : Electromagnetic

DC : Direct Current

PCB : Printed Circuit Board

RSSI : Received Signal Strength Indicator

INTEGRATION AND TESTING OF THE RFID-ENABLED SMART FACTORY

ABSTRACT

With the development of technology, factory needs in supply chain management from production to customers have started to change. Factories have started to frequently benefit from communication systems in product tracking, warehouse stock control and supply chain management. Radio Frequency Identification (RFID) system is one of the main components of IoT technologies, where data transfer occurs wirelessly and flexibly, instead of traditional tracking and monitoring methods. RFID systems, which are automatic identification systems such as barcode systems used for the last 30 years, offer many advantages as the identification is performed wirelessly through a silicon chip, without mechanical contact, compared to traditional methods. In this thesis, an RFID system operating in the UHF band was designed for a marble factory, transforming this factory into a smart factory environment, and integration and testing studies of the smart factory with an RFID system were carried out.

During the study, RFID system component requirements to be installed in a smart factory environment were determined, and literature and commercial resources were examined accordingly. After selecting the RFID reader, RFID tag and auxiliary components, a new RFID antenna design with 6.7 dBi gain and circular polarization are proposed for smart factory applications in the CST Studio Suite program in line with the examined antennas. Necessary reading distance tests of the proposed antenna design have been made. Simultaneously, for the scenarios in which the system will be used, the RFID tag design was redrawned with AutoCAD, transferred to CST Studio Suite, and Ansys HFSS environments and simulation studies were carried out with the necessary chip modelling. In addition to all these, a graphical user interface has been created with C# programming language in order for the system to be easily used by the end-user in the smart factory environment. Finally, integration and testing of all system components were carried out both in a laboratory environment and in a sample marble factory scenarios.

Keywords: Radio Frequency, Radio Frequency Identification, Smart Factory

RFID-ETKİN AKILLI FABRİKANIN ENTEGRASYONU VE TEST EDİLMESİ

ÖZET

Teknolojinin gelişmesiyle birlikte fabrikaların üretimden müşteriye kadar olan tedarik zinciri yönetimindeki ihtiyaçları da değişmeye başlamıştır. Fabrikalar ürün takibi, depo stok kontrolü ve tedarik zinciri yönetimi gibi konularda haberleşme sistemlerinden sıklıkla yararlanmaya başlamıştır. Geleneksel takip ve izleme metotları yerine, veri aktarımının kablosuz ve esnek bir şekilde gerçekleştiği, IoT teknolojilerinin ana bileşenlerinden birisi olan Radyo Frekansıyla Tanımlama (RFID) sistemleri de bu haberleşme teknolojilerinden birisidir. Hali hazırda son 30 yıldır kullanılan barkod sistemleri gibi otomatik tanımlama sistemlerinden biri olan RFID sistemleri, geleneksel metotlara karşın tanımlamanın mekanik bir kontakt olmadan, kablosuz bir şekilde bir silikon çip vasıtasıyla gerçekleşmesi sebebiyle birçok avantaj sunmaktadır. Bu tezde bir mermer fabrikası için, UHF bandında çalışan bir RFID sistemini tasarlanarak, bu fabrikanın bir akıllı fabrika ortamına dönüştürülmesi ve RFID sistemi ile akıllı fabrikanın entegrasyon ve test çalışmaları yapılmıştır.

Çalışma yapılırken, bir akıllı fabrika ortamına kurulacak olan RFID sistem bileşen gereksinimleri belirlenmiş ve bu doğrultuda literatür ve ticari kaynaklar incelenmiştir. RFID okuyucu, RFID etiket ve yan bileşenlerin seçimi yapıldıktan sonra, incelenen antenler doğrultusunda CST Studio Suite programında, akıllı fabrika uygulamalarına yönelik, UHF bandında çalışan, 6.7 dBi kazançlı ve dairesel polarizasyonlu yeni bir RFID anten tasarımı önerilmiştir. Önerilen anten tasarımının gerekli okuma mesafesi testleri yapılmıştır. Aynı zamanda sistemin kullanılacağı senaryolar konusunda, kullanılacak olan RFID etiketin tasarımı AutoCAD ile yeniden yapılıp, CST Studio Suite ve Ansys HFSS ortamlarına aktarılarak, gerekli çip modellemesi ile benzetim çalışmaları yapılmıştır. Bütün bunların yanında, sistemin akıllı fabrika ortamında son kullanıcı tarafından kolay şekilde kullanılabilmesi için, bir son kullanıcı ara yüzü C# programlama dilinde oluşturulmuştur. Son olarak tüm sistem bileşenlerinin entegrasyonu ve testleri hem laboratuvar ortamında hem de fabrika senaryosunda gerçekleştirilmiştir.

Anahtar kelimeler: Radyo Frekansı, Radyo Frekansıyla Tanımlama, Akıllı Fabrika

1. INTRODUCTION

With today’s technological developments, the needs of factories have started to change. Manufacturers are continually working on information and communication technologies that can increase value. These efforts to increase value have been named Industry 4.0 in Germany and pioneered the start of the 4th Industrial Revolution, which the whole world will adopt. Industry 4.0 aims to create an extensive communication network between production elements and create flexible and dynamic self-organized production processes for customizable products to provide advantages related to production. Smart factories depart from the definition of a place surrounded by four walls; Taking an active role in post-production issues such as post-production stock control, customer requests, problems, feedback, product usage life cycle, product improvement; It is a factory with a technological structure that can predict malfunctions that may occur in the production process, and make the process more efficient in the light of the data collected and analyzed. In terms of form, the proposals for Industry 4.0 and the IoT are very similar. The concept of IoT can be defined as the smart connection of smart devices through objects that can perceive and communicate with each other, with the definition presented by Bryce Barnes. The places working on manufacturing and distributing factories have already started applying this in matters such as worker, factory, and stock control. The smart factory is defined as a machine and equipment-based business environment where all processes are automated, and the process is possible to recover on their own. In other words, to integrate the real world and the virtual world, the smart factory is such an incredibly intelligent organism that can share data. Compared to today's factories, the smart factory, which requires the incorporation of commodity, information and communication systems into manufacturing and delivery processes, greatly improves the utilization of energy, decreases the packaging and delivery cycle of individual goods and guarantees that production takes place at the same time as consumer needs.

Furthermore, while the smart factory systems provide the mentioned benefits, they use the IoT structure together with information and communication technologies. One of these technologies is Radio Frequency Identification, RFID systems. Recent advances in IoT technology related to RFID systems have enabled real-time tracking, accessibility and interoperability of production management systems in the planning, implementation and management of smart factory facilities [1,2]. In light of these developments, RFID systems and smart factory environments are very open to complement each other. The visibility and traceability of the devices, personnel, and stock control in the factory can be increased with RFID systems.

1.1 Motivation

Inspection within a production factory is a critical issue. This control includes many elements within the factory as a concept. These elements include many things, such as factory-made products, factory-processed products, factory-working staff, factory-found devices. With the developing technology, it has become obligatory for the factories to meet some conditions. It is imperative to ensure the proper supply chain management and manage customer relations in the best way for the factory to exist in a competitive environment. In-plant visibility and traceability need to be increased to meet these obligations. RFID technology is a very important tool to ensure this situation. Today, automatic identification systems are used in many sectors, such as production, health, logistics, sales, and retail. Manufacturers and sellers need automatic identification technologies to follow up on their products and make a detailed sales analysis. Barcode technology has been used as an automatic identification technology in many sectors for many years. However, barcode technology is very insufficient for a factory that produces and will be made smart. The most suitable solution here would be to use RFID systems to enable data transfer and identification wirelessly, as mentioned above. In light of all these, this study's motivation is the use of RFID systems to increase the efficiency and value of a factory environment and make it smart.

1.2 Related Work and Literature Review

There are different studies about RFID systems and smart factories in the literature. While some studies dealt with RFID systems in subjects such as inventory and stock tracking, supply chain management, some studies dealt with the smart factory applications. This study covers both the antenna design, simulation, antenna production process, hardware, and software integration for making smart a factory. For this reason it can be think that this study is related to antenna design, supply chain management, smart factory, and RFID applications. After an initial overview of related work, we examine spesific prior work on RFID systems and smart factories. Biswal et al., explored the effects of RFID adoption in a non-profit supply chain scenario in order to research the effect of the available order-and-shrink recovery rate on the total costs at the warehouse level [3]. Lu et al. used RFID system for automating guided vehicle for smart factories [4] and Huang et al. used passive RFID system for lozalizating products on smart rack [5]. Also, there are various antenna design works for UHF RFID reader in literature, Li et al. designed an RFID antenna with circular polarization for UHF RFID reader applications [6]. Rong Cao and Shun-Chuan Yu designed circularly polarized UHF RFID reader antenna with two L-shaped strip lines and CPW-fed by an L-shaped feeding line [7]. Jui-Han Lu and Sang-Fei Wang designed planar broadband UHF RFID reader antenna with arc-shaped strip line and CPW-fed by an F-shaped feeding line [8]. Zhongbao Wang et al., designed circularly polarized stacked UHF reader antenna with arc-shaped strip line and CPW-fed by using a horizontally meandered strip feed technique [9]. Chow Yen Desmond Sim et al., designed slits loaded circularly polarized antenna for universal UHF RFID reader applications [10]. Also, Chow Yen Desmond et al., designed slits loaded circularly polarized antenna with parasitic element [11]. Zhi Ning Chen et al., designed circularly polarized 8.3 dBi antenna [12], Nasimuddin et al., designed wideband circularly polarized stacked slotted microstrip patch antenna with 7 dB gain [13]. Hang Leong Chung et al., designed circularly polarized stacked probe-fed patch UHF reader antenna [14]. Chow Yen Desmond Simd et al., designed slot loaded circularly polarized patch antenna for UHF RFID reader [15], Nasimuddin et al., designed asymmetric-circular shaped slotted microstip antenna for circular polarization and RFID applications [16] , Jiade Yuan et al., designed a compact low-profile ring antenna

for use in RFID readers [17]. Shu-An Yeh et al., designed circularly polarized crossed dipole antenna for handheld RFID reader application [18], Jong Moon Lee et al., designed a circular polarized metallic patch antenna for RFID reader [19] and Shu-An Yeh et al., designed slotline-fed circularly polarized annular-ring antenna for RFID reader [20]. All performance comparison about UHF RFID reader antennas such as physical dimensions of antennas, gain, center frequency, operating frequency band, 3-dB axial ratio center frequency, 3-dB axial ratio operating frequency band have been shown in Table 1.1 with details.

Table 1.1 Literature review of different UHF RFID antennas.

Reference Number	Physical Dimensions [mm^3]	Gain	Center Frequency (Bandwidth)	Operating Frequency Band	3-dB AR Center Frequency (Bandwidth)	3-dB AR Operating Frequency Band
[7]	120×120×0.8	3.41 dBic	808 MHz (380MHz)	618 – 998 MHz	957 MHz (332 MHz)	791 – 1123 MHz
[8]	126×12×0.8	6.8 dBic	931 MHZ (142 MHz)	860 – 1002 MHz	940 MHz (166 MHz)	857 – 1023 MHz
[9]	250×250×36.5	8.6 dBic	870.5 MHz (255 MHz)	758 – 983 MHz	898.5 MHz (121 MHz)	838 – 959 MHz
[10]	250×250×60	7.5 dBic	905 MHz (440 MHz)	685 – 1125 MHz	912.5 MHz (150 MHz)	836-986 MHz
[11]	200×200×57	7.6 dBic	861.5 MHz (487 MHz)	618 – 1105 MHz	914 MHz (56 MHz)	886 – 942 MHz
[12]	250×250×35	8.3 dBic	861.5 MHz (203 MHz)	760 – 963 MHz	891 MHz (146 MHz)	818-964 MHz
[13]	250×250×29.5	7.0 dBic	933 MHz (200 MHz)	833 – 1033 MHz	895 MHz (120 MHz)	835 – 955 MHz
[14]	250×250×17.3	6.5 dBic	890 MHz (180 MHz)	800 – 980 MHz	910 MHz (180 MHz)	820 – 1000 MHz
[15]	150×150×34	7 dBic	990 MHz (220 MHz)	880 – 1100 MHz	915.5 MHz (29 MHz)	901 – 930 MHz

Table 1.1 (cont.) Literature review of different UHF RFID antennas.

[16]	90×90×4.8	3 dBic	922.5 MHz (37 MHz)	904 – 941 MHz	923.5 MHz (11 MHz)	918 – 929 MHz
[17]	100×100×10	5.62 dBi	955 MHz (210 MHz)	850 – 1060 MHz	980 MHz (208 MHz)	876 – 1084 MHz
[18]	60×60×1.6	1.3 dBi	932 MHz (50 MHz)	907 – 957 MHz	925 MHz (12 MHz)	917 – 929 MHz
[19]	200×200×2.7	9 dBi	906.5 MHz (23 MHz)	918 – 895 MHz	910 MHz (9 MHz)	905.5 – 914.5 MHz
[20]	100×100×1.6	1.5 dBi	910 MHz (160 MHz)	830 – 990 MHz	915 MHz (34 MHz)	898 – 932 MHz

In addition to these, there are different studies on the effects of RFID systems. RFID systems have many effects on issues such as supply chain management, inventory control, loss control. Via advanced features such as specific product recognition, ease of communication and real-time information, RFID technologies provide diverse contributions to the supply chain [21,22]. For example of these contributions, RFID systems can increase efficiency, time-management and accuracy of stock control. These systems can also minimize handling and delivery costs and raise profits by reducing the number of stockouts [23]. RFID system contributions not limited with increasing efficiency of systems, it also improve the reorganization of systems. After deployment of RFID systems to Wal-Mart, it reduced inventory levels by 70% and it also improved service quality by 3% [24]. In recent years, RFID systems have become one of the focal points of both the supply chain and the academy. The first applications of this system, which was not a new technology, were used during the second world war to distinguish enemy aircraft from friendly aircraft [25]. Currently, RFID systems provide benefits for most areas. Examples of these fields are retail, healthcare, textile, production factories. Leung et al. [26], presented the RFID system benefits as in Figure 1.1 in three groups.

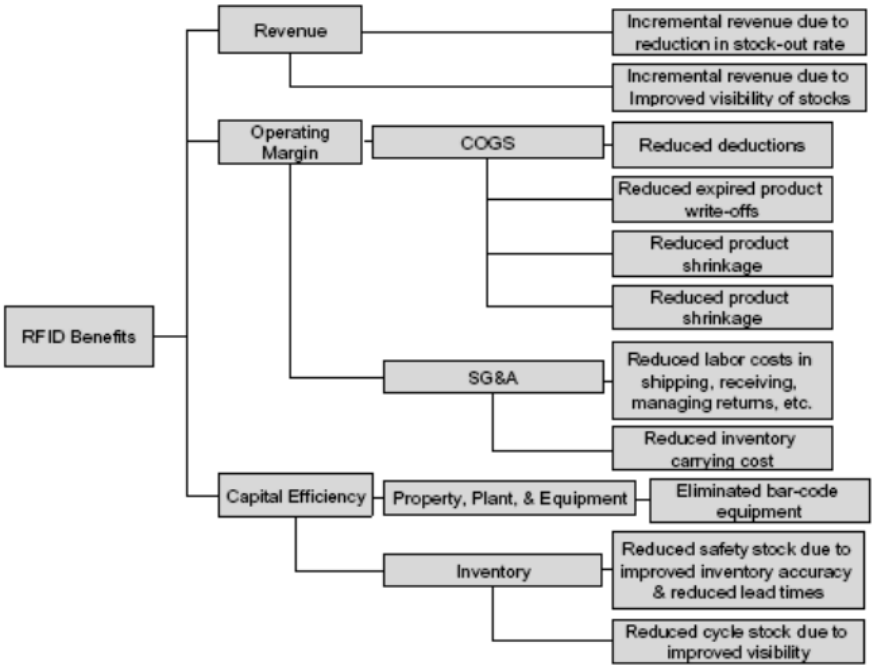

Figure 1.1 RFID benefits tree [27].

As a result, a high rate of positive feedback can be provided to companies or factories with the necessary work and RFID systems applications. There are many publications that evaluate these benefits academically. The authors investigating this issue generally focused on the possible problems that the RFID system can solve in the supply chain process. Atali et al. [28] , Kang and Gerswhin [29] and, Fleish and Tellkamp [30] researched about the inventory inaccuracy issues, Joshi [31], Lee et al. [32], and Fleisch and Tellkamp [30] researched about bullwhip effect, and Kok and Shang [33], Lee et al. [32] researched about replenishment policies. For analyzing the affects of RFID on supply chain in literature, there are four approaches, analytical approach, simulation approach, case studies and experiments. Analytical models are the simplifications of a specific system by mathematical expressions to evaluate and optimize the system according to an objective feature. Generally the discussion in analytical models is limited and about different replenishment policies [27]. There are many studies about anayltical approach in literature [29,34,43–46,35–42]. Simulation studies make it easy to understand a complex model. There are numereous examples in the literature using the simulation approach [47–54]. Finally, the case study and

experiments approach mentioned earlier also come to the fore in this study. Inferences were made from the results by applying the effects of smart factory integration using RFID system directly to a sample factory. There are numerous industrial applications for RFID system applications. Lefebvre [55] analyzed the effects of RFID application on warehouses with a pilot application. Wamba et al. [56] , examined the effects of the integration of RFID technology in the EPC network and e-commerce field. Tzeng et al. [57] has addressed the application of RFID technology in the field of health. Wang et al. [58] focused on the enhancement of RFID technology flow information in a construct supply chain. Chuang and Shaw [59], made a study about integration in supply chains. Huber et al. [60], researched about impact of RFID for tracking goods. Manik et al. [61] carried out an RFID application project in the automotive supplier business to increase the efficiency of the production process. Kim et al. [62], compare the benefits of RFID technology on supply chain management of U.S and Korean retailers.

1.3 Research Objective

Although there are many studies on RFID and smart factories separately in the literature, it has been observed that there is not enough work to make a factory smart with the integration of RFID system. There is currently no method that can inherently provide the smart factory opportunities with RFID system. The main objective of this work is to investigate methods for improving the RFID system abilities for factories to make it smart. To achieve this, the RFID systems has to be researched broadly in both antenna, system and software design. This study mainly research answers for RFID-enabled smart factory environment.The supply chain management and customer relations is really crucial issues for factories. In competition world, factories must follow the technological developments for improve the quality of their products and services. Regardless of the working area of factory, smartening the environment for both produce and workers is important. This study mainly aims the integration of marble factory for smart environment integration with RFID system. Also with this integration, improvement about the total efficiency of factory, quality of products, and services, time management have also been aimed.

Along with the main research questions, other research questions emerging from these questions can be listed as follows:

- Is it possible to improve the operation of the marble factory by providing smart factory integration with RFID system?
- Is it possible to save time by performing human-made operations in the factory with RFID system?
- Can the malfunctions / inaccuracies in stock and shipment issues (wrong stock count, wrong product shipment) be prevented by ensuring an effective control with the RFID system?
- How should RFID system component selections be made for smart factory integration?
- What should be considered in the design of the antenna to be used in the smart factory? Is it possible to design compact, high-gain, circular polarized UHF RFID antenna?
- How can the graphical user interface be designed to be used effectively and properly by the end user in the smart factory?
- How can system tests be performed after system components selection, antenna design and software development?

In the later stages of the thesis, the answers to these questions were sought both in academic and practical terms. In the light of the necessary theoretical information, different design, simulation and measurement results were made and in this context, the added value provided by the system in a real factory environment was discussed together with all system tests.

1.4 Thesis Outline

The following topics will be explained in detail in the remainder of the thesis.

In **Chapter 2**, the theoretical background of RFID systems is explained in detail. After a general summary of RFID technology, different issues are mentioned along with the mathematics behind the system. First of all, the antenna parameters and configurations that affect the system are explained. In the remainder of Chapter 2, RSSI and read range issues, propagation and path loss models, and link budget calculation for RFID systems are mentioned.

In **Chapter 3**, information about RFID reader antenna and tag antenna for smart factory applications is given, and RFID network planning is explained. Along with the antenna analysis found in commercial and literature, an RFID antenna design that can be used in smart factories is presented. In addition, in this section, simulations and measurements of the antennas in sample scenarios have been made and the results are presented in tables and graphics. In the RFID network planning section, different components and details that can be found in an RFID system are explained.

In **Chapter 4**, software studies made to integrate the RFID system into the factory environment and turn it into a smart factory are presented. An exemplary test includes a graphical user interface as well as an end-user interface specially coded for the factory. Besides, an example of an antenna designed with machine learning method is presented in this section. Also tests of the whole system have been carried out in one piece. With the designed antenna and software, the system was planned and installed, tested in a sample test scenario, and its advantages and disadvantages were presented.

In **Chapter 5**, the conclusion of this study has been presented.

2.THEORETICAL BACKGROUND OF RFID SYSTEMS

2.1 Radio Frequency Identification Overview

Radio Frequency Identification (RFID) is a wireless communication technology used to gather information that can be correlated with various identification characteristics of assets bearing RFID tags, such as object count, kind, expiration date, etc. In RFID systems, the identification process occurs by transferring electromagnetic waves between the object carrying RFID tag and reader antenna. Compared to other automatic identification systems, the most significant aspect of RFID systems, the automatic identification (Auto-ID) system, is that no mechanical contact is needed for the identification process. Mechanical contact is not a practical solution in the new era entered with the development of technology. Technically, the most accurate solution is RFID systems by transferring the data on the silicon chip inside the RFID tag wirelessly and without mechanical contact. Around the same time, another aspect that stands out in RFID systems is that the data on this silicon chip can be erased and rewritten depends on the form of RFID tag, so that the tag can be used over and over again. Depending on the storage capacity of the chip, the information can be stored in detail. In recent years, economic, social, military, health, and political service groups have realized RFID technology's potential. The usage rates of RFID tags are increasing in many areas, and thus communication performance and standardization levels are constantly improved. For example, with the UHF Gen2 protocol, the reliability and security level has increased in RFID systems. Large companies use RFID systems to increase efficiency in many areas, such as inventory tracking, supply chain management, and worker tracking. Consequently, the place and importance of RFID systems in our lives have become undeniable. In the continuation of this section, detailed technical information about components in RFID systems will be given. UHF RFID operating bands in different countries have been shown in Figure 2.1.

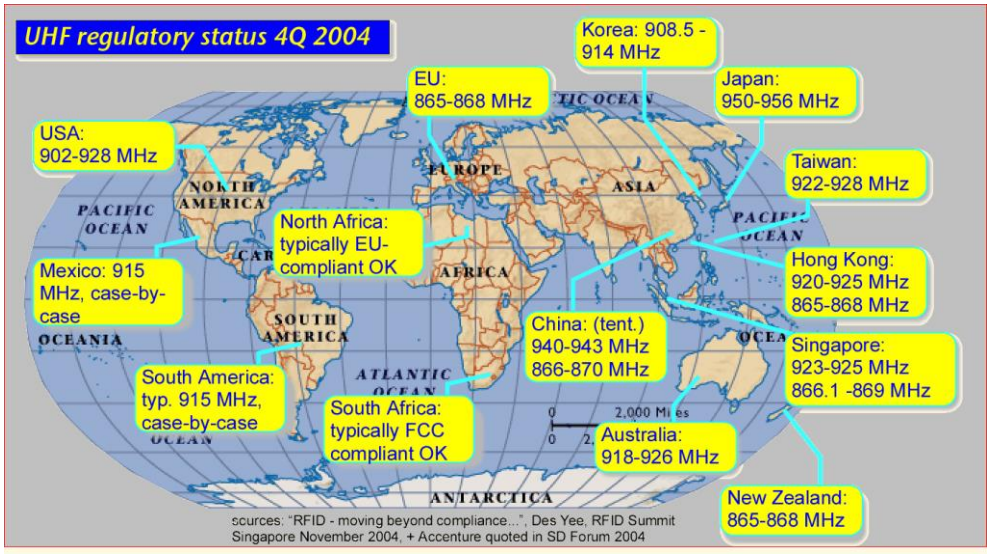

Figure 2.1 UHF RFID frequency bands for different countries [63].

2.1.1 Basics of RFID systems

Basically, RFID system are composed of three main components:

-RFID Transponder (Reader)

-Antenna for Reader

-RFID Tag

As a receiver and transmitter, the RFID tag antenna works. Electromagnetic signals are transmitted through the reader and tag so that information about the chip in the tag is transferred. The RFID reader is a tool that in the context of an electronic product code, makes sense of the data and introduces it to the end user. RFID tag, antenna and reader will be explained in details later in this section.

The **RFID tag** is a compact device with a small antenna and a chip inside. The RFID tag chip includes specific information called the Electronic Product Code (EPC) about the object attached to it. The RFID tag antenna for magnetic and electrical coupling systems varies. For magnetic coupling, the RFID tag antenna is basically a coil protected by a shielding surface; for electrical coupling, the RFID tag antenna is typically a dipole antenna structure.

The IC of the RFID tag includes multiple features, such as basic logic operations, multi-tag identification, data handling, and data modulation. RFID tags can be placed

on a single object or product, as well as on structures such as boxes or pallets that contain multiple products. In context by their structure, RFID tags can be divided into four general groups. These are: active, semi-active, passive, and semi-passive RFID tags. Figure 2.2 shows the single antenna RFID tag structure.

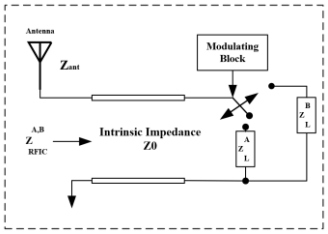

Figure 2.2 Single-antenna RF tag structure.

In order to enable wireless communication, **Active RFID tags** need an internal energy source. Generally, they have a small battery for energizing the tag. The active RFID communication model does not vary in general structure from other communication models which communicate using radio waves. As a result, active RFID tags will trigger communication with their readers and sometimes a peer-to-peer network to broadcast information. A very notable characteristic of active RFID tags is that they are longer than most RFID tags for identification distances. Since they have an internal power source, more reliable reading and reading from longer distances can be achieved compared to passive tags. However, considering the power supply cost of active tags, their prices remain higher than passive tags. For this reason, active RFID tags are generally used to track high-value products and products that require long-distance reading. In Figure 2.3, the active RFID communication model has been shown.

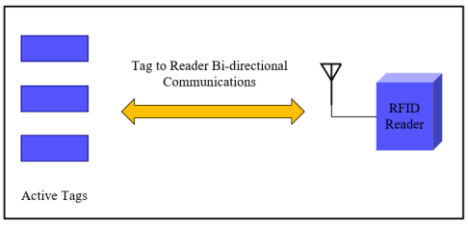

Figure 2.3 Active RFID communication model.

Semi-active RFID tags need an internal energy source to communicate like active RFID tags. These tags start to transmit RF signals when their internal batteries are

activated by the activation signal sent by the reader. However, unlike active RFID tags, semi-active RFID tags cannot initiate communication themselves. They remain in sleep mode until the activation signal is received from the reader. Semi-active RFID tags have a longer battery life than active tags. Reading distances are higher than passive tags. While the use of semi-active RFID tags and active RFID tags does not vary much, semi-active RFID tags are usually used at points where power consumption is significant. In Figure 2.4, the semi-active RFID communication model has been shown.

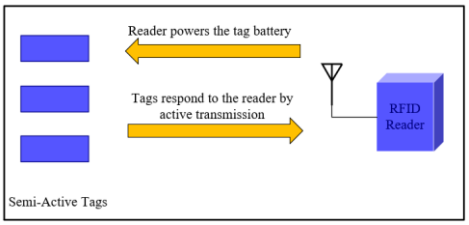

Figure 2.4 Semi-active RFID communication model.

Unlike the other tags mentioned, passive RFID tags do not have an inbuilt energy supply; instead they have the power needed to work by capturing the electromagnetic energy emitted by the RFID reader. Passive tags store little energy emitted from the RFID reader; by converting this energy to DC power and generating their responses, they provide the necessary power to the microchips inside. The passive tag antenna must therefore be configured to conduct two main duties:

(1) Gathering power from the RFID reader.

(2) Reflecting the outgoing backscatter signal. In Figure 2.5, the passive RFID communication model has been shown.

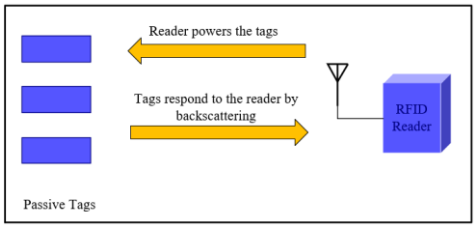

Figure 2.5 Passive RFID communication model.

Passive RFID tags, relative to other tags mentioned, are typically manufactured in very small architectures and are compact, lightweight, and inexpensive. In areas that need shorter distances and where there are a number of items, passive RFID tags are commonly used.

Semi-passive RFID tags have power sources and unlike active tags, are only enabled when the RFID reader awakens. The battery of semi-passive RFID tags will also last longer than active tags. Semi-passive tags, since semi-passive RFID tags have an internal battery, have a longer reading distance than passive tags. The battery in the semi-passive tags only supplies the required power to the tag circuit; so semi-passive tags do not activate tag-reader interaction by constantly transmitting RF signals. The tag-reader communication of these tags is focused on the backscattering process, such as passive RFID tags. These tags are more expensive than passive tags because of having an inbuilt battery source and are large in scale. However these tags fill in the distinction between short-range passive tags and expensive active tags**.** The semi-passive RFID communication model is given in Figure 2.6.

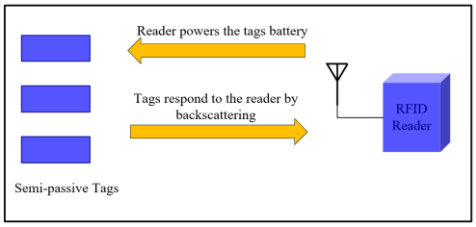

Figure 2.6 Semi-passive RFID communication model.

Above mentioned RFID tags have positive and negative aspects compared to each other. The technical summary of RFID tags has been presented in Table 2.1.

Table 2.1 Technical overview of types of main RFID tags.

	Active	**Semi-active**	**Semi-passive**	**Passive**
Battery Requirement	Required	Required	Required	Not required
Power source	Internal battery, continuously available	Internal battery, available only after a wake-up	Internal battery, available only after a wake-up	Obtain RF energy generated from the reader

Table 2.1 (cont.) Technical overview of types of main RFID tags.

Tag-reader communications	Low	Low	Low	High
Reader-to-tag signal strength (range dependant)	High	High	High	Low
Communication range	Longer than 100 m	Longer than 100 m	Longer than 100 m	~15m
Data storage capacity	Large	Large	Large	Small
Read/write capability	Yes	Yes	Yes	Read-only
Expense	High	High	Medium	Low
Application area	Large asset tracking	Large asset tracking	Electronic toll	Proximity cards

An **RFID reader** is an electronic device with its own hardware and operating system that sends and receives signals to RFID tags through antenna or antennas attached to it. Specifically, the RFID reader serves as a bridge for the transfer of information between software application and RFID tags.

One or more antennas can be connected to the RFID reader. There are RFID readers that can be fixed or used as portable. Below are some examples of portable and fixed reader models of some brands.

The operation of the tag is ensured for active RFID systems by listening to the signal coming from the RFID tags via the RFID transponder; for passive RFID systems by sending the RF signal required by the tag from the reader.

With two main EM coupling mechanisms, passive RFID readers activate the tags :

- “Magnetic Field Coupling”
- “Electric Field Coupling”

The method of coupling in which the tag antenna is inductively coupled by the electromagnetic field generated across the reader antenna is considered **magnetic coupling**. The concept is one that has been found in transformers, where under Faraday’s law, the primary coil creates a secondary coil voltage. The primary coil is the alternating magnetic field of the reader in this scenario, and the secondary coil is the antenna of the tag. In LF and HF RFID systems, nearfield coupling mostly happens, where the distance between the tag and the reader antenna is much shorter than their

wavelength. It offers minimal read ranges in RFID systems. The concept of a tag powering up with a magnetic coupling has been shown in Figure 2.7a.

Magnetically coupled RFID tags are antenna tags comprising multi-turn coils with LC circuits tuned to the desired frequency in order to optimize reader energy collection. For HF tag antenna coils, the turn number is less than the total number of turns on the antenna for LF tags. In this type of coupling, Tag-reader interactions are related to digital data modulation by changing the magnetic field intensity that effectively provides AM modulation for the digital information to flow. Magnetically coupled tags have no capacity to store energy; thus, during the tag query, the magnetic field should be continuously applied.

In microwave and UHF RFID tags at longer wavelengths and in the far-field region, **electric coupling**, unlike magnetic coupling, is used. In free space, field components of an antenna transmit as a single electromagnetic wave, far-field energy conversion is carried out. The inductive coupling system cannot be used in such a way that the far-field antenna and magnetic field can no longer be aligned. For electric field coupling, the backscatter method, which is the same concept used in radar, is used. In Figure 2.7b, electrically coupled RFID system representation has ben shown.

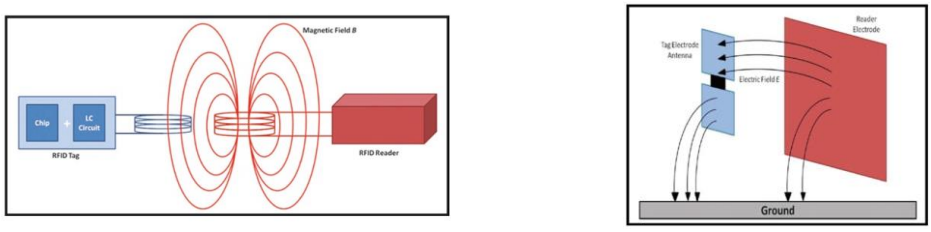

a) b)

Figure 2.7 a) Magnetically coupled RFID systems, b) Electrically coupled RFID systems [64].

Tag-reader interactions proceed through changes within that load impedance of the tag antenna in the electric coupling. This has resulted in a special backscatter signal which can be deciphered by the reader. In this modulation method, instead of absorbing it the

tag is purposely mistuned to the frequency of its antenna to reflect the obtained signal. Figure 2.8 illustrates the inductive coupling (LF) vs. electric coupling (UHF).

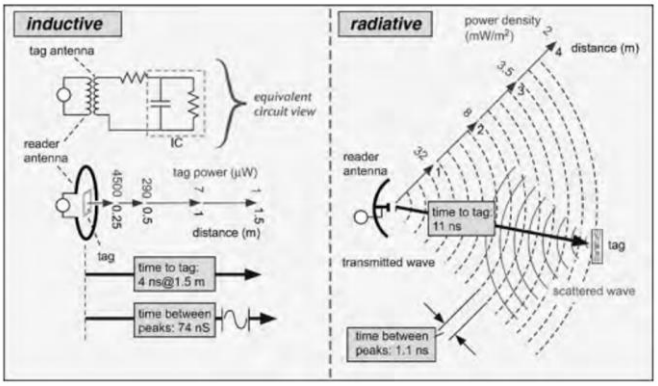

Figure 2.8 Magnetic Coupling (LF) vs. Electrical Coupling (UHF) [65].

2.2 Electromagnetic Fundamentals of RFID System

The method of reading an RFID tag is far more complex than just an RF receiver that identifies its backscatter. The RFID reader has to energize the tag via RF continuous wave (CW) transmission for a passive tag to function. The magnitude of this energy transfer is calculated using the following Friis equation, Equation 2.1:

$$P_R = P_T \frac{G_T(\theta_T, \emptyset_T) G_R(\theta_R, \emptyset_R) \lambda^2}{(4\pi r)^2} (1 - |\Gamma_T|^2)(1 - |\Gamma_R|^2)|\hat{p}_T \cdot \hat{p}_R|^2 \quad (2.1)$$

These three elements will help us to understand the antennas' behaviors and characteristics in the RFID system. In the Friis equation, the G_T and G_R define the reader and tag antenna gains and RFID system, respectively. The gains of the transmitter, receiver antennas are relative to the spatial positions for collecting and harvesting energy from the two antennas. Both the tag and the reader's polar coordinates are shown as functions of θ and $\emptyset$. The maximum transfer happens when the center lines of the planes coincide with each antenna. So the gains will start to drop if angles change out of the most appropriate orientation. It is important to know that the relative spatial alignments of the interrogator and tag antennas for determining the

real amount of power available on the tag. In addition to antenna gains, polarization is also an important question. Polarization relates to relative orientations, including electric fields generated by the RFID reader and tag antenna conductive elements. The distance between the interrogator and the tag, r, is another significant term in the Friis equation. In terms of both powering the tag and seeing the RCS difference of the tag antenna with ability in the reader's receiver, the tag-reader distance is vital. For RFID tag to operate, the power delivered by the interrogator should be sufficient. For reading backscatter signal from the tag by RFID reader, the change in the reflection coefficient of the tag Γ_T changes the power received by the reader P_R, this value is used to decipher the information from the RFID tag. There are variations between tags working close to the interrogator, depending on the wavelength of the frequency used. The closer distances are called the antenna's near-field operation area, and the far-field is called the greater distance operation area.

The Friis equation is related to the far field. It is often necessary to minimize the power required by the silicon chip and hence the tag, especially in the case of far-field UHF. Whenever the matching impedance within the tag is modified to modulate the backscattered RF, the reflection coefficient is altered. Thus, through this change in the reflection coefficient suggested in the Friis equation, the force harvested by the tag is altered (reduced). The power transmitted by the P_T antenna in the Friis equation is governed by the "Federal Communications Commission (FCC)". As determined by the antenna radiation pattern, this power is distributed over a three-dimensional region. The frequency used, 867 MHz in Turkey, has a wavelength λ, 0.346+ m. The transmit antenna gain, $G_T(\theta_T, \emptyset_T)$, means that the energy supplied to the antenna is focused to some extent, causing the energy density to be greater in some areas than it would have been if it had been spread evenly in all directions. The angular directions θ_T, $\emptyset_T$, discloses that the orientation of the tag will obtain the power that will differ with the transmitting energy along with all orientation angles. Another term in the Friis equation is tag antenna gain $G_R(\theta_R, \emptyset_R)$. In general, most of the RFID tag antennas available in the market are produced in a dipole structure. With a small distance between them the dipole can be thought of as two end-to-end linear wires. For the reader antenna and tag antenna, the gain is significant. Simultaneously, both antennas must be placed in the appropriate orientations to ensure accurate and consistent

reading. The important parameters related to the mathematics of RFID systems such as polarization, reflection, directivity, and gain are discussed in detail later in this section.

2.2.1 Polarization

Polarization is called the direction of oscillation of the electric field component of the electromagnetic wave emitted by an antenna. Polarization of antenna in RFID systems is important because to maximize the tag reading distance, polarization matching between reader and tag antenna should be ensured. The mutual polarization efficiency among the RFID tag antenna and the RFID interrogator antenna can be calculated using complex polarization ratios $e_1 e^{j\vartheta_1}$ and $e_2 e^{j\vartheta_2}$ of antennas, as shown in Equation 2.2 [66]:

$$p = \frac{1 + {e_1}^2 {e_2}^2 + 2e_1 e_2 \cos(\vartheta_1 - \vartheta_2)}{(1 + {e_1}^2)(1 + {e_2}^2)} \tag{2.2}$$

In Equation 2.2, e value denotes the antenna polarization ratio, and the absolute of this value is in relationship with the antenna axial ratio *AR*, as shown in Equation 2.3[67]:

$$AR[dB] = 20 \log \left| \frac{e + 1}{e - 1} \right|. \tag{2.3}$$

Most of the RFID tags commercially available are produced with linear polarization. But because of the tag readability in any direction of circularly polarized RFID antennas, generally, they are used in RFID systems. Their circular gains and axial ratios generally determine antennas. Tag reading distance is highly dependent on antenna gain, so understand the relationship between an antenna's polarization of gain is crucial in RFID systems. For an antenna's linear and circular gain, linear and circular isotropic sources are taken as a reference, respectively. The relationship between linear gain (dBil) and circular gain (dBic) have been expressed in equation Equation 2.4 [67,68] :

$$G[dBic] = G[dBil] + 3 + 20\log\left(\frac{1 + 10^{-A/20}}{2}\right) e \quad (2.4)$$

The 3 dB difference between the two gains is valid in only perfect circular polarization cases, and that is a nearly impossible case in practice. Also, the antenna's circular gain may be greater or smaller than its linear gain.

2.2.2 Reflection

The antenna's impedance matching the load (chip) impedance on the RFID tag is called reflection. Reflection is an important parameter because it gives essential information about the operating frequency and characteristics of an RFID antenna. The reflection coefficient are calculated with the difference of load impedance, Z_L, and antenna impedance, Z_A, divided by the sum of load impedance and antenna impedance as shown in Equation 2.5:

$$\Gamma = (Z_L - Z_A)/(Z_L + Z_A) \quad (2.5)$$

For maximizing the energy transfer of antenna, reflection coefficient should be minimum as possible in dB. The reference for reflection coefficient of resonant frequency of an antenna is generally -10 dB. Also, reflection coefficient is directly relates with the standing wave ratio which is equals 1+|Γ|/1-|Γ|. The standing waves occurs because of the impedance mismatch between the RFID antenna and transmission line. So for better transmission, standing waves not desired. The impedance mismatch is a crucial issue in antenna theory. While designing an RFID tag antenna, the chip of the RFID tag and antenna of tag should be matched. Sometimes matching tecniques are applied for impedance matching for minimize the reflection coefficient. To sum up, reflection coefficient is vital in mathematics behind the RFID systems and it may directly affects the overall performance of RFID system.

2.2.3 Antenna directivity and gain

The antenna directivity, [D(θ,∅)], is defined isotropically as the proportion of the radiated power density of the antenna at a distant point to the total radiated power

density of the antenna. It is expressed in decibels above a reference, where $[D(\theta,\emptyset)][dB]=10\log_{10}D(\theta,\emptyset)$. The directivity of an isotropic radiator is equals to 1. The antenna is driven by a source in practical applications where the total radiated power is not the total power that is obtainable from the power source. The effects of mismatch (reflection) losses in the antenna and source link can be attributed to loss factors that affect antenna efficiency. The total power transmitted to the antenna terminal is therefore equal to the ohmic (P_{ohmic}) losses plus the antenna, $P_{in} = P_{rad} + P_{ohmic}$, radiated power ($P_{rad}$).

One of the parameters that determines the propagation capacity of the antenna is **gain**. The antenna's absolute gain in a given direction is defined as the ratio of an antenna's power density propagating to a given far-field point to the power density emitted by a lossless isotropic emitter at the same point. It is expressed as Equation 2.6:

$$G = \frac{4\pi r^2 W_{rad}}{4\pi r^2 W_{rad}^i} = \frac{W_{rad}}{W_{rad}^i} \tag{2.6}$$

G denotes the gain of the subject antenna, and *r* denotes the distance from the antenna to a point in the far-field zone, which should be larger than $2D^2/\lambda$. W_{rad} is the radiation density generated at that point by the subject antenna, W_{rad}^i is the power density of the lossless isotropic emitter. Also gain can be expressed as Equation 2.7:

$$G = D_0 e_0 \tag{2.7}$$

where e_0 is the overall efficiency and D_0 is the directivity of antenna, $e_0 = e_{cd} e_r$.

In lossless cases, the radiation efficiency of antenna $e_{cd} = 1$. But there is also another parameter that must taken into account for gain value which is the reflection efficiency which calculated by $1-|\Gamma|^2$. With using this value maximum realized gain can be calculated. For an example case of antenna that has directivity value of 1.697, gain versus reflection efficiency relationship has been shown in Figure 2.9.

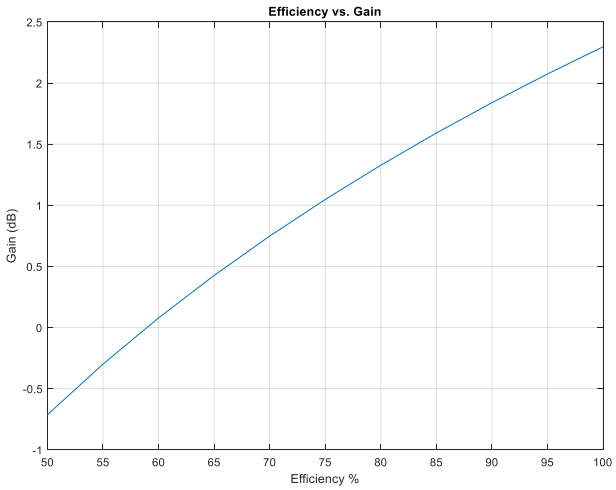

Figure 2.9 Relationship between the total efficiency vs. antenna gain.

To summarize, RFID system performance depends on many parameters included in the Friis equation. Since these parameters directly affect the antenna performance, they can directly affect the RFID system performance to be used in the smart factory environment. For this reason, the necessary analyzes should be made in the design part of the whole system and the design should be carried out accordingly. In the continuation of this section, antenna configurations in RFID systems, which is an important issue in the system to be designed for the smart factory, will be examined.

2.3 Antenna Configurations in RFID Systems

The antenna configuration in RFID systems is important for maximizing the reading distance. The polarization, gain, and EIRP of the antenna directly affects the reading distance. Also, for convenient indentification and decipher process of the tag antenna signals, good isolation between communication channels is vital for RFID systems [65]. Various RFID readers are commercially available such as fixed, handheld, etc. Antenna selection is a significant factor that affects the RFID system performance; for different application areas, different types of RFID antennas could be used. As an example, while circular polarized RFID antennas used in inventory tracking applications, linear polarized RFID antennas used in access control systems.

While designing an RFID system RF front end antenna configuration, the isolation between communication channels is critical. There are two main selections in the

design stage; these are bistatic antenna configuration, monostatic antenna configuration. Also, an RFID reader can use both configurations by switching between them [69]. The environment where the system is placed and other objects in the propagation environment cause reflections in both configurations. These reflections may negatively affect the overall RFID system performance.

2.3.1 Bistatic antenna configuration

The antenna configuration type that is used for separate transmit and receive antennas is called bistatic antenna configuration (Figure 2.10a). In this type of configuration, receive and transmit antennas are separated via polarization. Bistatic systems generally use circularly polarized antennas in polarization (RHCP-LHCP) with opposite polarization for transmitting and receiving. Bistatic systems are generally used in places where there is space for more than one antenna to be placed, RFID portals, and doors [70].

2.3.2 Monostatic antenna configuration

In the monostatic antenna configuration, an RF isolator and a single RFID antenna are used for transmitting and receiving, as shown in Figure 2.10b. In RFID readers, circulator and directional coupler structures are mostly used as isolators [71]. In most cases, the isolation between channels in monostatic antenna configurations is lower than in bistatic antenna configuration. Monostatic antenna configurations are used in cases where the antenna size and the area where the antenna will be placed are important, such as handheld RFID readers. It is technically difficult to create a small-sized antenna with the desired high gain, polarization, and beam-width in a monostatic configuration due to size restrictions [72].

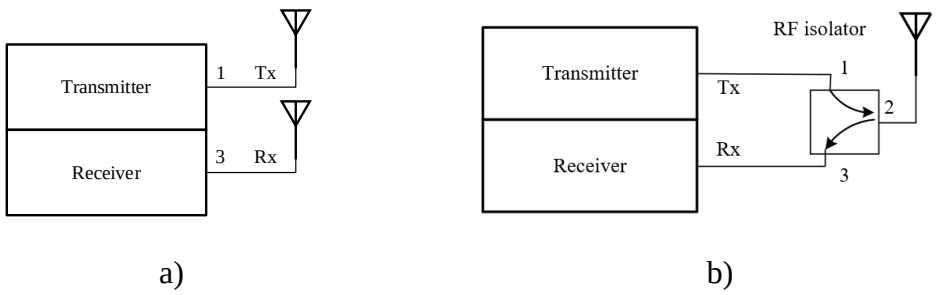

Figure 2.10 Antenna configuration types a) Bistatic antenna configuration, b) Monostatic antenna configuration.

When directional couplers and circulators are used on RF front-end modules, directional couplers cause extra receive path attenuation loss. Because of this situation, in these cases, the receiver must have better radiosensitivity. On the other hand, the tag signal's Signal-to-Noise Ratio is limited by the transmitted signal leakage, not thermal noise. In monostatic antenna configurations, the return loss of the antenna generally defines the Tx/Rx isolation. As a result, the tag signal for couplers and circulators is approximately the same as shown in the example in Table 2.2, where the SNR value is constructed using typical values.

Table 2.2 Tag signal Signal-Noise Ratio for two RF isolators [71].

(dB)	**Return Loss**	**Coupling Between Antennas**	**Isolator S_{12}**	**Isolator S_{23}**	**Isolator S_{13}**	**Isolation between Tx/Rx**	**Tag Signal SNR**
Bistatic	-20	-30	Not av.	Not av.	Not av.	-30	P_r/P_t +30
Monostatic (Coupler)	-20	Not av.	-1	-20	-45	-41	P_r/P_t +21
Monostatic (Circulator)	-20	Not av.	-1	-1	-25	-22	P_r/P_t +21

2.4 RSSI and Read Range in RFID Systems

2.4.1 RSSI model

In passive RFID reader and tag communication, the sensitivity of the RFID tag chip is important for communication to take place. If the sensitivity of the chip is greater than the power emitted by the tag, the tag sends back the unique information inside the chip using the principle of backscatter modulation. The tag antenna has two impedance load states, which are conjugate matching impedance load Z_{CM} and short circuit impedance load $Z_{SC,}$ and the backscattered signal by the RFID tag is modulated according to changing the Z_{CM} and Z_{SC} impedance load states [73]. After the backscatter signal from

the RFID tag side, when the RFID reader side is examined, the modulated signal amplitude is made available by the Received Signal Strength Indicator (RSSI). Let's consider a closed space with two-dimensional borders with an RFID reader and RFID tag at certain points. In this closed area, let's assume that x and y coordinates indicate the RFID tag position with respect to the reader antenna and d stands for the distance between the RFID reader and the RFID tag.

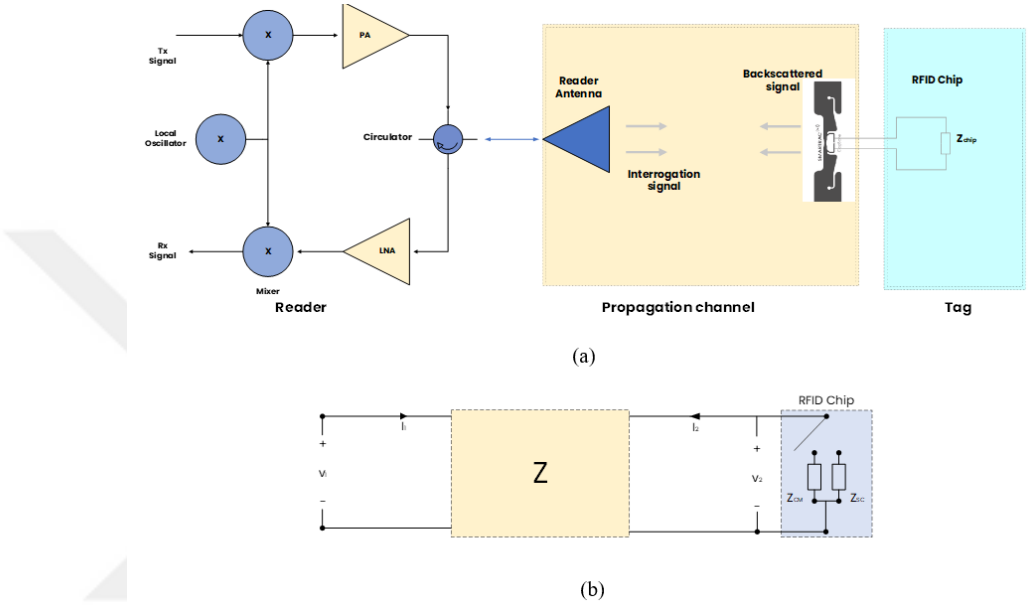

Figure 2.11 a) Schematic representation of a tag equipped with an antenna – RFID chip – the reader – the latter consisting of an antenna – circulator – power amplifier for the transmitted signal (backward link). b) Equivalent impedance matrix representing the reader antenna, the tag antenna, the propagation channel between them. Z_{CM}: conjugate matching impedance load or a short circuit Z_{SC}: short circuit impedance.

Based on the equivalent circuit in Figure 2.11, in terms of the difference between the reflection coefficients corresponding to the above two tag impedance load states Γ_{CM} and Γ_{SC}, the obtained signal strength on the reader side can be expressed. The obtained signal strength known as RSSI can be displayed as a digital value by any RFID reader compliant with the standardized EPC Gen1 and Gen2 protocols. In Equation 2.8, the RSSI can be expressed as follows with Alice Buffi's study [74], where Z_{in} is the input impedance seen at the reader antenna connector, and K is a constant, independent of the tag position:

$$RSSI = K|\Gamma_{CM}(x,y) - \Gamma_{SC}(x,y)|^2 \quad (2.8)$$

With Equation 2.9

$$\Gamma = \frac{b_1}{a_1} = \frac{Z_{in} - R_0}{Z_{in} + R_0} \quad (2.9)$$

Where R_0 is the reader antenna feeding line's characteristic impedance, and b_1 and a_1 are the complex amplitudes of the reflected and incident voltage waves, respectively, at the reader antenna port. The reflection coefficient Γ depends on the tag antenna load and on the electromagnetic coupling between tag and reader antennas.

There will be changes in the RSSI value calculation depending on the size of the two-dimensional closed area we initially assumed, and therefore, whether it is near or far-field. Calculation of the RSSI value depends on whether wireless communication takes place in the near field or in the far-field. If the tag-reader distance is less than a wavelength value, this area is called the near field of the antenna. The electric field component in the near field contains terms that are proportional to 1/d, $1/d^2$, and $1/d^3$. Conversely, situations where the tag-reader antenna distance is much higher, is called the far-field region of the reader antenna. The radiated electric field in the far-field region of the antenna can be approximated with a local plane wave whose amplitude decreases as 1/d. As a result, in antenna near-field operation area, the RSSI amplitude is proportional to $1/d^4$ [71], while the RSSI value for the far-field of the antenna can be expressed in terms of the gain of the reader and tag antennas, obtained by classical radar equation and differential radar cross-section [75].

2.4.2 Sensitivity, range, and differential RCS

The **RFID tag sensitivity** is an indicator of threshold power at the location of the tag for a tag to operate [71]. This value depends on different parameters such as the RFID chip power sensitivity, the gain of the antenna, match between RFID tag antenna – RFID chip and tag sensitivity is an independent value from propagation medium. There is a direct relationship between the field sensitivity of RFID and RFID tag power

sensitivity. The collected power by RFID antenna chip with a perfect impedance match can be expressed as Equation 2.10 [71] where S is incident power density:

$$P_{tag}G = SA_e, \tag{2.10}$$

A_e denotes the RFID tag antenna effective area and with using this value the relationship between tag power sensitivity and received power on tag can be shown as in Equation 2.11:

$$\frac{|E_{tag}|^2}{120\pi}\frac{\lambda^2}{4\pi}G = P_{received_{tag}} = P_{tag}G \tag{2.11}$$

By combining the power density equation with these equations, the following Equation 2.12 can be obtained [71]:

$$E_{tag} = \frac{4\pi}{\lambda}\sqrt{30P_{tag}} \tag{2.12}$$

and with using Equation 2.12, the relationship between field sensitivity and power sensitivity of RFID tag can be obtained as shown in Figure 2.12:

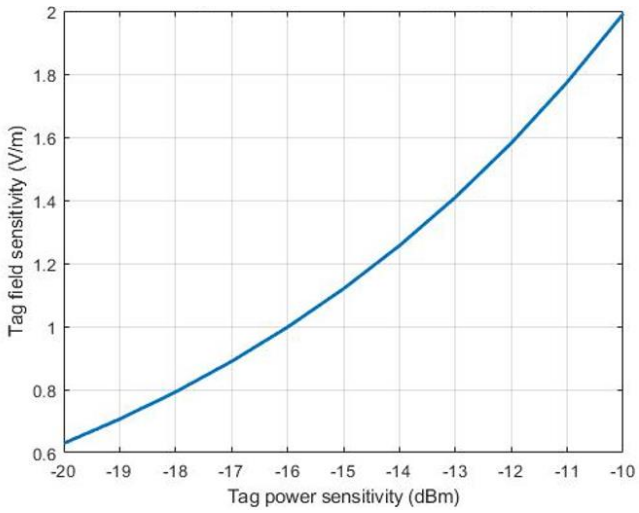

Figure 2.12 Relationship between field sensitivity and power sensitivity of RFID tag at 867 MHz.

The RFID tag power sensitivity can also be calculated as follows in Equation 2.13 using chip sensitivity P_{th}, impedance matching coefficient τ, and polarization efficiency p [71]:

$$P_{tag} = Gp\tau P_{th} \tag{2.13}$$

Equation 2.13 can be used for finding the minimum power required at the location of the RFID tag for the RFID chip to activate.

The **tag range** is the longest distance that the RFID tag can read by the reader antenna. It is an important performance feature because it can be measured directly and interpreted easily. Tag range depends on different parameters such as transmitted EIRP, path loss on propagation environment, RFID tag sensitivity, RFID tag field sensitivity, and other system parameters. While describing tag range, the writing range and reading range of a tag differs, and the writing range of the tag is generally about 70 percent less in the reading range because of the more power required to write on the RFID tag. If the only restriction about maximum tag range is RFID tag sensitivity, tag range can be expressed as Equation 2.14 in an arbitrary propagation environment [71].

$$P_t G_t L_{path}(d) = P_{tag} \tag{2.14}$$

In some special cases, if the inverse function of the distance-dependent path loss is known, the above equation can be solved analytically for the tag range. For an example case, when the path loss is relative to the distance with d^{-2}, the RFID tag range can be calculated as follows Equation 2.15 [71] :

$$r_{tag} = \frac{\lambda}{4\pi}\sqrt{\frac{P_t G_t G p \tau}{P_{th}}} \tag{2.15}$$

As can be seen in Equation 2.16, in free space, there is a relationship between tag range, and field sensitivity, and power sensitivity of a tag [71]:

$$r_{tag} = \frac{\sqrt{30P_tG_t}}{E_{tag}} = \frac{\lambda}{4\pi}\sqrt{\frac{P_tG_t}{P_{tag}}} \tag{2.16}$$

Below are graphs regarding the change of tag range according to different parameters. Figure 2.13a shows the relationship between tag field sensitivity and tag range; Figure 2.13b shows the relationship between chip power sensitivity and tag range. EIRP is 1 W. The RFID tag to be used in graphs, Smartrac Dogbone R6, has a reading sensitivity of -20 dBm and a writing sensitivity of -16.7 dBm. RFID operating frequency is 867 MHz in Turkey. The RFID tag antenna gain is taken as 2 dBi, and the impedance matching coefficient is assumed as 1. Figure 2.14a shows the relationship between tag antenna gain and tag range, and Figure 2.14b shows the relationship between impedance matching coefficient with tag distance. The necessary information about the other parameters that affect the relationship between tag range has been given in these graphs. Fields marked with dots show the theoretical tag range values of the RFID tag to be used as a reference.

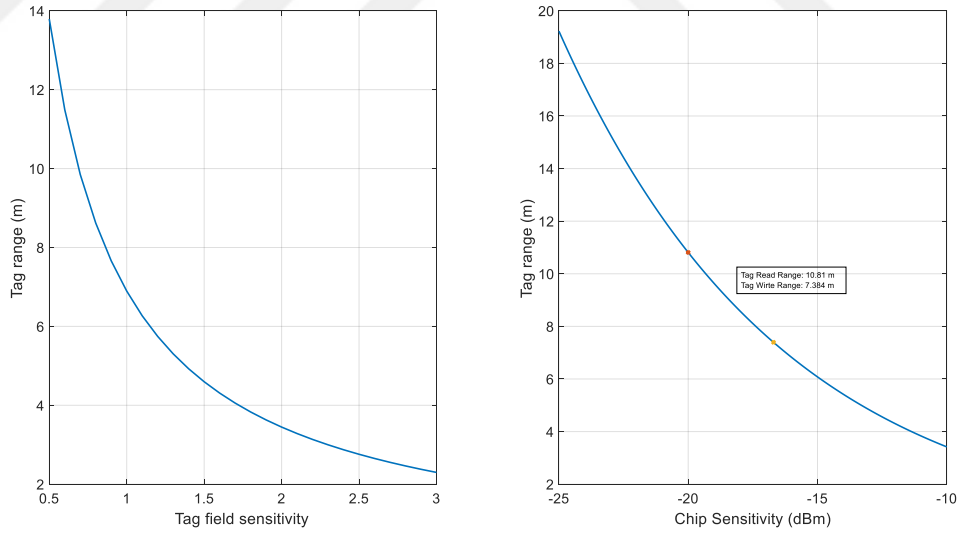

a) b)

Figure 2.13 a) Tag field sensitivity – tag range, at 867 MHz, EIRP 1 W, b) Chip sensitivity vs. Tag range, frequency 867 MHz, Chip read sensitivity -20 dBm; Chip write sensitivity -16.7 dBm.

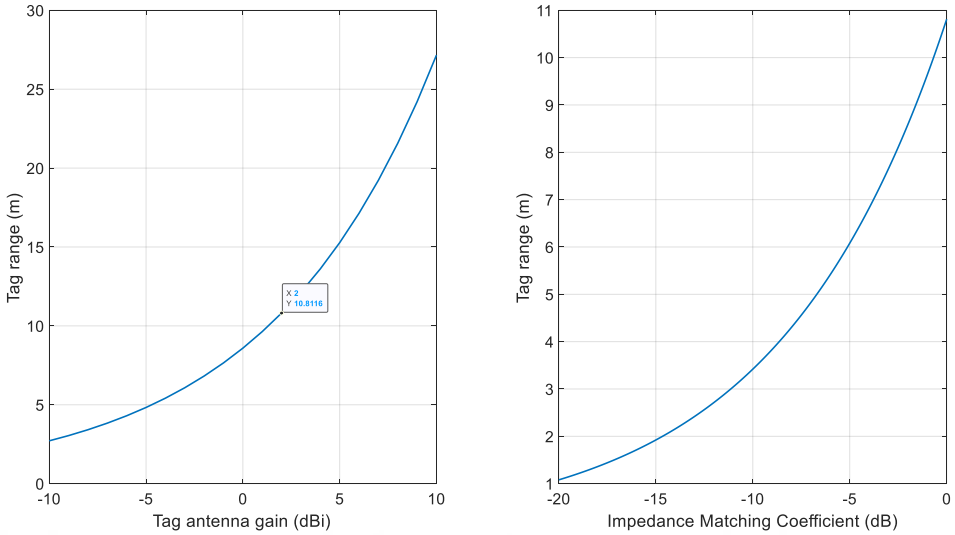

a) b)

Figure 2.14 a) Tag antenna gain vs. Tag range, frequency 867 MHz, free space, Chip read sensitivity -20 dBm, 1 W EIRP, perfect impedance match, b) Impedance matching coefficient vs. Tag range, frequency 867 MHz, free space, Chip read sensitivity -20 dBm, 1W EIRP.

Differential RCS $\Delta\sigma$ is another tag performance attribute that depends on the tag itself, such as tag sensitivity. Differential RCS specifies the modulated backscattered signal power from the RFID tag to the RFID reader. The differential RCS of an RFID tag can be expressed with the antenna effective area A_e and the backscatter modulation loss factor K as follows in Equation 2.17 [71]:

$$\Delta\sigma = A_e K \tag{2.17}$$

and K can be calculated using Equation 2.18 [71] :

$$K = \alpha|\rho_1 - \rho_2|^2 \tag{2.18}$$

The coefficient α varies according to the different modulation cases, and the reflection coefficients ρ_1, ρ_2 between the tag impedance Z_a – the chip impedance according to different modulation states $Z_{1,2}$ can be expressed as follows in Equation 2.19 [71]:

$$\rho_{1,2} = \frac{Z_{1,2} - Z_a^*}{Z_{1,2} + Z_a^*} \tag{2.19}$$

The delta RCS definition given in Equation 2.17 uses the coefficient a = 1. This implies that the maximum observable radar cross section of the minimum scattering antenna switching between open and matched loads is equal to the scalar radar cross section of the same antenna connected to the corresponding load, in accordance with classical antenna theory. In addition, the modulation conditions required to calculate the time-averaged signal strength are not taken into account in this definition.

For a case that the modulated signal of the tag has a 50% duty cycle value and the reference level of the received voltage is in the middle point of the modulation states, α coefficient can easily be calculated as 1/4. With 50% duty cycle, Table 2.3 shows the K values for various chip impedance cases.

Table 2.3 K value for various chip impedance states.

Z_1	Z_2	ρ_1	ρ_2	K
Matched	Short	0	-1	-6 dB
Matched	Open	0	1	-6 dB
Short	Open	-1	1	0 dB

As can be seen in Table 2.3, the maximum modulation efficiency occurs when Z_1 is short Z_2 is open. Selecting these modulation states does not allow any RF signal power to be acquired by the RFID tag chip, but is still a great option for semi-passive tags. Generally, Z_1 matched Z_2 short case with -6 dB modulation loss is used in RFID tags. At the same time, the delta RCS and K values can be calculated from the strength of the signal received from the RFID tag with the classical radar equation.

2.5 Link Budget and Propagation Analysis

2.5.1 Propagation analysis in RFID systems

In the theoretically described cases, different environmental conditions between the reader and tag are not considered. However, the progression of propagation in real life is very different. In real conditions, in an RFID system, the electromagnetic wave emitted from the reader antenna interacts with many other objects besides the tag. Naturally, the electromagnetic wave emitted by the RFID antenna does not reach the RFID tag as it is. To better understand the propagation in real life, it is necessary to understand the issues such as path loss and reader-tag link.

2.5.2 Path loss

Path loss is an important parameter that depends on the propagation medium between two communication antennas and shows the attenuation of the electromagnetic wave through space. It is a wide-range research area in wireless communication technologies, and there are many studies on UHF RFID systems in the literature. [76–79].

For a multi-path condition with numerous single reflections and line-of-sight, the path loss among the RFID reader – RFID tag antennas expressed as in Equation 2.20 [71]:

$$L_{path} = \left(\frac{\lambda}{4\pi d}\right)^2 \left| 1 + \sum_{n=1}^{N} \Gamma_n \frac{d}{d_n} e^{-jk(d_n - d)} \right|^2 \tag{2.20}$$

In Equation 2.20, d denotes the direct ray path length, Γ_n and d_n represent the reflection coefficient and reflected ray path length, where N is the total number of reflections. In an electromagnetically complex environment, the path loss is generally proportional to d^{-n}. The value of n, which is 2 in free space, may vary between 1 and 4.

Figure 2.15 shows the classical two-ray ground reflection of antenna transmits at 867 MHz at a specified height h [80].

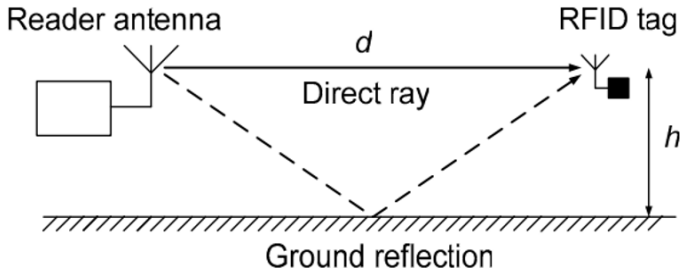

Figure 2.15 Two-ray ground reflection [71].

The magnitude and phase of the ground reflection are dependent on many parameters in the shown two-ray ground reflection case. Wave polarization, incident angle, and ground characteristics are these parameters. Assuming that reflections from the ground are ideal and the antenna is isotropic, the path loss for the 2-ray ground reflection model can be expressed as Equation 2.21 [71]:

$$L_{path} = \left(\frac{\lambda}{4\pi d}\right)^2 \left|1 - \frac{d}{d_1} e^{-jk(d_1 - d)}\right|^2 \tag{2.21}$$

In Equation 2.21, d denotes the distance to the RFID tag from the line-of-sight, and $d_1 = \sqrt{d^2 + (2h)^2}$ is the reflected ray path length. The path loss given by Equation 2.20 is proportional to d^{-4} over long distances.

With the L_{path} the value is given in Equation 2.21 and the transmitted EIRP, the signal power at the tag point can be obtained as Equation 2.22:

$$P_{tag} = P_t G_t L_{path} \tag{2.22}$$

In Equation 2.22, P_t is equal to the RFID reader transmitter's output power, and G_t is the reader antenna's gain. By multiplying these two values, the transmitted EIRP value is obtained (P_tG_t). The signal intensity at the tag location can be perceived as the power absorbed by the RFID chip, which is perfectly matched to the 0 dBi tag antenna.

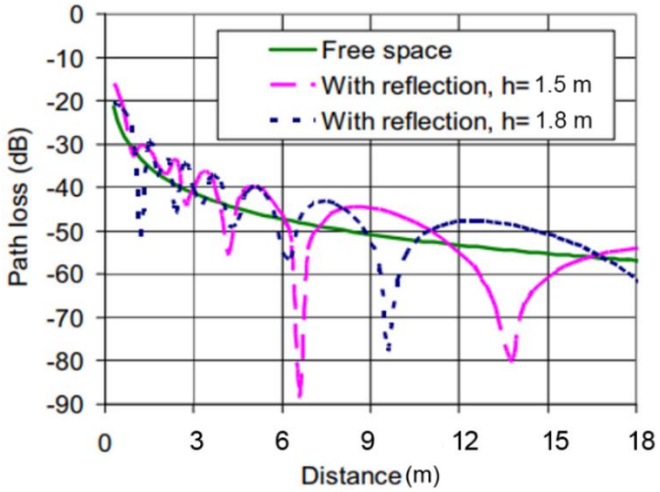

Figure 2.16 Path loss vs. tag read distance for various antenna elevations above the ground in the ground reflection example.

In Figure 2.16, the path loss given by Equation 2.21 is plotted for two separate reader antenna height values above ground. Because of the multipath, it can be observed that the signal sent there would encounter major distance variations. Consider that the RFID reader transmits 4 W EIRP. Also, for theoretical read-range calculations, assume that the above Smartrac Dogbone R6 RFID tag is used.

In order to power up, the Smartrac Dogbone R6 RFID requires an incident signal strength of -20 dBm. This tag's overall reading distance will be reduced to -50 dB of path loss. The path loss of -50 dB correlates, from Figure 2.19, to the full tag range of 8.2 meters in free space. This distance will be increased to 11.2 meters (h=1.5 meters) and 14.6 meters (h=1.8 meters) by the presence of ground reflection, but it can also establish dead zones within that range, leading to places where the path loss drops below -50 dB. For reasons such as multiple reflections, diffractions, etc this case would be quite complicated in a real propagation scenario. The average indoor root mean square delay spread<300 ns is typically not a concern due to the comparatively low data rate of UHF RFID systems, and the communication link between the reader-tag is mainly influenced by the signal power received. Some conditions with low loss propagation will have slightly lower path loss than free space and as a result, significantly longer read distance for tags. An example is a waveguide-like environment where only dominant directions [81,82] are propagated by waves. Remember that every actual propagation environment, no matter how dynamic, is

always symmetrical-the path losses between the two transmitting antennas are identical between the forward and reverse channels. Any calculated asymmetry is typically due to calibration of RF hardware.

2.5.3 Forward and reverse channels

The communication direction of the reader-to-tag is called the forward channel, and the opposite direction as tag-to-reader communication direction is called reverse channel. The forward channel path loss determines the maximum tag reading length in cases where the sensitivity of the RFID reader is too high, while in cases where the sensitivity of the RFID reader is limited, the path loss of the reverse channel determines the maximum tag range. The two channels mentioned are widely studied [76–79] in the literature. The RFID tag can be interpreted in passive UHF RFID systems as an RF source that emits a modulated differential EIRP signal and can be expressed as Equation 2.23 [71]:

$$\Delta EIRP = S\Delta\sigma = P_{tag}G^2K \tag{2.23}$$

In Equation 2.23, *S* denotes the power density of an electromagnetic wave incident on the RFID tag, *G* denotes the gain of the tag antenna, $\Delta\sigma$ is the tag delta radar-cross-section, and *K* is the backscatter modulation loss. In free space, the power density *S* can be calculated by using Equation 2.24 [71]:

$$S = \frac{E^2}{120\pi} \tag{2.24}$$

Where E is the electrical field of the incoming wave. The power of the modulated tag signal obtained by the monostatic reader antenna in an arbitrary propagation condition can be written in differential EIRP as Equation 2.25 [71]:

$$P_r = G_t L_{path} \Delta EIRP \tag{2.25}$$

Equation 2.25 can be interpreted in free space in the form of the classical radar equation, Equation 2.26 [83]:

$$P_r = P_t {G_t}^2 \frac{\lambda^2 \Delta\sigma}{(4\pi)^3 d^4} = P_t {G_t}^2 \left(\frac{\lambda}{4\pi d}\right)^2 G^2 K \quad (2.26)$$

Where the distance to the tag is d. Equation 2.26 is useful for interpreting link budget calculations in RFID systems [65,71,84–87].

2.5.4 Link budget and link margin

In a link budget, the different terms in the aforementioned Friis formula are normally evaluated and tabulated separately; each of these variables can be evaluated separately in terms of their net impact on the power obtained. Besides that, extra loss factors may be included in the link budget, including the line losses, impedance mismatch, atmospheric attenuation, and polarization mismatch. One of the important terms in the link budget is the path loss mentioned earlier, which explains the decrease in signal strength with the distance between transmitter and receiver (see Equation 2.20). The path loss depends on the wavelength (frequency), which is normalization for units of distance. Using the Friis equation, the link budget for an RFID system can generally be written as follows in Table 2.4:

Table 2.4 Link budget terms in Friis equation

Receive Power	P_r
"Transmit antenna line loss"	(-)L_t
"Transmit antenna gain"	G_t
"Path loss"	(-)L_p
"Atmospheric attenuation"	(-)L_A
"Receive antenna gain"	G_r
"Receive antenna line loss"	(-)L_r
"Transmit Power"	P_t

Assuming all terms are in dB or dBm, the received power can be expressed as Equation 2.27:

$$P_r(dBm) = P_t - L_t + G_t - L_p - L_A + G_r - L_r. \quad (2.27)$$

Also if transmit and/or receive antennas is not perfectly impedance matched, impedance mismatch will reduce the received power by the factor of 1- $|\Gamma|^2$, where Γ

is the appropriate reflection coefficient. The resulting impedance mismatch loss as Equation 2.28,

$$L_{imp}(dB) = -10\log(1 - |\Gamma|^2) \geq 0, \quad (2.28)$$

can be included in the link budget to account for reduction in received power. The polarization matching of the transmit and receive antennas is another potential entry in the link budget, as maximum power transmission among the transmitter-receiver requires both antennas to be polarized in the same manner. For example, if a transmit antenna is vertically polarized, maximum power is delivered only to a vertically polarized receiving antenna, while zero power is delivered to a horizontally polarized receiving antenna and half of the available power is delivered to a circularly polarized receiving antenna.

The obtained power level should be higher in communication systems than the threshold needed for the minimum acceptable standard of service (usually expressed as the minimum carrier-to-noise ratio (CNR) or minimum SNR). The link margin is referred to as this design allowance for the received power and can be expressed as the difference between the design value of the received power and the minimum threshold value of the receiving power, as Equation 2.29:

$$Link\ margin(dB) = LM = P_r - P_r(min) > 0 \quad (2.29)$$

Where all quantities are in dB.

The link margin has to be a positive value varying between 3-20 dB. Having an appropriate link margin is critical against signal fading due to weather, mobile phone users, problems with the multipath propagations, and other unforeseeable factors that may degrade the performance of the system. Link margin that is used to account for fading effects is sometimes referred to as the *fade margin*. Link budget and link margin can be enhanced by increasing received power or by decreasing threshold power. However, in this case, it is necessary to make many swaps, such as increasing the

antenna gain and improving the receiver. Trying to increase the link margin too much is often avoided as it adds cost and complexity.

The following graphs show the relationship between maximum RFID tag distance with different parameters and different situations. Green dots in the graphics indicate the distances where the RFID tag can be defined, while the red dots indicate the distances that cannot be defined. G_t value on the figures indicates reader antenna gain, G_r value tag antenna gain, EIRP reader power, ML modulation loss, L_t and L_r cable induced losses, L_a atmospheric loss, and PL path loss. For better understanding the factors that affect the tag range, these values have also been taken into consideration, along with the chip sensitivity of the RFID tag and the sensitivity of the RFID reader. In Figure 2.17, RFID reader sensitivity has been taken as -84 dBm, tag chip sensitivity as -20 dBm, G_t 8 dB, Gr 2 dB, L_t, and L_r -6.4 dB. In this case, the theoretical maximum RFID tag distance is approximately 18 meters.

In Figure 2.18, reader sensitivity is -84 dBm; tag sensitivity is -12 dBm, G_t 2 dB, G_r 2 dB; in this case, the RFID tag cannot be identified theoretically. In Figure 2.19, unlike Figure 2.18, the G_t value is 4 dB; in this case, the maximum distance that the RFID tag can be read is 2 meters. In Figure 2.20, the G_t value is taken as 8 dB, and in Figure 2.21, the G_t value is taken as 10 dB, and the maximum reading distances are 6 and 12 meters, respectively. Figure 2.22 and Figure 2.23 have been created with the RFID reader sensitivity as -70 dBm. Many parameters are taken into consideration in the calculation of the link budget. In order for the RFID tag to be identified consistently, the signal from the reader must be greater than the tag chip sensitivity, and the signal returned to the reader must be greater than the reader sensitivity. As a result, there are many limitations in the definition of an RFID tag. A tag with very high chip sensitivity, although very high gain, cannot be identified, and a tag with very good chip sensitivity cannot be identified by a high sensitivity RFID reader. The high and low sensitivity concepts mentioned for sensitivity are in dBm.

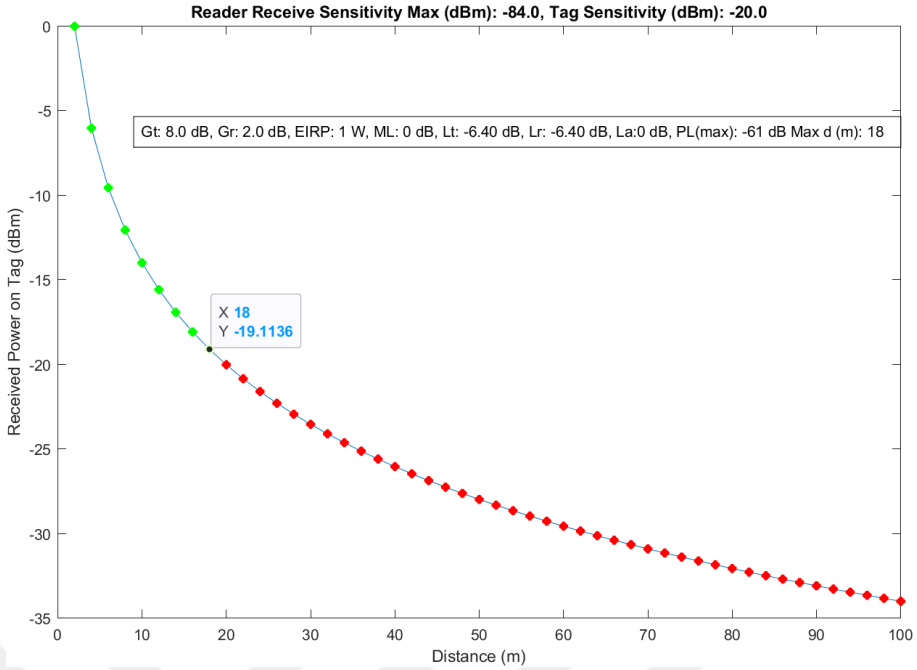

Figure 2.17 Received Power on Tag vs Distance (m) (Reader Receive Sensitivity Max (dBm): -84.0, Tag Sensitivity (dBm): -20.0 G_t: 8.0 dB, G_r: 2.0 dB, EIRP: 1 W, ML: 0 dB, L_t: -6.40 dB, L_r: -6.40 dB $P_{L(max)}$: -61 dB Max d (m): 18).

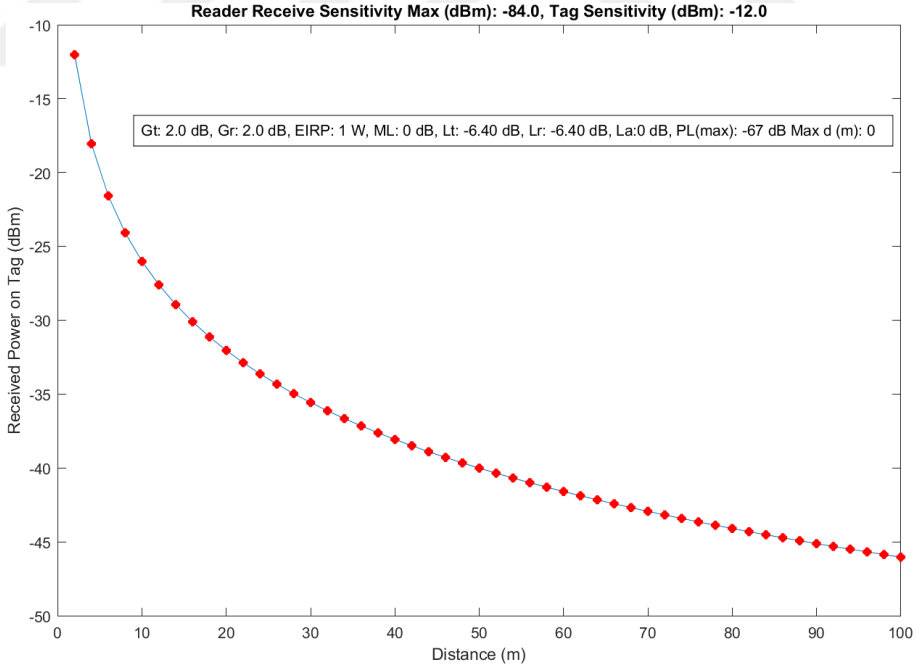

Figure 2.18 Received Power on Tag vs Distance (m) (Reader Receive Sensitivity Max (dBm): -84.0, Tag Sensitivity (dBm): -12.0 G_t: 2.0 dB, G_r: 2.0 dB, EIRP: 1 W, ML: 0 dB, L_t: -6.40 dB, L_r: -6.40 dB $P_{L(max)}$: -67 dB Max d (m): 0).

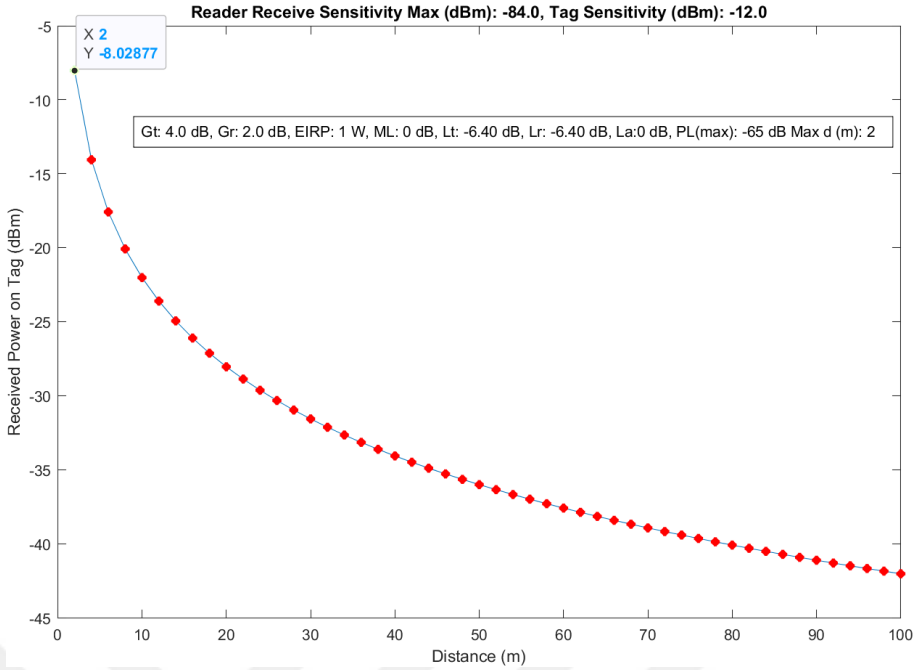

Figure 2.19 Received Power on Tag vs Distance (m) (Reader Receive Sensitivity Max (dBm): -84.0, Tag Sensitivity (dBm): -12.0 G_t: 4.0 dB, G_r: 2.0 dB, EIRP: 1 W, ML: 0 dB, L_t: -6.40 dB, L_r: -6.40 dB $P_{L(max)}$: -65 dB Max d (m): 2).

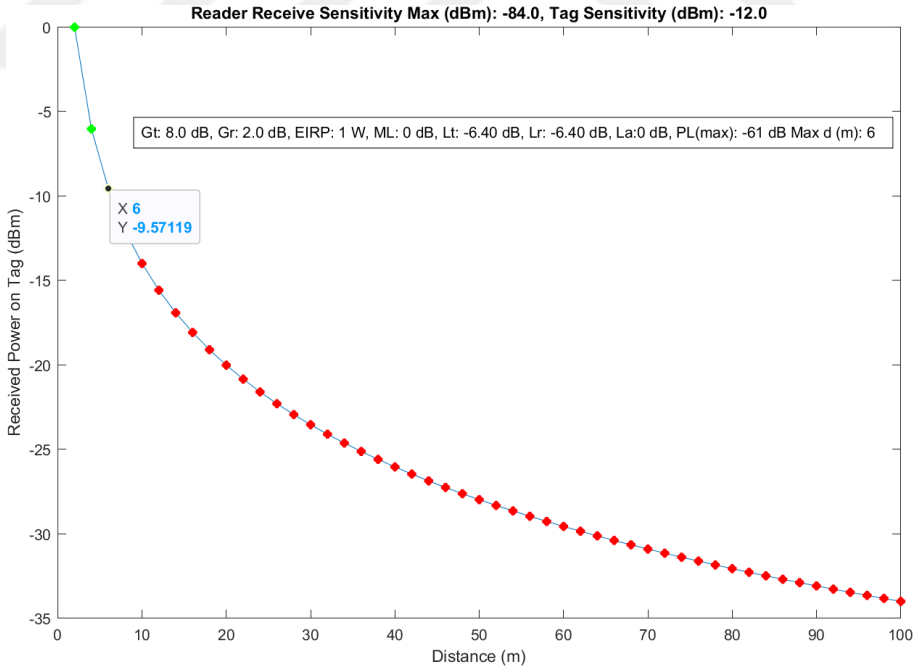

Figure 2.20 Received Power on Tag vs Distance (m) (Reader Receive Sensitivity Max (dBm): -84.0, Tag Sensitivity (dBm): -12.0 G_t: 8.0 dB, G_r: 2.0 dB, EIRP: 1 W, ML: 0 dB, L_t: -6.40 dB, L_r: -6.40 dB $P_{L(max)}$: -61 dB Max d (m): 6).

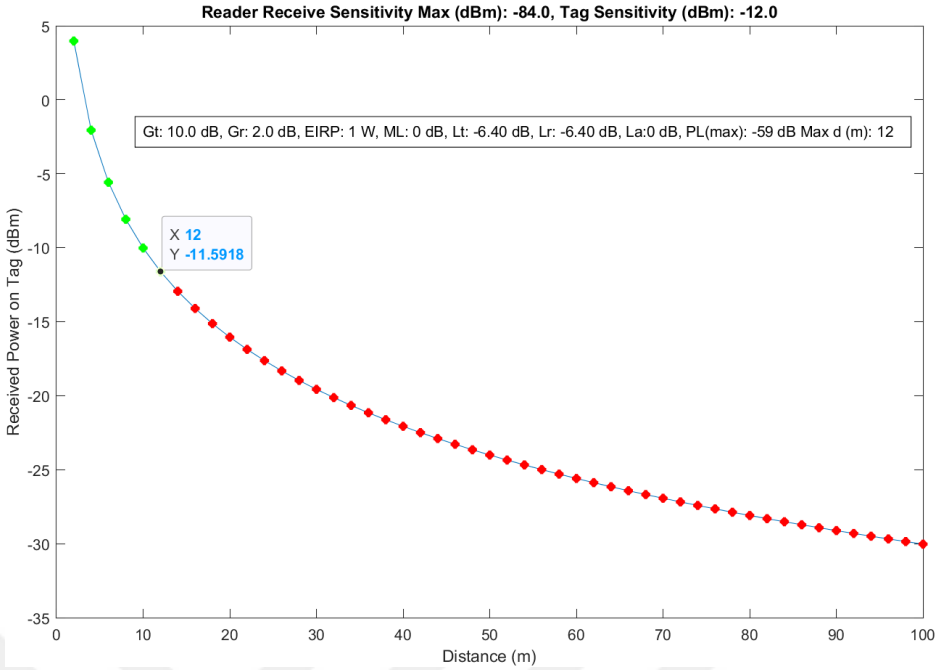

Figure 2.21 Received Power on Tag vs Distance (m) (Reader Receive Sensitivity Max (dBm): -84.0, Tag Sensitivity (dBm): -12.0 G_t: 10.0 dB, G_r: 2.0 dB, EIRP: 1 W, ML: 0 dB, L_t: -6.40 dB, L_r: -6.40 dB $P_{L(max)}$: -59 dB Max d (m): 12).

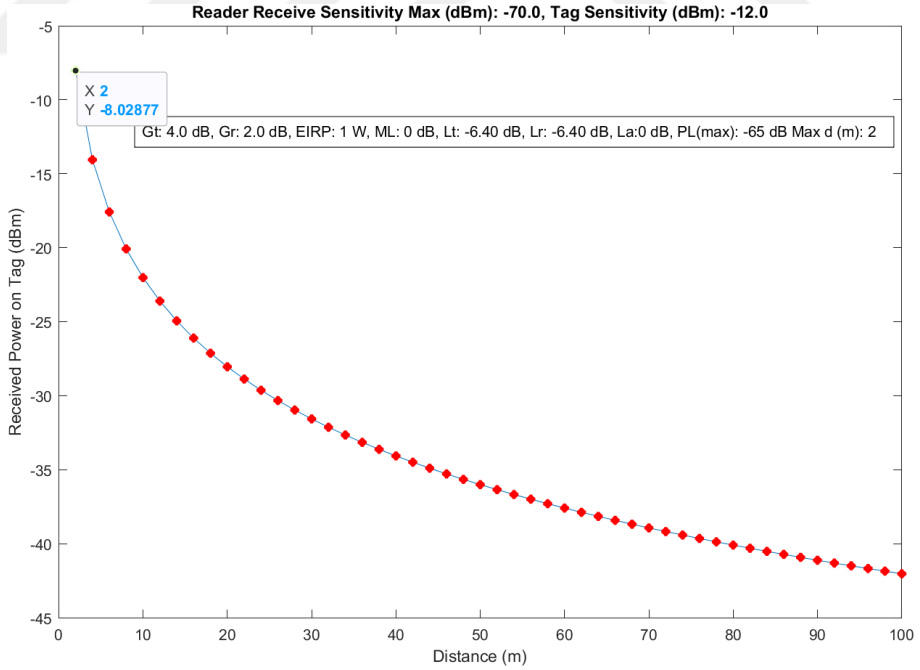

Figure 2.22 Received Power on Tag vs Distance (m) (Reader Receive Sensitivity Max (dBm): -70.0, Tag Sensitivity (dBm): -12.0 G_t: 4.0 dB, G_r: 2.0 dB, EIRP: 1 W, ML: 0 dB, L_t: -6.40 dB, L_r: -6.40 dB $P_{L(max)}$: -65 dB Max d (m): 2).

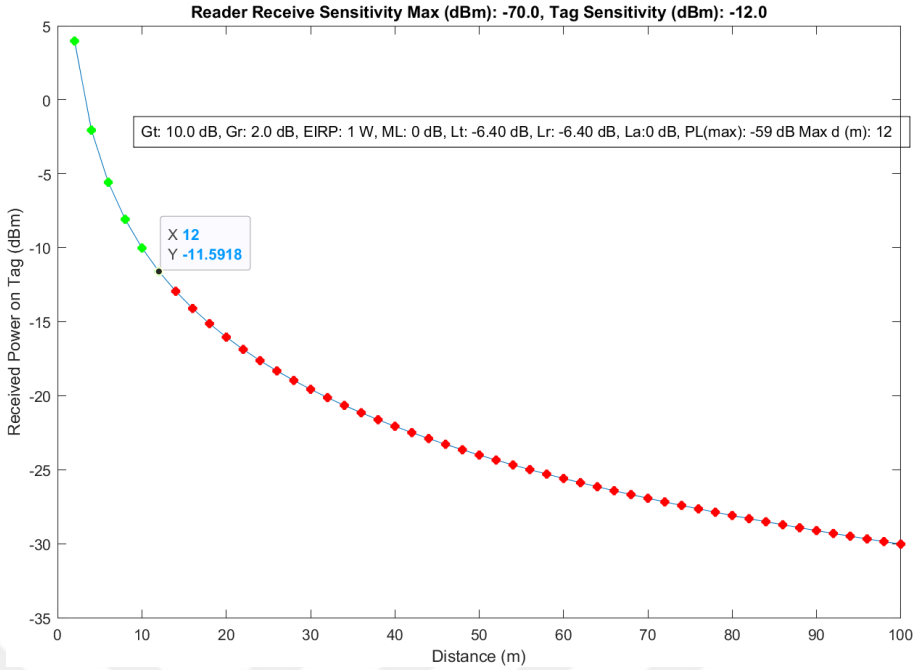

Figure 2.23 Received Power on Tag vs Distance (m) (Reader Receive Sensitivity Max (dBm): -70.0, Tag Sensitivity (dBm): -12.0 G_t: 10.0 dB, G_r: 2.0 dB, EIRP: 1 W, ML: 0 dB, L_t: -6.40 dB, L_r: -6.40 dB $P_{L(max)}$: -67 dB Max d (m): 12).

3. RFID ANTENNA AND SYSTEM DESIGN FOR SMART MARBLE FACTORY ENVIRONMENTS

3.1 Determining UHF RFID Antenna Parameters

RFID reader antennas play a vital role in RFID systems. The reader antenna performance parameters, such as reflection coefficient, gain, directivity, etc., directly and mainly affect the overall performance of the system. While measuring the field performance of RFID systems, the antenna tag reading distance, the total number of reads of the tag, and the receiving signal strength (RSSI) values have been examined. Based on these values, a conclusion can be drawn about the antenna performance within the system. In general, if the antenna tag chip will not be used for EPC writing, it is desirable that the antenna's communication distance be long. The longer the reading distance, the more objects can be identified. However, the long reading distance alone is not a sufficient criterion for the antenna to be considered as working with high performance. The antenna's directivity and polarization is also an important factor in the number of objects to be identified. Different conditions become essential depending on the environment where the RFID system will be used and different scenarios. In cases such as parking lot entrance systems, the antenna needs to read from a very long distance, but the number of objects to be defined is not very important according to different scenarios. In order to open the parking gates, it is sufficient to define the vehicle that will enter the parking lot at that moment. In such cases, it would be more reasonable to use high gain antennas with linear polarization. However, when the RFID system is desired to be used in cases such as warehouses and sales areas with many stacked products, it will be more appropriate to use circularly polarized antennas as it will be necessary to identify products that are not directly in the antenna's line of sight.

Since there will be an RFID system to be designed to work in smart factories in this study, it is necessary to design an RFID antenna suitable for the environment and scenarios to be used. The factory environment is an electromagnetically complex environment due to its structure. There are many different mechanisms and systems, especially in factories that manufacture and process products. Most of the products contain metal components, and electromagnetic waves reflect in metal environments, and these reflections make it difficult for the RFID system to operate in this complex environment. For this reason, these issues should be taken into consideration while designing the antenna. To carry out the study, firstly, the antennas found in the academic literature and used commercially have been examined. Simulation results of these antennas and measurement results in sample scenarios are presented in detail. in sections 3.2 and 3.3, together with the designed antenna and developments.

3.2 UHF RFID Antenna Design Considerations for Smart Factory Environments

In simulation studies, reflection coefficients, far-field directivity, and gain values of RFID antennas have been examined. While analyzing the performance of RFID antennas, the first commercially available Litum 7.5 dBic RFID antenna [88] has been redesigned and examined in the CST Studio Suite environment. The antenna's gain value is given as 7.5 dBi, operating frequency 865-870 MHz, physical dimensions 190x190x30 mm. This antenna, which has an acceptable gain value and circular polarization, can be used in many applications. Simulation studies have been carried out again to see the commercial antenna's performance analysis with other antennas in the simulation environment. The necessary designs have been made by analyzing the internal structure of the purchased antenna. When the structure of the antenna has been examined, it has been seen that it has been designed as a patch antenna on the reflector structure. The inverted E openings in the patch part affect circular polarization. While designing, FR-4 has been used as the antenna substrate, and copper plate with 0.5 mm thickness has been used for the ground plane.

The front, back, and perspective view of the antenna, together with the image taken from the site of the Litum company, have been given in Figure 3.1.

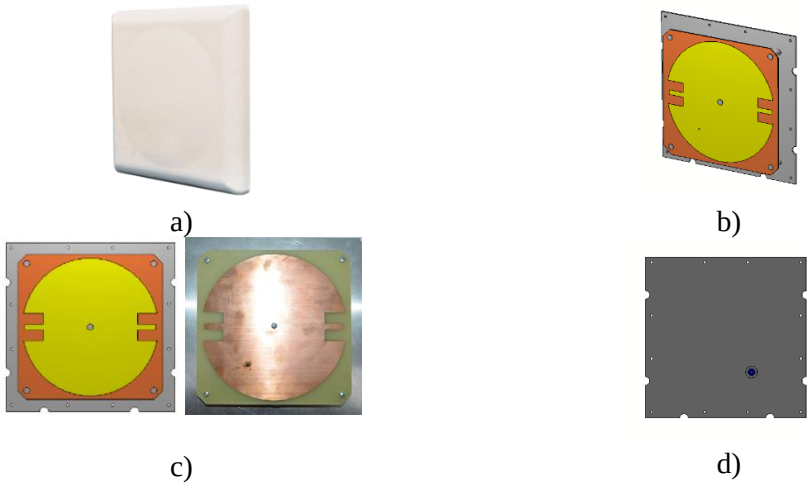

Figure 3.1 a) Image taken from Litum's website [88], b) Perspective view of commercial antenna, c) Front view of Commercial antenna, d) Back view of commercial antenna.

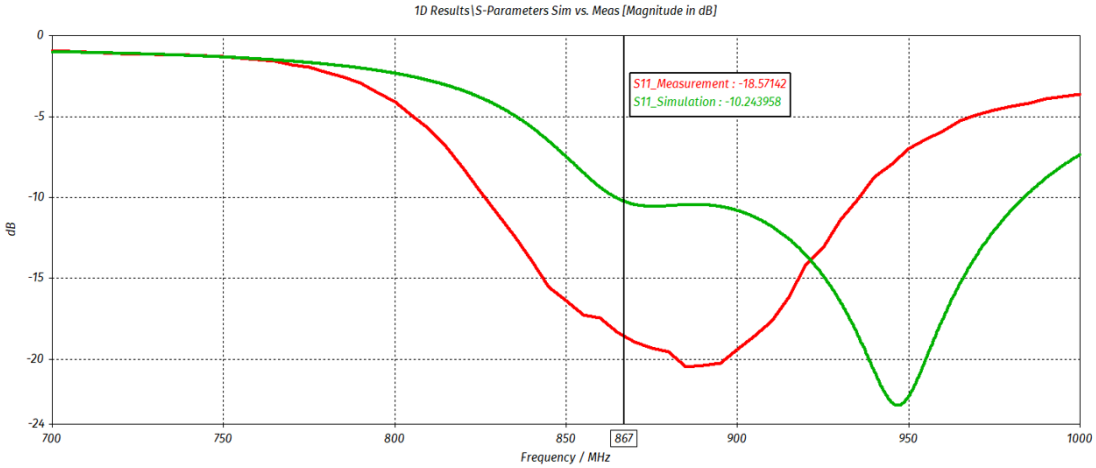

Figure 3.2 S_{11} simulation vs. measurement results of commercial antenna.

Table 3.1 Bandwidth, Resonant Frequency, and S_{11} value at 867 MHz of commercial antenna.

	Bandwidth	**Resonant Frequency**	**S_{11} @867 MHz**
Simulation	864-982 MHz (118 MHz)	946.9 MHz	-18.57 dB
Measurement	826-935 MHz (109 MHz)	885 MHz	-10.24 dB

When the S11 simulation and measurement results in Figure 3.2 of the antenna have been examined, it is seen that with some differences, both results confirm that the antenna operates at 867 MHz and RFID band. When the measurement results in Table

3.1 have been examined, the antenna has an S_{11} value of -10.24 dB at 867 MHz and a bandwidth of 109 MHz. The resonance frequency of the antenna is 885 MHz. However, when examining the simulation studies, it is not correct to make a definite conclusion about the operation of the antenna only from the S_{11} results. S_{11} results alone do not provide sufficient information about the performance of the antenna. It is not enough for the antenna to operate at the specified frequency. The far-field results of the antenna at that frequency should be examined, and more detailed information about its performance should be obtained. For this reason, the far-field results of the antenna should be examined in detail. In Figure 3.3, the antenna's gain, directivity, and other far-field results at different angles have been presented in detail.

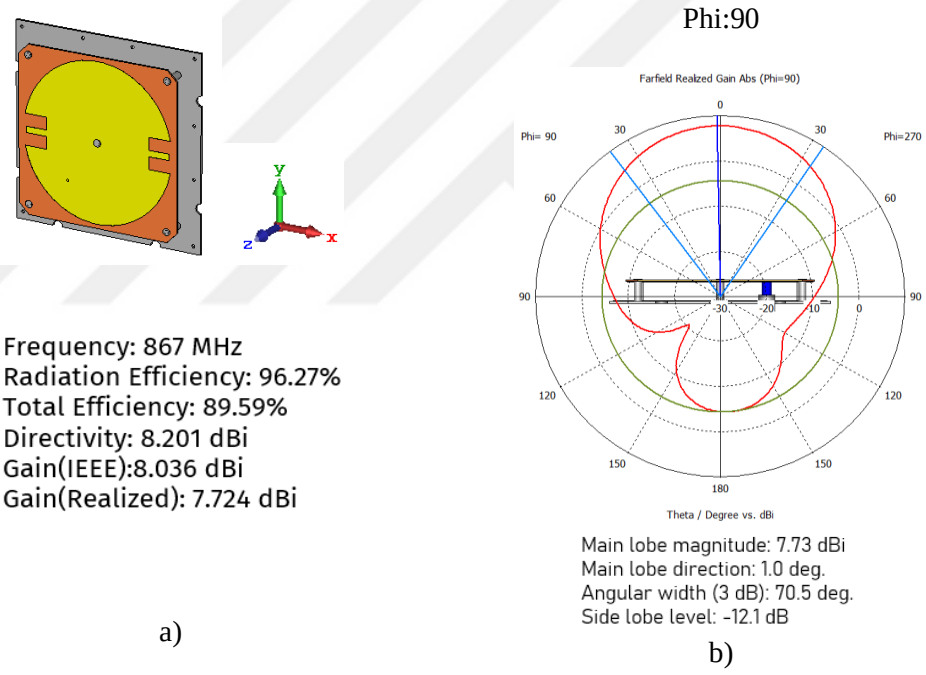

Figure 3.3 The 2D and 3D radiation patterns of commercial RFID antenna at the resonance frequency of 867 MHz: a) Design and coordinate system, b) X-Y plane, c) X-Z plane, d) Y-Z plane, and e) 3D results.

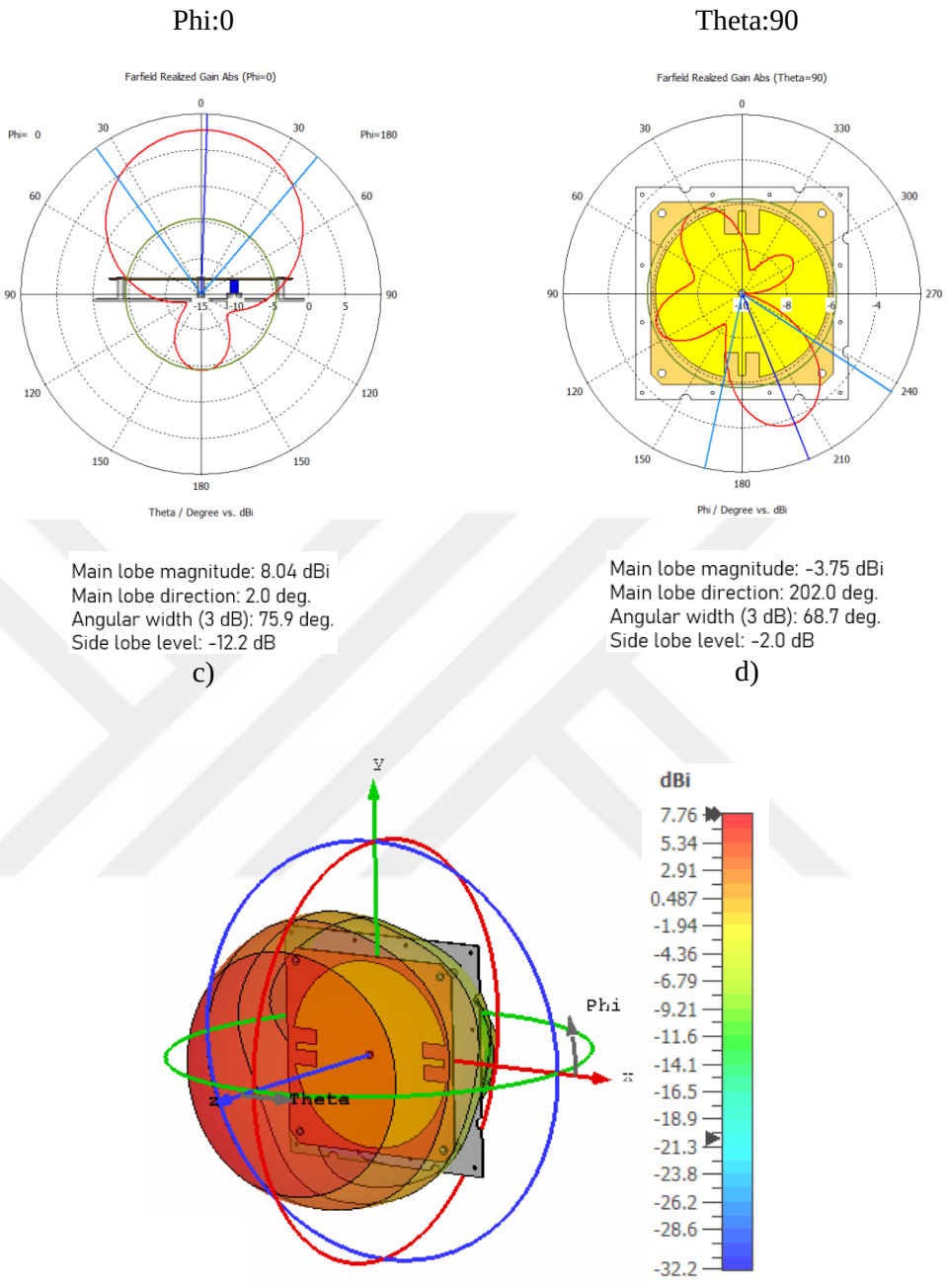

Figure 3.3 (cont.) The 2D and 3D radiation patterns of commercial RFID antenna at the resonance frequency of 867 MHz: a) Design and coordinate system, b) X-Y plane, c) X-Z plane, d) Y-Z plane, and e) 3D results.

The far-field results show that the antenna has a gain of 7.72 dBi and a directionality value of 8.20 dBi. At the same time, the radiation pattern of the antenna at Phi = 90,

Phi = 0 and Theta = 0 degrees is given. In addition to all these values, the commercial antenna has an efficiency value of 89.59%. After examining the commercial antenna, simulation and realization studies of the half e-shaped antenna with circular polarization found in the academic literature which design by Li et al. [6] have been carried out. The E-shaped antenna consists of three simple parts:

- Modified half E-shaped patch,
- Corner truncated square patch,
- Four rotated metallic plates on the edge of the ground plane

Antenna dimensions are 150x150x25 mm, and different views of the half e-shaped antenna are given in Figure 3.4.

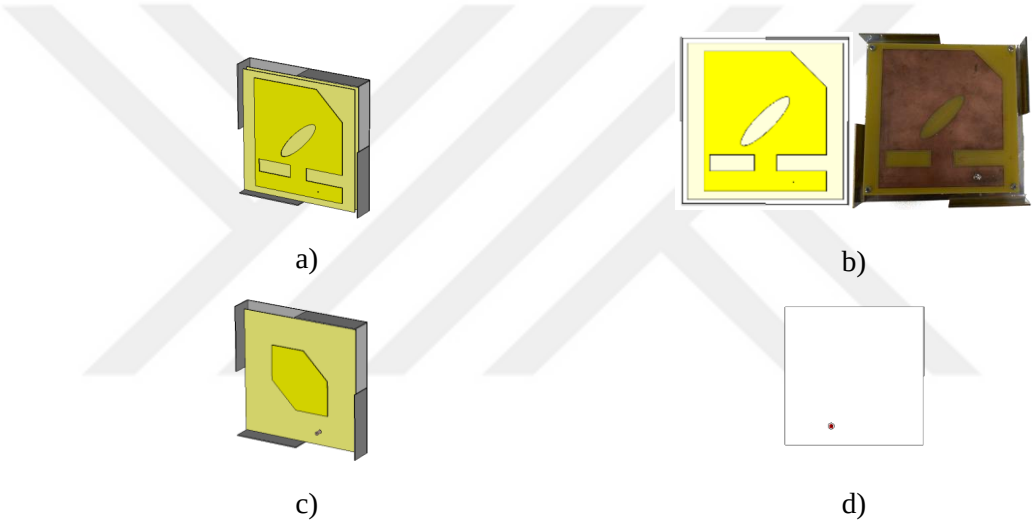

Figure 3.4 a) Perspective view of Half E-Shaped antenna, Front view of Half E-Shaped antenna, c) Perspective view of near field resonant parasitic, Back view of Half E-Shaped antenna.

S_{11} simulation and measurement results also confirm that the antenna operates at 867 MHz and RFID band like commercial antenna. When the measurement results in Table 3.2 have been examined, the antenna has an S_{11} value of -12.69 dB at 867 MHz and a bandwidth of 100 MHz. In Figure 3.6, the antenna's gain, directivity, and other far-field results at different angles have been presented in detail.

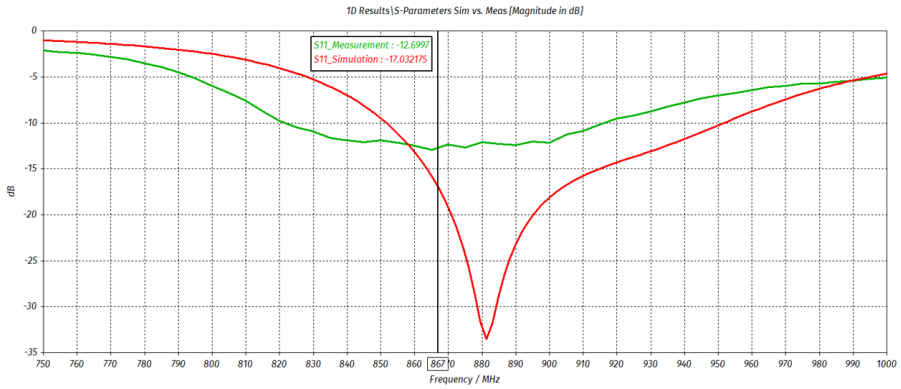

Figure 3.5 S_{11} simulation vs. measurement results of Half E-Shaped antenna

Table 3.2 Bandwidth, Resonant Frequency, and S_{11} value at 867 MHz of Half E-Shaped antenna.

	Bandwidth	**Resonant Frequency**	**S_{11} @867 MHz**
Simulation	821-915 MHz (94 MHz)	881.25 MHz	-17.03 dB
Measurement	850-950 MHz (100 MHz)	865 MHz	-12.69 dB

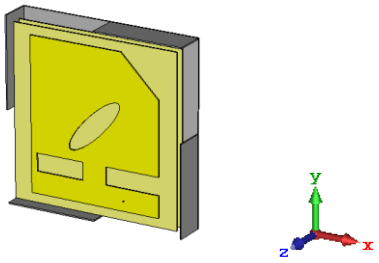

Frequency: 867 MHz
Radiation Efficiency: 95.67%
Total Efficiency: 93.05%
Directivity: 7.332 dBi
Gain(IEEE):7.140 dBi
Gain(Realized): 7.019 dBi

a)

Phi:90

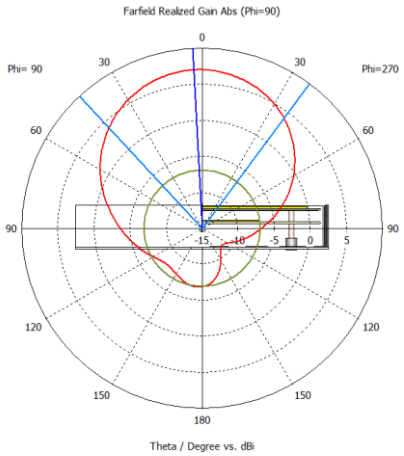

Main lobe magnitude: 7.02 dBi
Main lobe direction: 3.0 deg.
Angular width (3 dB): 79.2 deg.
Side lobe level: -13.9 dB

b)

Figure 3.6 The 2D and 3D radiation patterns of half e-shaped RFID antenna at the resonance frequency of 867 MHz: a) Design and coordinate system, b) X-Y plane, c) X-Z plane, d) Y-Z plane, and e) 3D results.

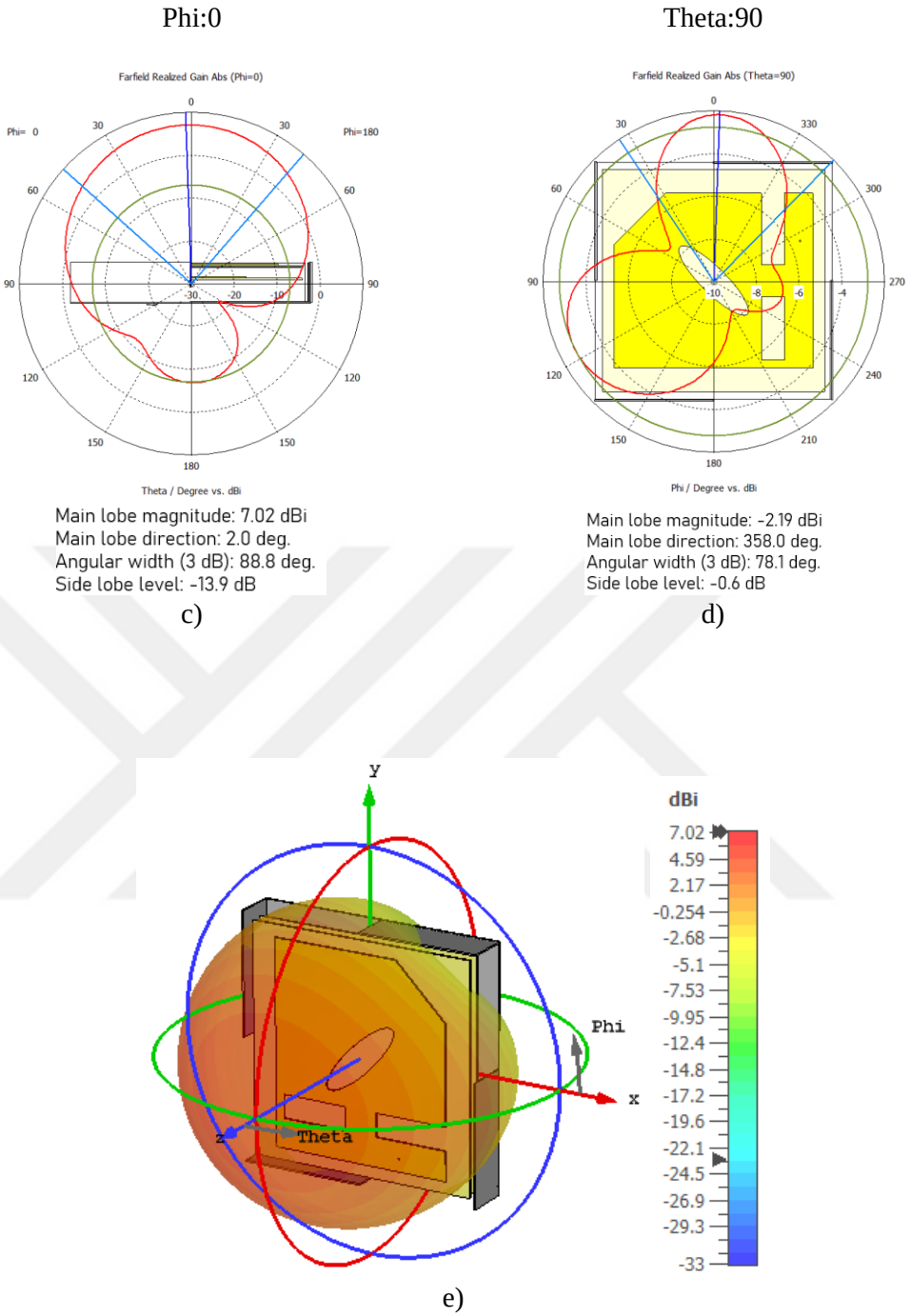

Figure 3.6 (cont.) The 2D and 3D radiation patterns of Half E-shaped RFID antenna at the resonance frequency of 867 MHz: a) Design and coordinate system, b) X-Y plane, c) X-Z plane, d) Y-Z plane, and e) 3D results.

The far-field results show that the antenna has a gain of 7.01 dBi and a directionality value of 7.33 dBi. At the same time, the radiation pattern of the antenna at Phi = 90, Phi = 0 and Theta = 0 degrees is given. In addition to all these values, the half e-shaped

antenna has an efficiency value of 93.05%. Upon examining the commercial antenna and the antenna taken as an example from the academic literature, it has been studied on the design of a high-gain, compact, and circular polarization antenna that can be used in smart factories. Along with classical design methods, developments on different antennas found in the academic literature, design stages, methods that can be used to achieve circular polarization have been examined.

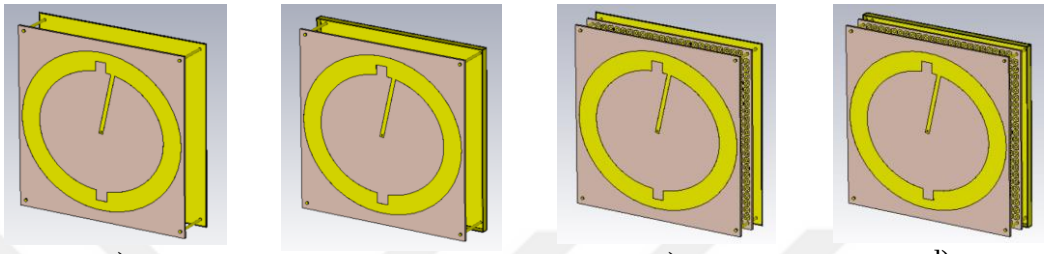

Figure 3.7 Design stages of antenna a) Patch + Flat Ground, b) Patch + Truncated Ground c) Patch + AMC + Flat Ground, d) Patch + AMC + Truncated Ground.

There are many versions at the antenna design stages. In the antenna design process, the radiating part is a standard patch structure, and the reflector part is flat Figure 3.7a. When the results of this structure have been examined, it has been seen that it has a 4.68 dBi gain value and 14.2 dB axial ratio at 867 MHz. In order to achieve circular polarization, the axial ratio must be below 3 dB. There is a requirement that the antenna to be designed must be of circular polarization. Because the products to be identified in the factory environment to be used will not always be found in the direct line of sight of the antenna. Also, the antenna gain value should be increased because the reading distance of the antenna will increase with the gain. For this reason, many improvements have been made to the antenna after the first version. The first improvement has been bending the metal reflector part in Figure 3.7b. After bending the reflector, the antenna gain has been decreased, but the axial ratio has been increased. This improvement has not been enough for the requirements for a smart factory. For increasing the gain value of the antenna, a middle layer has been added to the design. This middle layer acts as an artificial magnetic conductor (AMC) in Figure 3.7c. First, this structure has been tried with flat ground. AMC structure is not suitable for requirements with the flat ground because it has low gain and a higher than 3 dB axial ratio. Because the gain value has been decreased to 3.70 dBi, and the axial ratio

has been increased to 11.70 dB. For this reason, in the fourth and final design in Figure 3.7d with clock shaped patch, AMC and corner truncated ground have been used. In this case, also can be seen in Table 3.3, the antenna has a 6.70 dBi gain value and 2.4 dB axial ratio. It can be said that the antenna has a high gain for its dimensions; also antenna is circularly polarized. The dimensions of the antenna are 130x130x30 mm. Also, the s-parameters of each antenna design have been shown in Figure 3.8.

Table 3.3 Gain, Directivity, Axial Ratio values for different design stages.

	Patch + Flat Ground	**Patch + Truncated Ground**	**Patch + AMC + Flat Ground**	**Patch + AMC + Truncated Ground**
Gain	4.68 dBi	4.2 dBi	3.7 dBi	6.7 dBic
Directivity	6.4 dBi	5.2 dBi	4.4 dBi	7.15 dBic
Axial Ratio	14.2 dB	3.1 dB	11.7 dB	2.4 dB

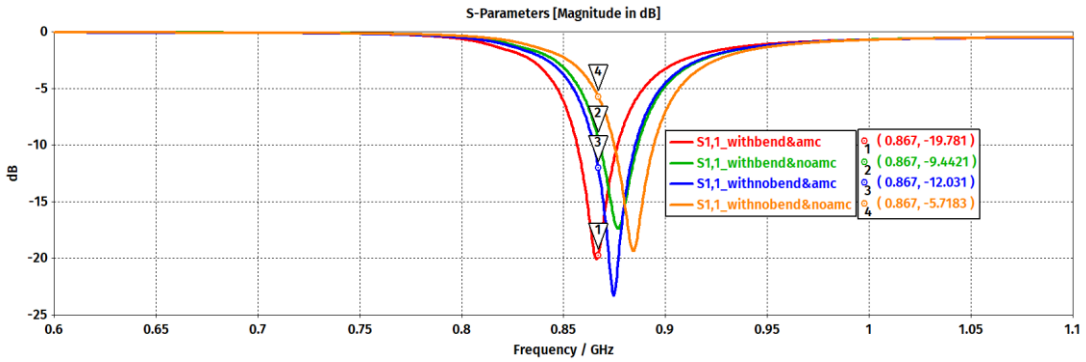

Figure 3.8 S-parameters of different design stages of Clock-Shaped antenna.

In Table 3.3, different design structures' gain, directivity, and axial ratio results have been shown. When examining Table 3.3, the most suitable option for smart factories has been the fourth design. After these design steps, the antenna has been produced with a printed circuit board machine. Then the reflection coefficient values of this antenna have been measured. Different views of the antenna have been shown in Figure 3.9. The detailed results about the antenna have been shown in Figure 3.10, Table 3.4, and Figure 3.11. In Figure 3.10, simulated and measured reflection

coefficient values have been shown. Bandwidth, resonant frequency, and S_{11} value at 867 MHz of the antenna can be seen in Table 3.4. The detailed far-field results of the antenna have been shown in Figure 3.11.

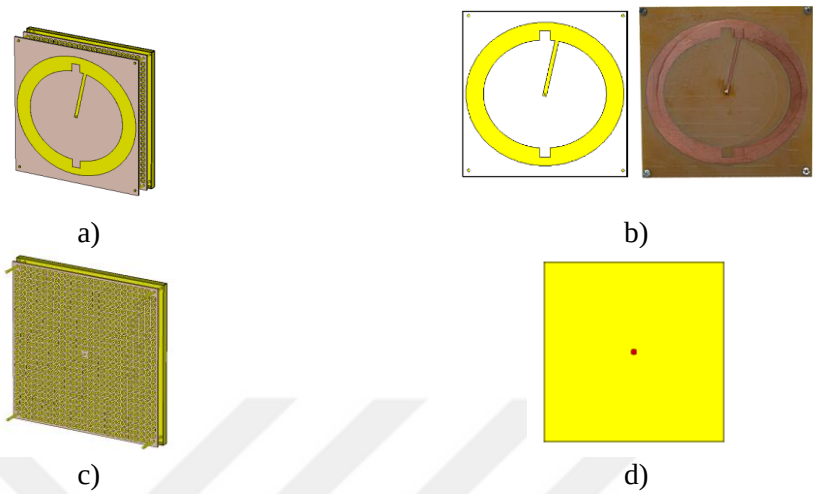

Figure 3.9 a) Perspective view of Clock Shaped antenna, b) Front view of Clock Shaped antenna, c) Perspective view of middle layer, d) Back view of Clock Shaped antenna.

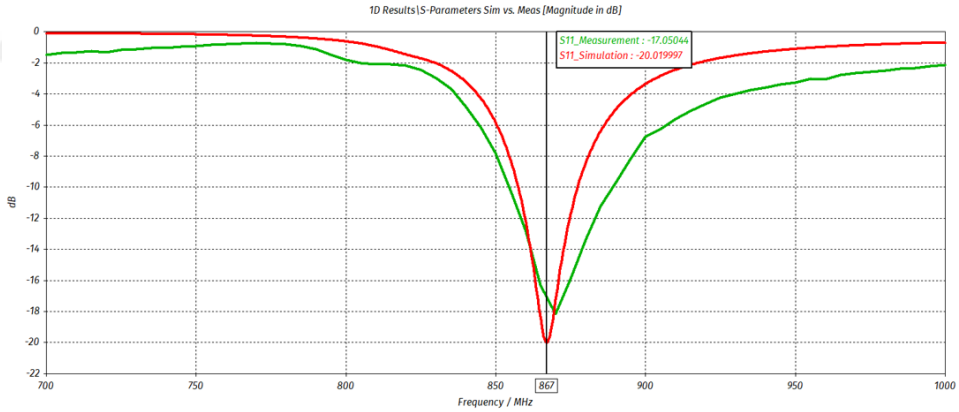

Figure 3.10 S_{11} simulation vs. measurement results of Clock Shaped Antenna.

Table 3.4 Bandwidth, Resonant Frequency, and S_{11} value at 867 MHz of Clock Shaped antenna.

	Bandwidth	**Resonant Frequency**	**S_{11} @867 MHz**
Simulation	857-877 MHz (20 MHz)	867 MHz	-20.02 dB
Measurement	854-888 MHz (34 MHz)	870 MHz	-17.05 dB

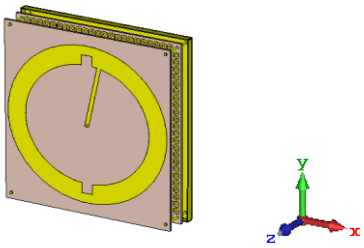

Frequency: 867 MHz
Radiation Efficiency: 90.56%
Total Efficiency: 90.25%
Directivity: 7.155 dBi
Gain(IEEE): 6.724 dBi
Gain(Realized): 6.710 dBi

a)

Phi:90

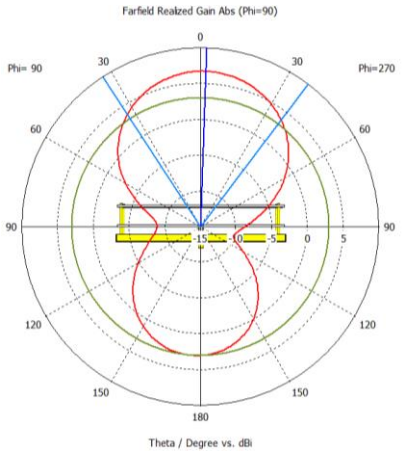

Main lobe magnitude: 7.02 dBi
Main lobe direction: 3.0 deg.
Angular width (3 dB): 79.2 deg.
Side lobe level: -13.9 dB

b)

Phi: 0

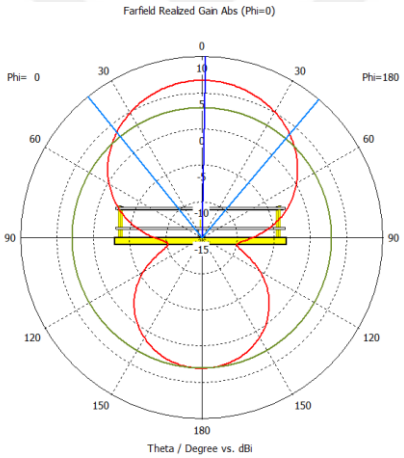

Main lobe magnitude: 6.71 dBi
Main lobe direction: 1.0 deg.
Angular width (3 dB): 79.1 deg.
Side lobe level: -3.7 dB

c)

Theta:0

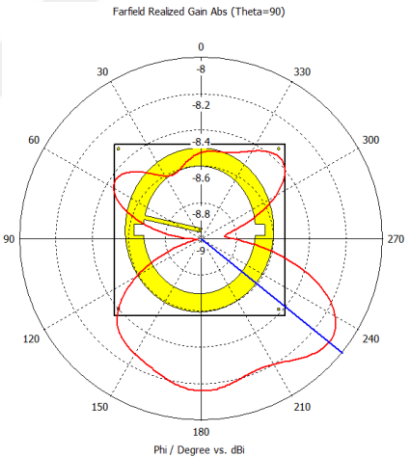

Main lobe magnitude: -8.1 dBi
Main lobe direction: 231.0 deg.

d)

Figure 3.11 The 2D and 3D radiation patterns of clock-shaped RFID antenna at the resonance frequency of 867 MHz: a) Design and coordinate system, b) X-Y plane, c) X-Z plane, d) Y-Z plane, and e) 3D results.

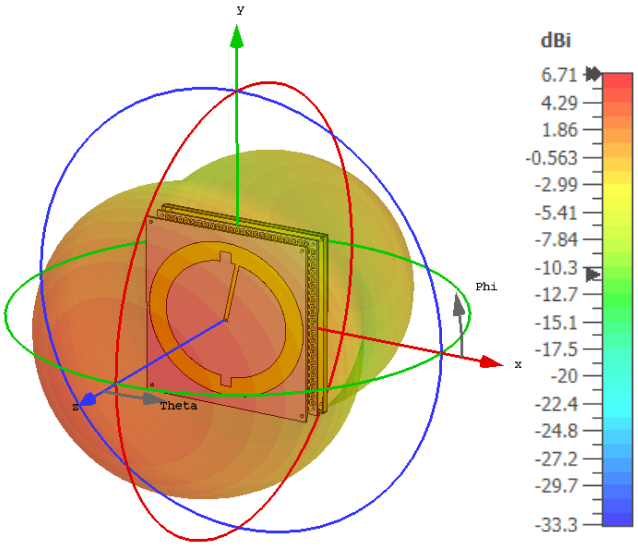

e)

Figure 3.11 (cont.) The 2D and 3D radiation patterns of clock-shaped RFID antenna at the resonance frequency of 867 MHz: a) Design and coordinate system, b) X-Y plane, c) X-Z plane, d) Y-Z plane, and e) 3D results.

The final design has a 6.70 dBi gain, 2.40 dB axial ratio. These simulation and measurement studies are only covered the S_{11} values and far-field results. For evaluating the antenna performance in an RFID system, different measurement methods have been taken into account. The application field of the RFID system is the marble factory. So simulation and measurement studies have been applied to marble blocks. For demonstrating the environment, the sliced marble blocks by 25x25x30 mm have been used on the desk in laboratory. Smartrac Dogbone R6 RFID tags have been attached to marble blocks, and their Electronic Product Codes (EPC) have been written to the tags. The reason for choosing Smartrac Dogbone R6 has been explained in section 3.4, and the different measurement methods and their results have been explained in section 3.3.

3.3 Measurement Results of RFID Antennas

For testing and benchmarking RFID antennas, different scenarios have been implemented in the RFID laboratory. An RFID system is a system that can be affected by environmental and material conditions. For different materials to be identified, different systems have to be used. Metal environments are electromagnetically complex environments due to their characteristics. Electromagnetic waves reflect from

metal environments. This reflection cause interferences and the object which wanted to identify cannot identify because of the reflection. This is an issue to solve in RFID systems, but first, the antennas have been tested for marble blocks. A marble is a dielectric material, so identifying marble is easier than metal objects. However, in smart factory environments, there are not always dielectric objects. So, different scenarios about different materials have been implemented in the RFID laboratory for benchmarking RFID antennas.

For simulating RFID system behaviors on marble, the material properties of marble have to be known. The **dielectric constant** is a measure of the amount of electric potential energy in the form of induced polarization stored in a given volume of material under the action of an electric field. It is essential to know this value for simulating RFID tags with marbles because electromagnetic simulators usually do not default.

For this reason, research has been done on the dielectric properties of marble. As a result of this research, in the study conducted by Arnold H. Scott, it has been concluded that the dielectric constant is different according to the type of marble and its dry or wet feature [89]. While doing the simulations, the dielectric constant of the marble was taken as 8.3. However, since this value will change for different marble types, the simulation and measurement results will also be different when using different marbles.

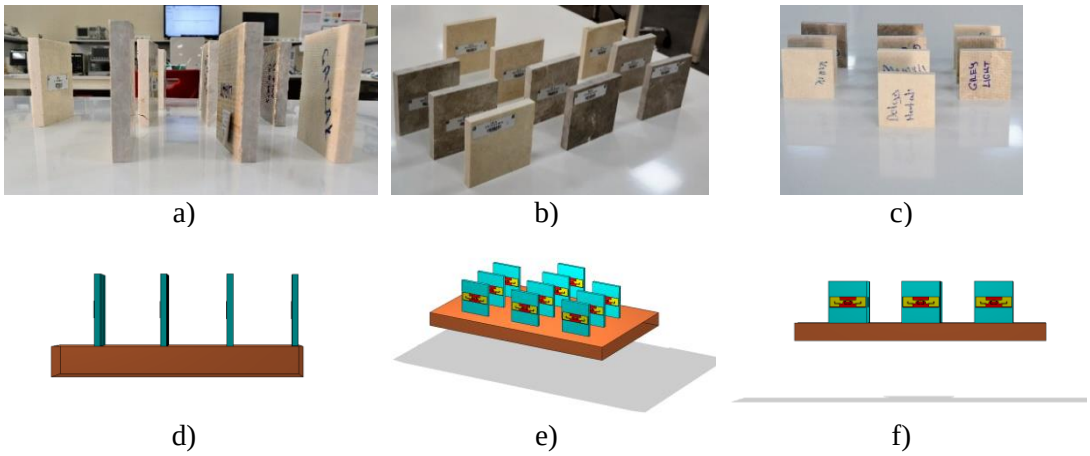

Figure 3.12 Marble orientations on the desk a) Side view, b) Perspective view, c) Back view, d) Sim. side view, e) Sim. perspective view, f) Sim back view.

First of all, each of the marbles has been tagged with Smartrac Dogbone R6 RFID Figure 3.12. The marbles have been placed on the desk with a 10 cm gap between them. While performing antenna performance tests, it has been checked whether the RFID tags on the marble have been read at different distances and different power levels. Impinj brand Speedway R420 RFID reader has been used during the tests. On the graphical interface named ItemTest provided by the reader, the reader's power level can be adjusted according to different antenna ports. The interface reports the RFID tag's minimum, maximum, average RSSI value, phase angle value, first reading, last reading time, and the number of reads. RSSI values and tag reads have been included in antenna performance tests. Antenna benchmarking steps have been implemented for the commercial, academic, and prosoposed antenna. With ten marble blocks, reading tests have been done.

For understanding the antenna performance and results, different marbles have been selected in different scenarios. Also, simulation studies have been done in CST with desk setup.

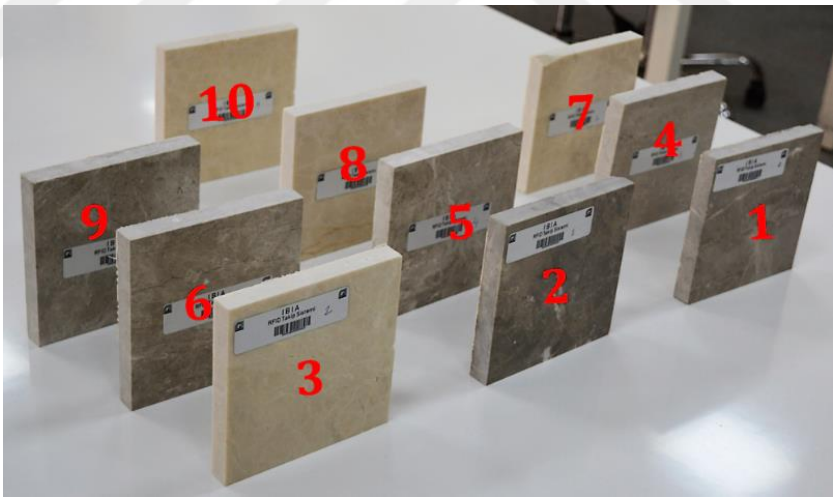

Figure 3.13 Orientation of different marbles on desk setup.

The measurement results taken from Impinj Speedway R420 RFID reader have been converted to .csv files, and with Python programming language, these results have been converted to graphs and tables. The simulation studies have also been done in CST Studio for analyzing the transmission coefficients on tags attached to different marbles. The numbers and order of marbles have been shown in Figure 3.13. The

number of marbles represents the last character of electronic product codes. The measurement results for different distance values have been shown in Table 3.5, Table 3.6, Table 3.7, and Table 3.8 for the commercial antenna.

Table 3.5 Measured RSSI values for Marble 2 with Commercial Antenna.

Marble	Read Count	AvgRSSI (dBm)	MaxRSSI (dBm)	MinRSSI (dBm)	Distance (cm)
2- Grey Marble (Mersin)	136	-38.64	-38.0	-39.0	50
2- Grey Marble (Mersin)	25	-44.24	-44.0	-45.0	75
2- Grey Marble (Mersin)	21	-53.34	-52.0	-54.0	100
2- Grey Marble (Mersin)	18	-53.8	-52.5	-54.5	150
2- Grey Marble (Mersin)	37	-55.93	-54.5	-58.0	200
2- Grey Marble (Mersin)	21	-72.14	-69.0	-73.5	250
2- Grey Marble (Mersin)	36	-66.65	-63.5	-72.5	300
2- Grey Marble (Mersin)	6	-73.28	-73.0	-73.5	350
2- Grey Marble (Mersin)	24	-70.56	-69.5	-72.0	400
2- Grey Marble (Mersin)	39	-64.68	-62.0	-68.0	450

Table 3.6 Measured RSSI values for Marble 6 with Commercial Antenna.

Marble	Read Count	AvgRSSI (dBm)	MaxRSSI (dBm)	MinRSSI (dBm)	Distance (cm)
6- Grey Marble (Mersin)	136	-67.0	-63.5	-73.0	50
6- Grey Marble (Mersin)	25	-64.03	-62.0	-65.5	75
6- Grey Marble (Mersin)	21	-63.28	-61.5	-64.0	100
6- Grey Marble (Mersin)	18	-73.01	-72.0	-74.5	150
6- Grey Marble (Mersin)	37	-67.83	-64.5	-71.5	200
6- Grey Marble (Mersin)	28	-69.17	-68.0	-72.0	250
6- Grey Marble (Mersin)	36	-62.64	-61.5	-66.0	300
6- Grey Marble (Mersin)	25	-63.89	-61.5	-65.5	350

Table 3.7 Measured RSSI values for Marble 7 with Commercial Antenna.

Marble	Read Count	AvgRSSI (dBm)	MaxRSSI (dBm)	MinRSSI (dBm)	Distance (cm)
7- Noble Beige (Burdur)	136	-59.64	-56.5	-61.0	50
7- Noble Beige (Burdur)	21	-74.1	-73.0	-75.0	75
7- Noble Beige (Burdur)	20	-72.83	-70.5	-74.0	100
7- Noble Beige (Burdur)	18	-61.83	-60.0	-63.5	150
7- Noble Beige (Burdur)	37	-62.64	-60.0	-64.5	200
7- Noble Beige (Burdur)	28	-62.1	-59.5	-63.5	250
7- Noble Beige (Burdur)	36	-62.16	-59.5	-64.5	300

Table 3.7 (cont.) Measured RSSI values for Marble 7 with Commercial Antenna.

7- Noble Beige (Burdur)	24	-66.87	-64.0	-68.5	350
7- Noble Beige (Burdur)	24	-67.0	-65.5	-68.0	400
7- Noble Beige (Burdur)	4	-74.31	-73.5	-75.5	450

Table 3.8 Measured RSSI values for Marble 10 with Commercial Antenna.

Marble	Read Count	AvgRSSI (dBm)	MaxRSSI (dBm)	MinRSSI (dBm)	Distance (cm)
10- Noble Beige (Burdur)	136	-57.57	-55.5	-60.5	50
10- Noble Beige (Burdur)	25	-66.85	-64.5	-68.5	75
10- Noble Beige (Burdur)	20	-66.36	-64.5	-67.5	100
10- Noble Beige (Burdur)	17	-68.18	-65.5	-70.0	150
10- Noble Beige (Burdur)	3	-75.12	-75.0	-75.5	200
10- Noble Beige (Burdur)	28	-73.82	-72.0	-74.5	250
10- Noble Beige (Burdur)	25	-72.06	-69.5	-73.0	350
10- Noble Beige (Burdur)	24	-73.31	-72.5	-74.5	400

Average RSSI value and read count results have been shown in Figure 3.14, Figure 3.15, Figure 3.16, Figure 3.17, and the comparison of results have been shown in Figure 3.18 and Figure 3.19.

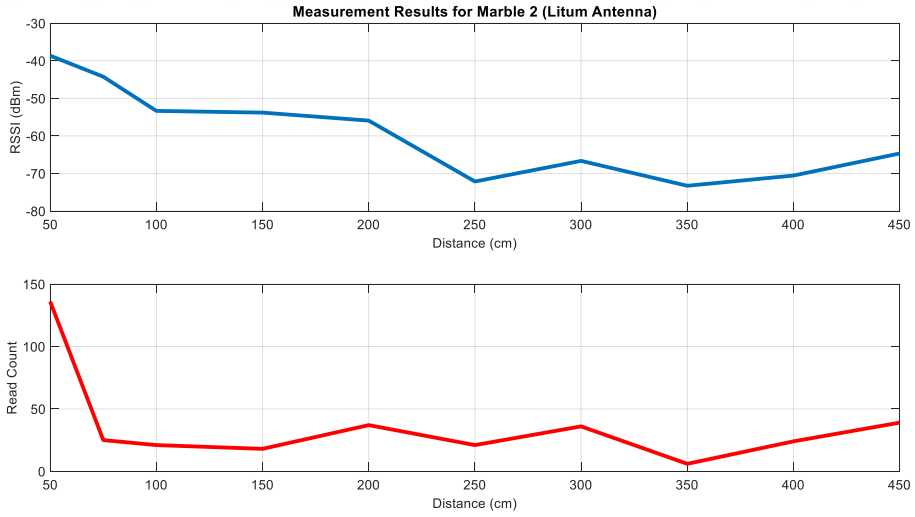

Figure 3.14 RSSI and Read Count results for Marble 2.

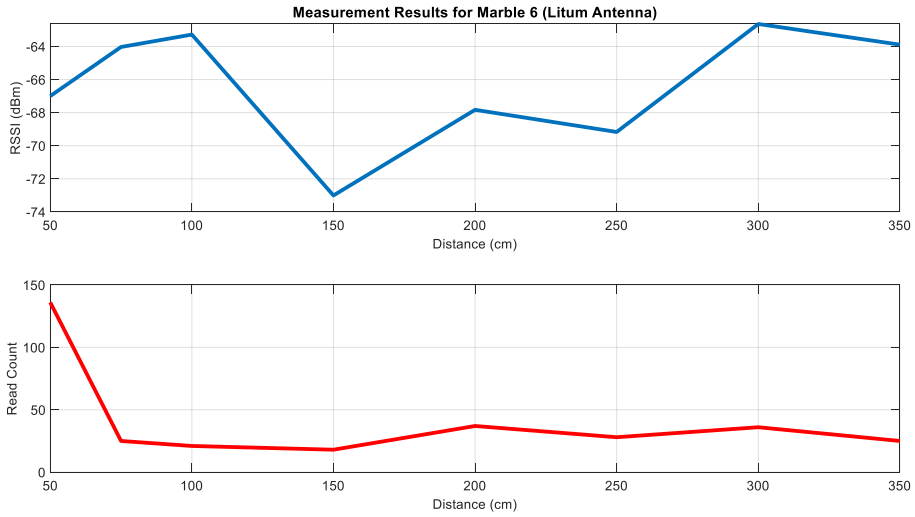

Figure 3.15 RSSI and Read Count results for Marble 6.

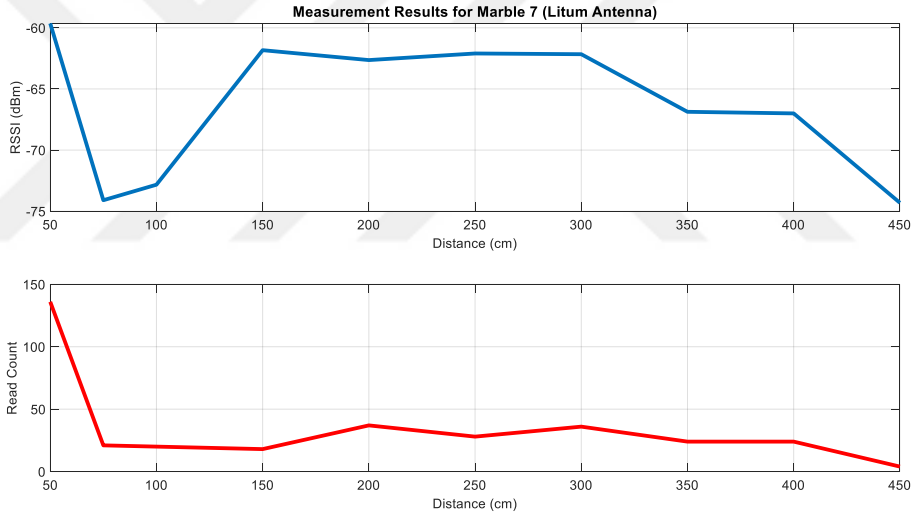

Figure 3.16 RSSI and Read Count results for Marble 7.

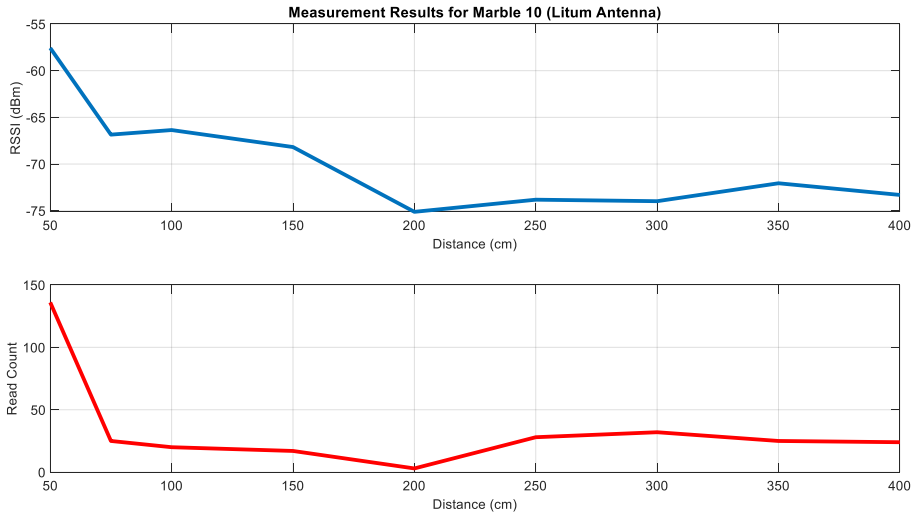

Figure 3.17 RSSI and Read Count results for Marble 10.

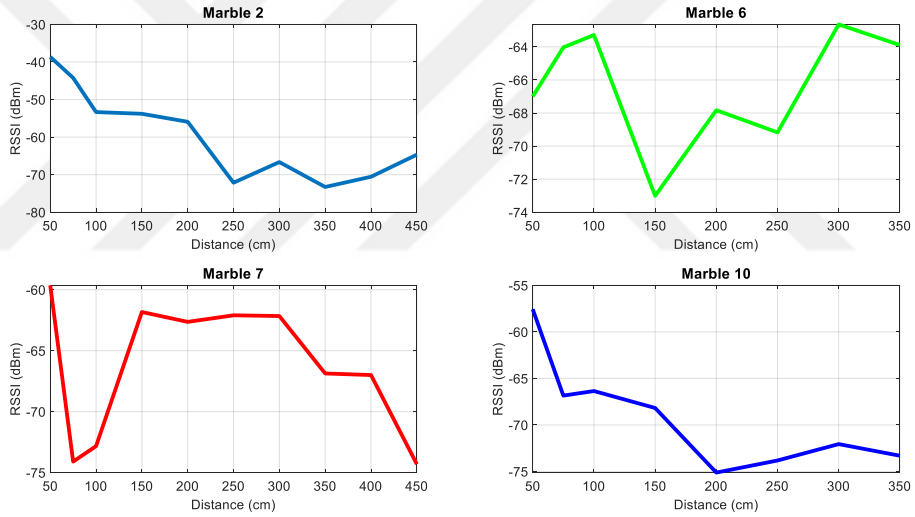

Figure 3.18 RSSI measurement comparison of marbles (2,6,7, and 10).

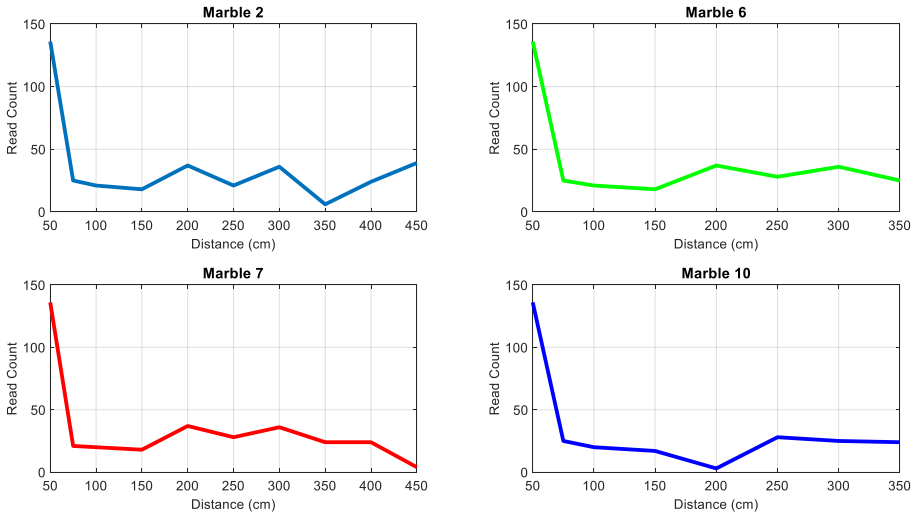

Figure 3.19 Read Count measurement comparisons of marbles (2,6,7, and 10).

With the RSSI measurements made, the transmission between the antenna and the tags on the marble numbered 2,6,7, and 10 have been examined on the CST Studio program. Transmission results have been presented in two ways: different distances for marbles and by distance for a single marble in Figure 3.20 and Figure 3.21.

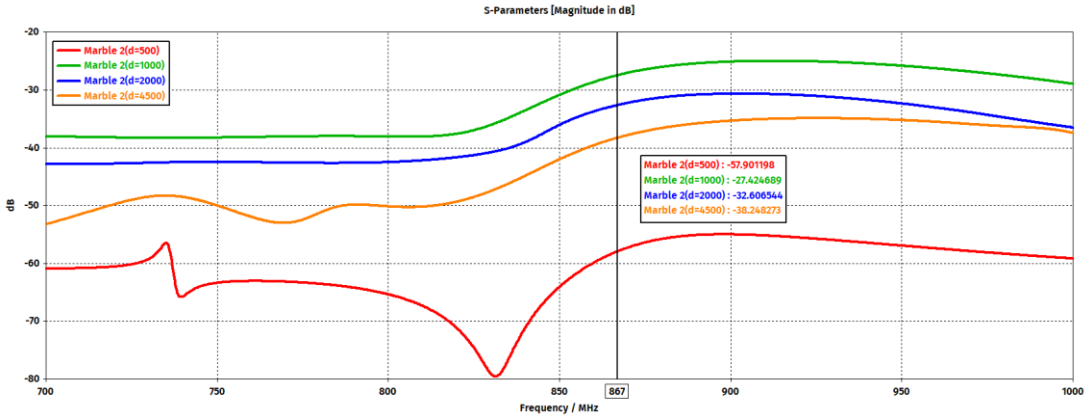

Figure 3.20 Transmission results for Marble 2 (Commercial antenna).

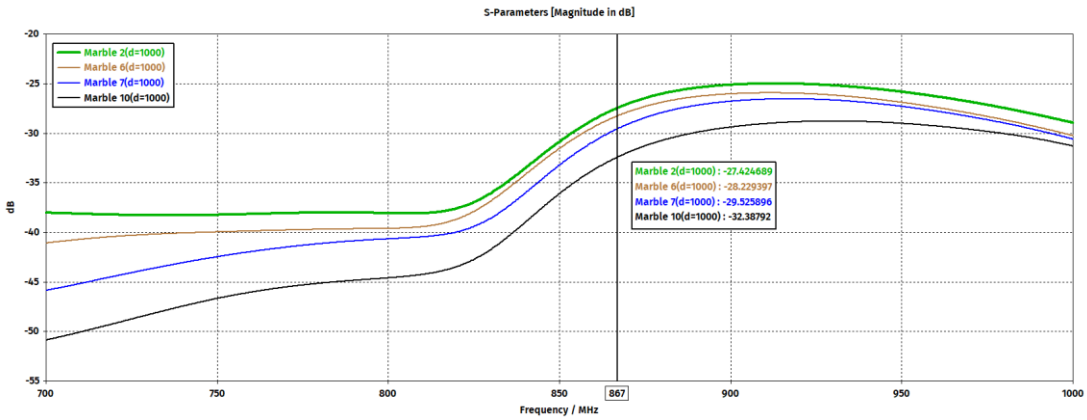

Figure 3.21 Transmission results for different marbles (Commercial antenna).

When the measurement results have been examined, it has been seen that the RSSI value decreases depending on the distance. Numbers 6 and 7 marbles could not be read consistently at distances greater than 400 cm. The receive sensitivity of the RFID reader used is -80 dBm, and possibly due to the different types of marbles from each other and environmental conditions, sufficient transmission could not be achieved for the 6th and 7th marbles. When the reading numbers in Figure 3.19 have been examined, it has been observed that all the marbles have been read in the same numbers at the beginning, while some marbles have been observed to be inconsistent in the reading numbers as the distance increased. The number of reads is naturally directly proportional to the RSSI value.

In some cases, a single reading of the RFID tag is sufficient, while in some cases, time is an important concept. The report received from the reader also includes values such as the first reading time of the RFID tag and the last reading time. The desired situation is to read the tag faster, with the highest RSSI value and the most times. When the results have been examined, it has been observed that the marbles that are more prominent are read better and more. As electromagnetic waves pass through marble, which is a dielectric material, they are weakened. For this reason, the signal coming to the marbles in the front and the marbles at the back will not be the same. However, because of the circular polarization of the antenna used, the marbles that are not in the direct line of sight of the antenna can also be identified. However, when all the results have been examined, it has been seen that all marbles up to 4 meters can be identified without any problems. No measurement has been performed for a distance of fewer

than 50 centimeters. The very short distance between the RFID antenna and the RFID tag can also cause negative consequences due to their affecting each other. The results regarding this situation have also been detailed in the simulation results with marbles. After observing the effect of different distances on the identification, measurement studies have been carried out on the effect of different power levels on the identification on the same distance.

Table 3.9 RSSI measurement results for different power levels.

Marble	Count	AvgRSSI (dBm)	MaxRSSI (dBm)	MinRSSI (dBm)	Power (dBm)
2- Grey Marble (Mersin)	124	-61.72	-61.5	-62	17
2- Grey Marble (Mersin)	244	-58.27	-56.5	-60.5	20
2- Grey Marble (Mersin)	172	-57.05	-55.5	-58.5	25
2- Grey Marble (Mersin)	120	-55.72	-54	-57	28
2- Grey Marble (Mersin)	18	-53.8	-52.5	-54.5	30
2- Grey Marble (Mersin)	72	-54.45	-52.5	-58	31.5
6- Grey Marble (Mersin)	172	-69.62	-69.5	-70	25
6- Grey Marble (Mersin)	120	-67.6	-65.5	-69	28
6- Grey Marble (Mersin)	18	-73.01	-72	-74.5	30
6- Grey Marble (Mersin)	68	-66.46	-65	-68	31.5
7- Noble Beige (Burdur)	120	-70.69	-70	-71	28
7- Noble Beige (Burdur)	18	-61.83	-60	-63.5	30
7- Noble Beige (Burdur)	68	-68.55	-66	-70	31.5
10- Noble Beige (Burdur)	172	-70.28	-70	-70.5	25
10- Noble Beige (Burdur)	120	-68.26	-66	-69.5	28
10- Noble Beige (Burdur)	17	-68.18	-65.5	-70	30
10- Noble Beige (Burdur)	68	-67.66	-65	-71.5	31.5

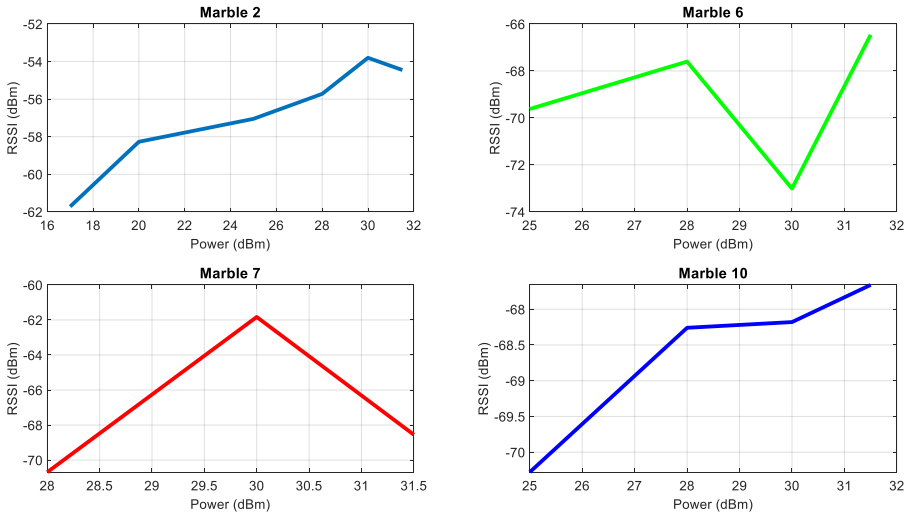

Figure 3.22 Power vs. RSSI measurements for commercial antenna.

Measurement results for different power levels are shown in Figure 3.22. Results have been shown for Marble 2, 6,7, and 10. As shown in the figures, there is a relationship between the power level and the RSSI value, but it is not always the linear proportion due to the environmental conditions affect. Although this difference may be due to environmental conditions, it may also be due to the different types of marbles from each other. Not all marbles described are identical in structure. There are also faulty, cracked, and broken marbles among them. To see the different effects in these marbles, measurement studies have also been carried out on different marbles under the same conditions. Measurement results of different types of marbles have been shown in Table 3.10.

Table 3.10 Measurement results for different types of marbles.

Marble	Count	AvgRSSI	MaxRSSI	MinRSSI	Power
Grey Marble (Burdur)	18	-56.26	-55.5	-57	31.5
Noble Beige (Mersin) – Cracked	18	-57.94	-56.5	-59	31.5
Grey Marble Light (Burdur)	30	-63.26	-60.5	-65	31.5
Noble Beige (Mersin) – Broken	26	-63.42	-59	-65.5	31.5
Noble Beige (Mersin) – Fill Fault	16	-63.69	-61.5	-64.5	31.5
Noble Beige (Mersin)-Veined	18	-64.47	-62	-66	31.5

Table 3.10 (cont.) Measurement results for different types of marbles.

Travertine (Denizli)	16	-61.99	-59	-72	31.5
Emparador (Konya)	21	-56.30	-56	-74	31.5
Yuco Extra (Burdur)	20	-54.91	-54	-56	31.5
Yuco Com (Burdur)	19	-59.69	-55.5	-61.5	31.5

Measurement studies for different marbles have been done for the same distance at 150 cm and the same power level. However, when the results have been examined, it has been seen that marble types also affect the RSSI value besides the effect of power level and distance. RSSI values were different in measurements performed under the same conditions. If the RFID reader's sensitivity has been -60 dBm, only three marbles in the table could be read.

Same measurements have also been done for the Clock-Shaped RFID antenna for comparison. The general perspective about these measurements have been declared for commercial antenna and under same conditions, the Clock-Shaped RFID antenna have been measured. These tests includes, RSSI vs distance, read count vs distance, and power vs distance. The simulation studies for transmission results have also been done for Clock-Shaped RFID antenna. The measurement results for different distance values have been shown in Table 3.11, Table 3.12, Table 3.13, and Table 3.14 for the Clock-Shaped RFID antenna.

Table 3.11 Measured RSSI values for Marble 2 with Clock-Shaped antenna.

Marble	Read Count	AvgRSSI (dBm)	MaxRSSI (dBm)	MinRSSI (dBm)	Distance (cm)
2- Grey Marble (Mersin)	56	-56.32	-54.5	-58.5	50cm
2- Grey Marble (Mersin)	68	-67.07	-62.5	-72.0	75cm
2- Grey Marble (Mersin)	60	-62.77	-60.0	-75.0	100cm
2- Grey Marble (Mersin)	22	-70.39	-62.0	-76.0	150cm
2- Grey Marble (Mersin)	31	-68.52	-64.5	-76.0	200cm
2- Grey Marble (Mersin)	23	-73.97	-72.0	-76.5	250cm
2- Grey Marble (Mersin)	1	-74.5	-74.5	-74.5	300cm
2- Grey Marble (Mersin)	25	-73.83	-71.0	-76.5	350cm
2- Grey Marble (Mersin)	33	-72.16	-67.5	-76.0	400cm
2- Grey Marble (Mersin)	30	-72.75	-70.0	-76.5	450cm

Table 3.12 Measured RSSI values for Marble 6 with Clock-Shaped antenna.

Marble	Read Count	AvgRSSI (dBm)	MaxRSSI (dBm)	MinRSSI (dBm)	Distance (cm)
6- Grey Marble (Mersin)	56	-73.28	-70.0	-74.5	50cm
6- Grey Marble (Mersin)	70	-72.21	-69.0	-74.5	75cm
6- Grey Marble (Mersin)	61	-66.22	-64.0	-72.5	100cm
6- Grey Marble (Mersin)	62	-70.57	-63.5	-76.0	150cm
6- Grey Marble (Mersin)	24	-72.09	-67.5	-76.5	200cm
6- Grey Marble (Mersin)	44	-72.19	-66.0	-76.5	250cm
6- Grey Marble (Mersin)	25	-71.48	-67.5	-76.5	300cm
6- Grey Marble (Mersin)	41	-70.59	-63.0	-77.0	350cm
6- Grey Marble (Mersin)	51	-71.92	-67.0	-76.0	400cm
6- Grey Marble (Mersin)	29	-70.31	-67.0	-76.5	450cm

Table 3.13 Measured RSSI values for Marble 7 with Clock-Shaped antenna.

Marble	Read Count	AvgRSSI (dBm)	MaxRSSI (dBm)	MinRSSI (dBm)	Distance (cm)
7- Noble Beige (Burdur)	56	-73.63	-70.5	-76.5	50cm
7- Noble Beige (Burdur)	51	-68.36	-66.0	-76.0	75cm
7- Noble Beige (Burdur)	8	-74.86	-73.0	-76.5	100cm
7- Noble Beige (Burdur)	38	-74.23	-68.5	-76.5	150cm
7- Noble Beige (Burdur)	39	-74.72	-70.5	-76.5	200cm
7- Noble Beige (Burdur)	22	-74.1	-71.5	-76.5	250cm
7- Noble Beige (Burdur)	23	-74.39	-73.0	-76.0	300cm
7- Noble Beige (Burdur)	5	-74.68	-73.5	-76.0	350cm
7- Noble Beige (Burdur)	10	-73.59	-72.5	-76.5	400cm
7- Noble Beige (Burdur)	7	-72.97	-70.0	-75.5	450cm

Table 3.14 Measured RSSI values for Marble 10 with Clock-Shaped antenna.

Marble	Read Count	AvgRSSI (dBm)	MaxRSSI (dBm)	MinRSSI (dBm)	Distance (cm)
10- Noble Beige (Burdur)	56	-70.54	-68.0	-72.5	50cm
10- Noble Beige (Burdur)	3	-77.0	-77.0	-77.0	75cm
10- Noble Beige (Burdur)	8	-71.25	-68.5	-77.0	100cm
10- Noble Beige (Burdur)	56	-68.82	-63.5	-76.5	150cm
10- Noble Beige (Burdur)	25	-71.23	-66.5	-76.0	200cm
10- Noble Beige (Burdur)	36	-71.89	-67.5	-75.5	250cm
10- Noble Beige (Burdur)	28	-72.34	-69.0	-75.0	300cm
10- Noble Beige (Burdur)	10	-73.36	-71.5	-75.5	350cm
10- Noble Beige (Burdur)	11	-73.15	-70.5	-75.5	400cm
10- Noble Beige (Burdur)	6	-74.35	-71.5	-76.5	450cm

Average RSSI value and read count results for Clock-Shaped antenna have been shown in Figure 3.23, Figure 3.24, Figure 3.25, Figure 3.26, and the comparison of results have been shown in Figure 3.27 and Figure 3.28.

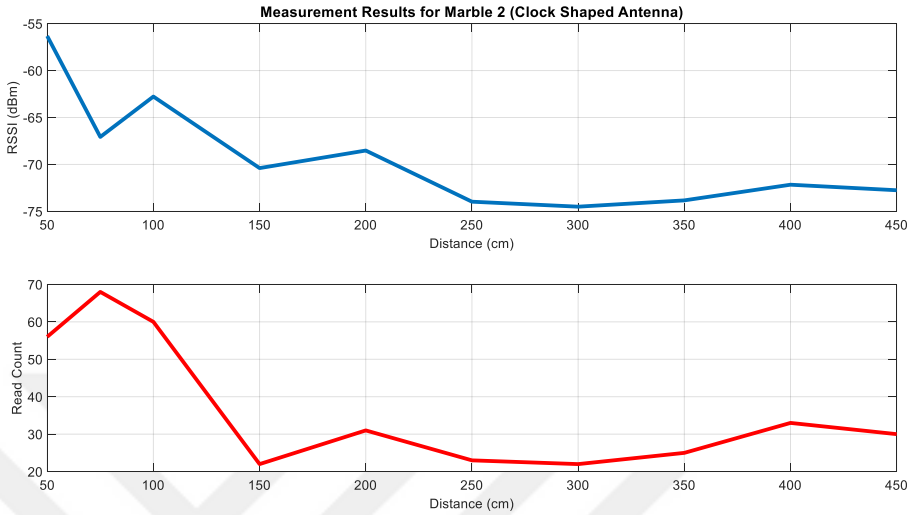

Figure 3.23 RSSI and Read Count Results for Marble 2 with Clock-Shaped antenna.

Figure 3.24 RSSI and Read Count Results for Marble 6 with Clock-Shaped antenna.

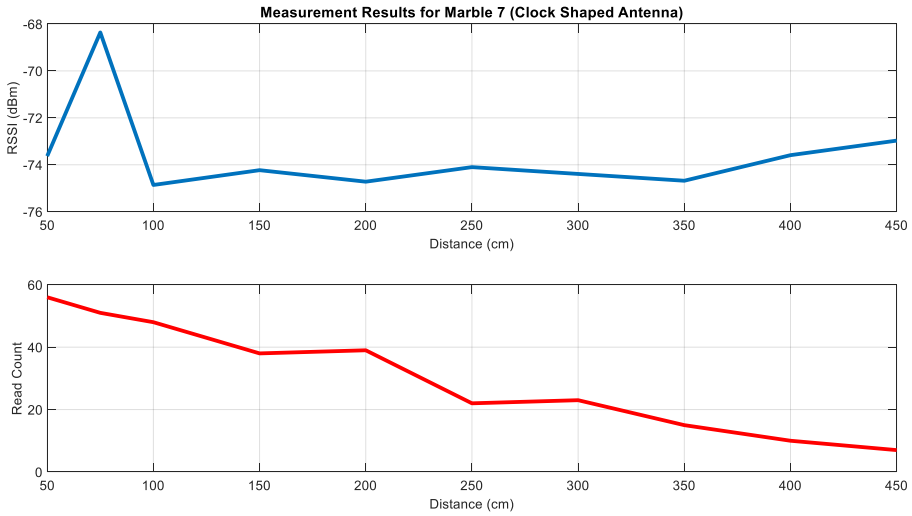

Figure 3.25 RSSI and Read Count Results for Marble 7 with Clock-Shaped antenna.

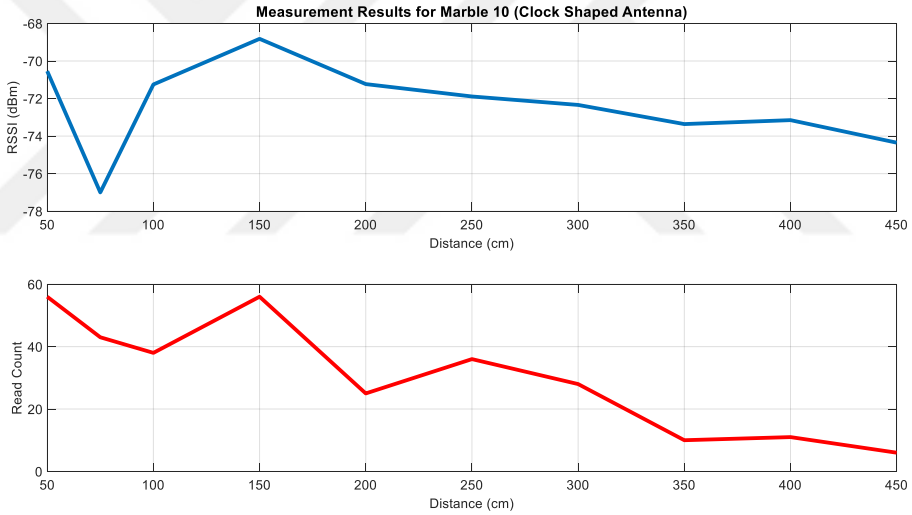

Figure 3.26 RSSI and Read Count Results for Marble 10 with Clock-Shaped antenna.

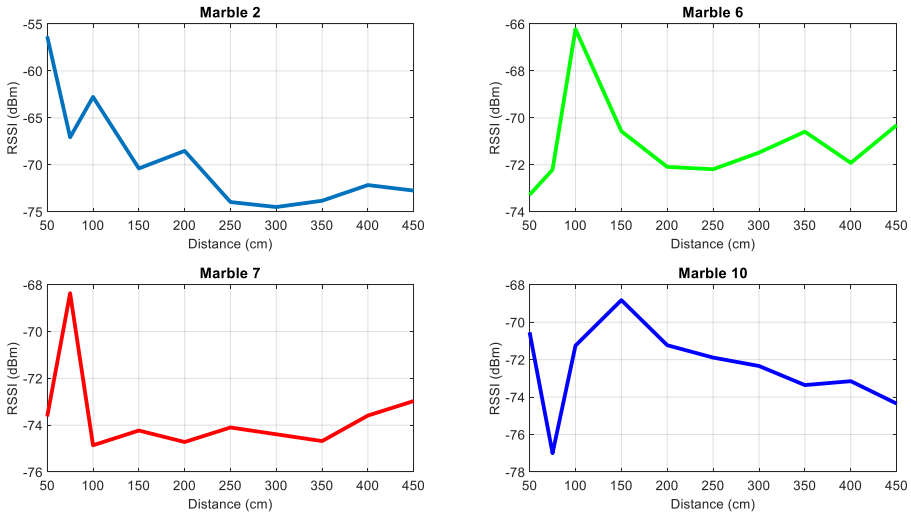

Figure 3.27 RSSI Comparison of Marbles (2,6,7, and 10) with Clock-Shaped antenna.

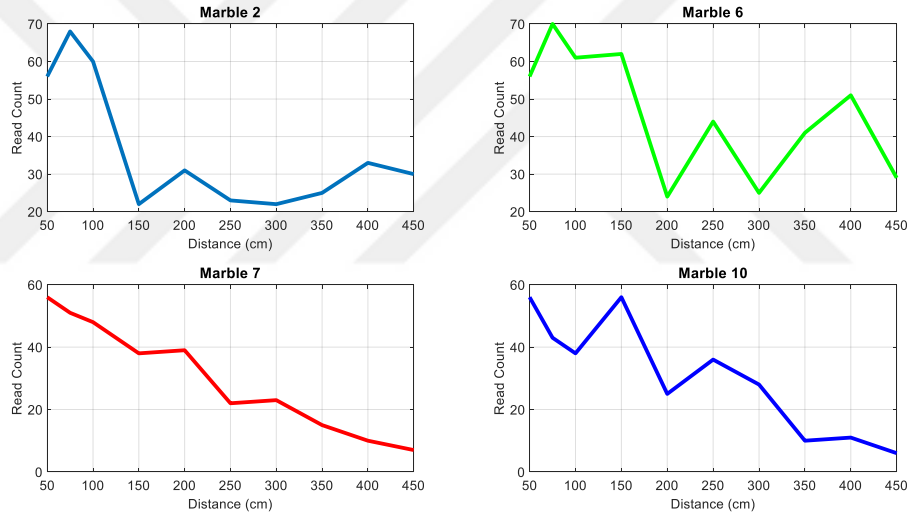

Figure 3.28 Read Count Comparison of Marbles (2,6,7, and 10) with Clock-Shaped antenna.

As with the other antenna, the transmission results for the designed Clock-Shaped antenna were also examined. Transmission results have been presented in two ways: different distances for marbles and by distance for a single marble in Figure 3.29 and Figure 3.30.

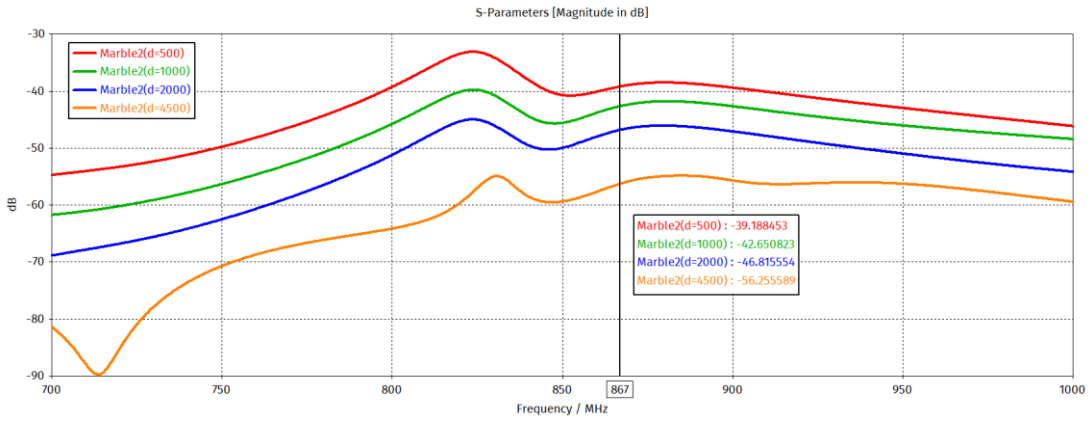

Figure 3.29 Transmission Results for Marble 2 (Clock-Shaped antenna).

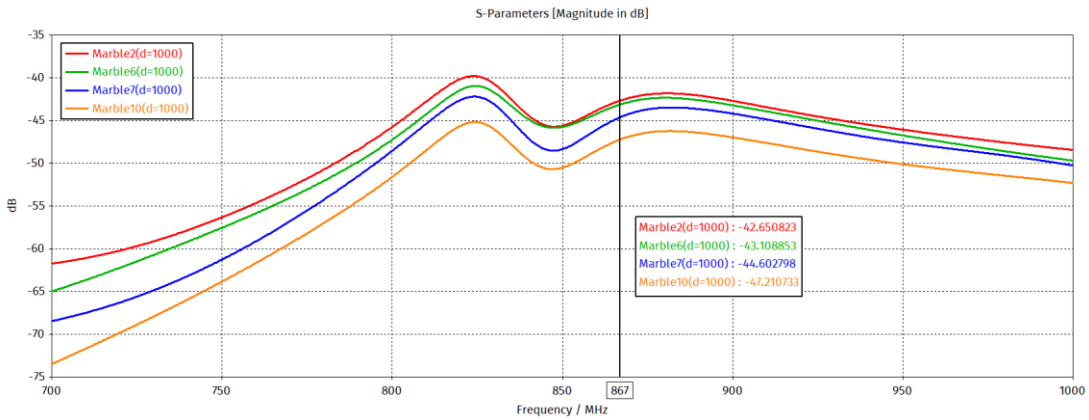

Figure 3.30 Transmission Results for Different Marbles (Clock-Shaped antenna).

With these results, it can be clearly seen that the distance is vital issue for RFID antennas. It can be limited by various issues and in this context, the antenna performance parameters have been investigated. The important of power to RSSI also been shown in Table 3.15 and Figure 3.31.

Table 3.15 RSSI Measurement results for different power levels with Clock-Shaped antenna.

Marble	Count	AvgRSSI (dBm)	MaxRSSI (dBm)	MinRSSI (dBm)	Power (dBm)
2- Grey Marble (Mersin)	119	-62.55	-61.5	-63.5	17.0
2- Grey Marble (Mersin)	124	-59.67	-58.0	-62.0	20.0

Table 3.15 (cont.) RSSI measurement results for different power levels with Clock-Shaped antenna.

2- Grey Marble (Mersin)	103	-57.73	-56.0	-59.5	25.0
2- Grey Marble (Mersin)	53	-56.78	-56.0	-57.5	28.0
2- Grey Marble (Mersin)	51	-56.14	-55.0	-57.0	30.0
2- Grey Marble (Mersin)	41	-55.99	-54.5	-57.0	31.5
6- Grey Marble (Mersin)	103	-68.81	-68.0	-70.0	25.0
6- Grey Marble (Mersin)	53	-66.74	-63.5	-67.5	28.0
6- Grey Marble (Mersin)	51	-66.1	-62.0	-67.5	30.0
6- Grey Marble (Mersin)	41	-64.53	-61.0	-67.5	31.5
7- Noble Beige (Burdur)	53	-72.15	-71.5	-72.5	28.0
7- Noble Beige (Burdur)	51	-71.71	-69.0	-73.0	30.0
7- Noble Beige (Burdur)	35	-71.65	-70.0	-76.5	31.5
10- Noble Beige (Burdur)	4	-70.47	-70.0	-71.5	25.0
10- Noble Beige (Burdur)	53	-70.47	-69.5	-71.5	28.0
10- Noble Beige (Burdur)	51	-69.63	-68.0	-71.0	30.0
10- Noble Beige (Burdur)	41	-69.3	-68.0	-70.5	31.5

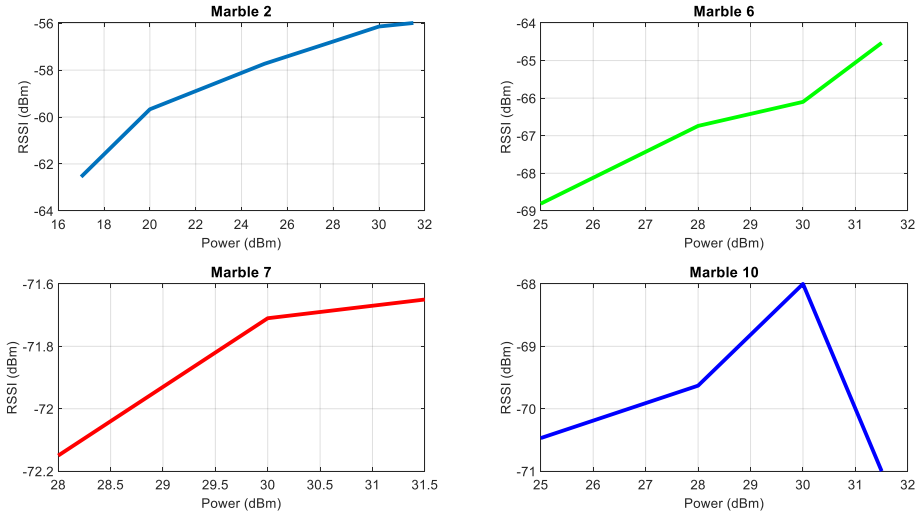

Figure 3.31 Power vs. RSSI measurements for Clock-Shaped antenna.

The affect of power level can be seen with these above results. When all the results of Clock-Shaped RFID antenna have been investigated it can be seen that antenna has enough performance for using smart factory environments. While in some cases its performance results lower than commercial antenna, it can be improved by material and build quality. But for summarized results, it can used for many environments because of its circular polarization and sufficient far-field-results. The gain of commercial antenna has been known value from its catalogue. For designed Clock-Shaped antenna, the gain value has been measured with using reference antenna as shown in Figure 3.32.

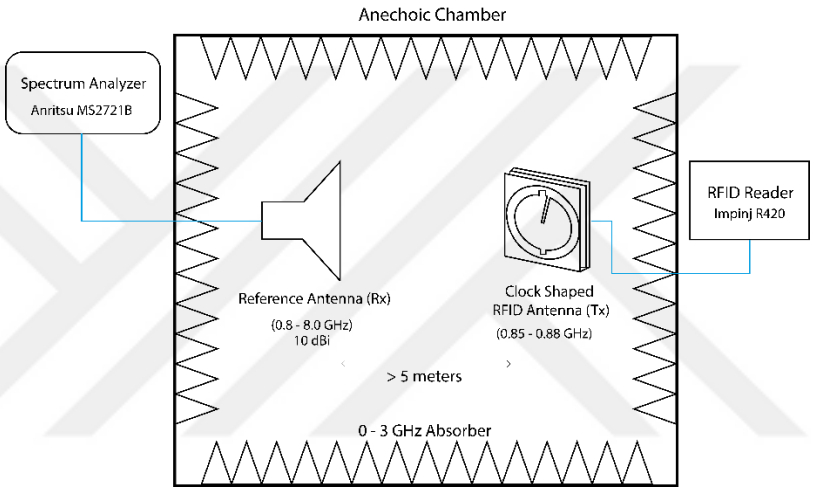

Figure 3.32 Gain measurement setup for Clock-Shaped RFID antenna.

The gain was measured for Clock-Shaped RFID antenna in anechoic chamber environment with Anritsu MS2721B spectrum analyzer and Impinj Speedway R420 RFID reader using a reference antenna with known values. This gain value, calculated using the Friis equation, is approximately 7.2 dB.

In summary, in the measurement evaluations in this section, different issues that may affect the operating performance of an RFID system to be used in a smart factory environment are emphasized. Distance, power level, and type of object to be identified are significant for system performance.

For this reason, a unique system for the smart factory environment to be used must be designed and developed. While making selections, many issues such as reader sensitivity, tag sensitivity, antenna gain should be considered. In this section, only the

results on the performance of the reader antennas have been examined. However, the material and RFID tag to be used have a significant effect on system performance. Measurements have been made on the RFID tag, which has been decided due to different tests. The simulation results made by redesigning the RFID tag together with the reason for the tag selection have been explained in section 3.4, together with the importance of tag selection. Network planning will enable the system to operate consistently in the smart factory environment after the reader antenna and tag selection have been described in section 3.5.

3.4 Tag Selection in RFID Systems

Tag selection is an important issue that should be considered in RFID systems. As mentioned in Chapter 2, there are various RFID tags, passive, active, semi-active, semi-passive. The tags to be selected according to the application areas differ. RFID tags to be used in this study have been selected to be adapted to the smart factory environment. Since the factory to be adapted to the smart factory environment is a marble factory, the type of material to be defined will not cause significant problems. Due to the large volume of the factory to be applied, price is also an essential factor.

For this reason, the tag to be used has been chosen as a passive RFID tag. There are many different brands and many different passive RFID tags on the market. These tag samples have been taken and subjected to different measurements, identified with the same reader and the same antenna, and compared. According to the results of the comparison, it has been decided which tag would be selected. Of course, in this decision-making process, not only these issues but also the size of the tag and the ability to print on it have been taken into account.

Reading tests of 6 RFID tags in total were performed under the same conditions. RSSI values were examined to examine the tag performance. The measurements have been carried out at 3 meters distance and circular polarized reader antenna in free space with 30 dBm EIRP. The images of RFID tags and measurement results table have been shown in Figure 3.33 and Table 3.16.

Table 3.16 Measurement results of different RFID tags.

RFID Tag	RSSI (Average)	RSSI (max)	RSSI (min)
1	-65,50	-61,5	-71,5
2	-68,10	-61,5	-73,5
3	-69,46	-67,5	-72,5
4	-68,09	-65	-71
5	-59,25	-55	-63,5
Smartrac Dogbone R6	-57,5	-55,5	-59,5

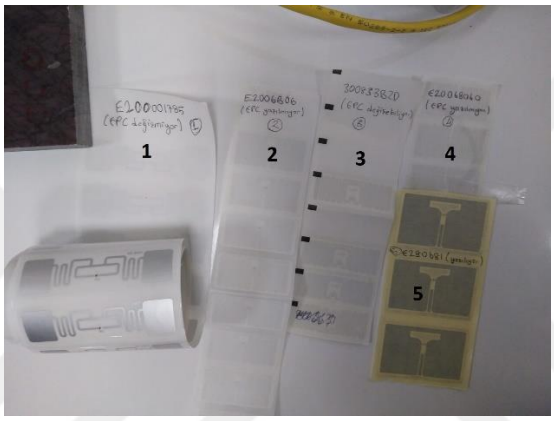

Figure 3.33 Different RFID tags for performance comparison.

When Table 3.16 analyzed, it can be clearly seen that the Impinj's Smartrac Dogbone R6 has better reading performance that others, also it has ability to write different EPC on its chip. So the final selection has been Smartrac Dogbone R6 for system's RFID tag.

This RFID tag, which stands out in laboratory measurements, was redesigned in the AutoCAD program and simulated by transferring it to the CST Studio program. Thus, the tag's behavior under different conditions can be examined by placing it on the materials in the simulation environment. The simulation results of the tag in the free space differ from the simulation results on any material. Many different studies have been conducted to examine these differences and to examine the behavior of the tag. The tag shape drawn in the AutoCAD environment has been shown in Figure 3.34.

Figure 3.34 Smartrac Dogbone R6 RFID Tag sketch in AutoCAD.

The RFID tag drawn in the AutoCAD environment has been converted to .dxf format and transferred to CST Studio ve Ansys HFSS environment as shown in Figure 3.35 and Figure 3.37.

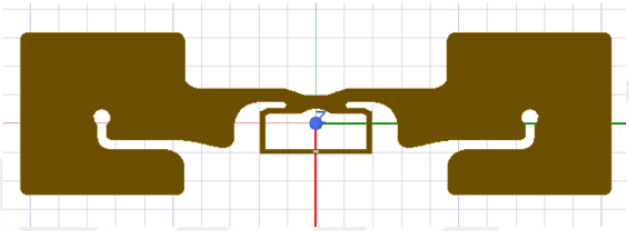

Figure 3.35 Smartrac Dogbone R6 RFID Tag design in Ansys HFSS.

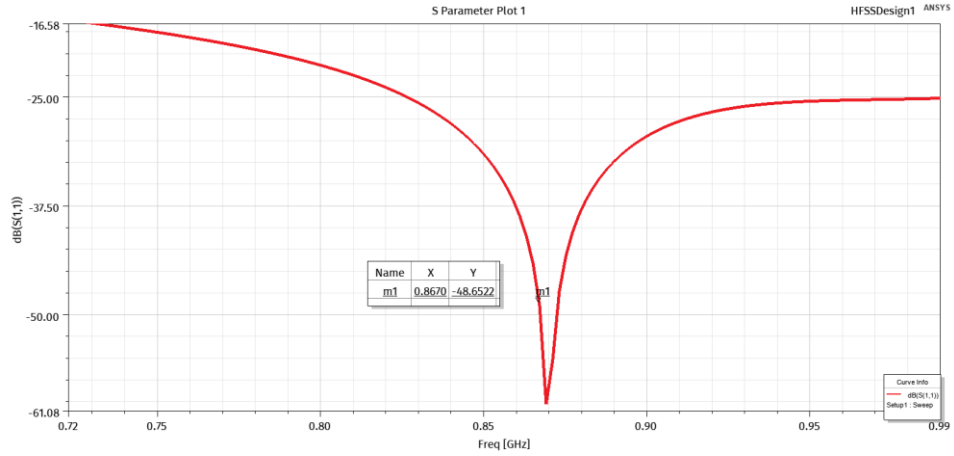

Figure 3.36 Smartrac Dogbone R6 S_{11} simulation results in Ansys HFSS.

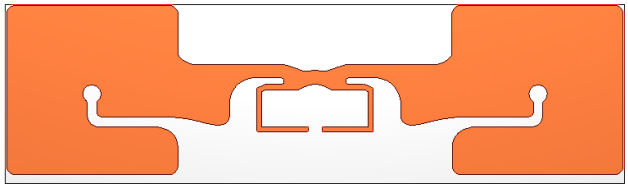

Figure 3.37 Smartrac Dogbone R6 RFID Tag design in CST Studio Suite.

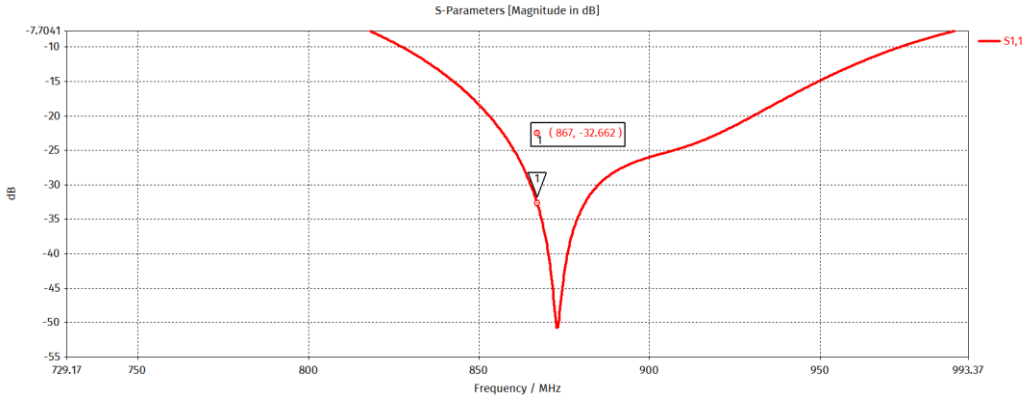

Figure 3.38 Smartrac Dogbone R6 S_{11} simulation results in CST Studio Suite.

Drawing and simulated S_{11} results transferred to the Ansys HFSS program have been shown in Figure 3.35, Figure 3.36 drawing, and simulated S_{11} results transferred to CST Studio Suite are shown in Figure 3.37 and Figure 3.38. When simulating the RFID antenna, it is not enough to draw the antenna geometrically and with the necessary materials because passive RFID tags contain a silicon chip that contains an electronic product code for identification. This silicon chip has its impedance. As such, the designed antenna must match the impedance of the chip at the desired frequency. To determine this value, the required complex conjugate matching values have been given in the datasheet of the Smartrac Dogbone R6 RFID tag. Different ways have been used in Ansys HFSS and CST Studio Suite program to model the chip. While modeling the chip in the Ansys HFSS program, impedance can be written as real and imaginary parts directly; in the CST Studio Suite program, it is necessary to place a capacitor corresponding to the required impedance the location of the chip in order to perform this modeling.

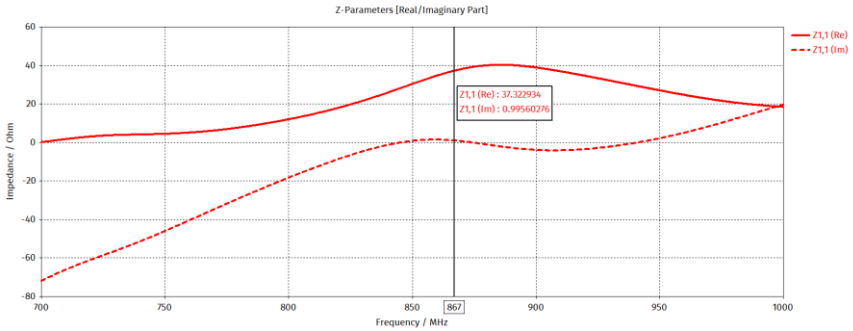

Figure 3.39 Z-Parameters of Smartrac Dogbone R6 RFID Tag.

To verify the impedance matching, the impedance on the port has been examined as real and imaginary in the Z matrix results on the CST Studio Suite. The imaginary part of the impedance is almost zero, as seen in Figure 3.39, the imaginary part of the impedance is almost zero, which indicates that there is an impedance match between the chip and the antenna itself. After ensuring that the designed RFID tag antenna works correctly in the simulation environment, the tag has been placed on the marble, and the S_{11} results have been examined again.

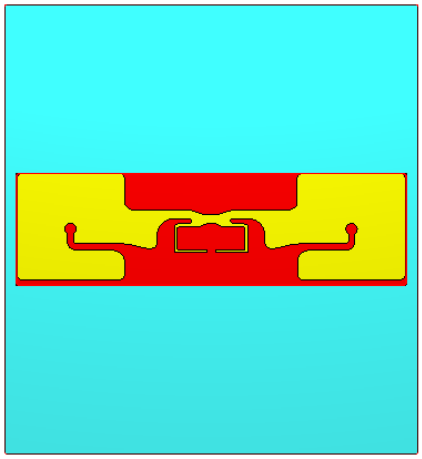

Figure 3.40 Smartrac Dogbone R6 RFID Tag placed on marble.

Paper material has been used as a substrate under the tag in the CST Studio program. Paper is a material with a low dielectric constant compared to marble. When the tag's results on the marble in Figure 3.40 have been examined again, differences are seen according to the free space environment. However, when the results have been examined, it can be said that the tag also works on marble with Figure 3.41. While marble was modeled in CST Studio environment, its features were taken as average from the article written by Arnold H.Scott [89]. The electrical properties of the marble vary according to the dry or wet property, according to its type and the frequency used. In the study, the electrical properties of marble were used as in Table 3.17 while simulating.

Table 3.17 Electrical and thermal properties of marble (average).

Dielectric Constant	8.3 (867 MHz)
Power Factor	1.1
Loss Tangent	0.00567
Conductivity	2.6 [W/K/m]
Spesific Heat	880 [J/K/kg]
Diffusivity	1.12769e-06 [m^2/s]

Table 3.18 Electrical and mechanical properties of different types of marbles [90].

Specimen colour	**Light green**	**Black**	**Pink**	**Zebra green**	**White**
Density (g cm^{-1})	2.72	2.66	2.66	2.74	2.62
Volume fraction, V_f	0.375	0.337	0.277	0.258	0.187
Dieletric constant at 100 kHz	1.376	1.372	1.263	1.248	1.220
Dielectric constant at 10 MHz	1.348	1.332	1.255	1.240	1.187

Table 3.19 Comparison of Relative Dielectric Constant for different types of marbles [91].

Types of Marble	**Green**	**Pink**	**White-1**	**White-2**
Highest Relative Dielectric constant	7.53698 at 9.4 GHz	9.673022 at 8.8 GHz	6.855717 at 9.6 GHz	7.464399 at 9.4 GHz
Lowest Relative Dielectric constant	3.088722 at 11.0 GHz	2.569849 at 10.0 GHz	1.244868 at 9.0 GHz	3.06345 at 12.0 GHz
Resonance Frequencies	9.4,10.6,11.6 & 12.0 GHz	8.8,9.8,10.6 & 11.8 GHz	9.6, 10.2, 11.2 & 11.8 GHz	9.4 10.4 & 11.0 GHz
Average Relative Dielectric constant	5.06878	4.74840	4.183437	5.099932

Table 3.20 Comparison of Relative Dielectric Loss Tangent for different types of marbles [91].

Types of Marble	**Green**	**Pink**	**White-1**	**White-2**
Highest Loss tangent	0.0687796 at 10.4 GHz	0.0236978 at 10.0 GHz	0.01446073 at 8.8 GHz	0.016075198 at 11.4 GHz
Lowest Loss tangent	0.0006495 at 9.2 GHz	0.000201261 at 9.0 GHz	0.000635667 at 11.4 GHz	0.00072297 at 9.0 GHz
Resonance Frequencies	9.2, 9.8, 10.6, 11.0, 11.8 & 12.0 GHz	9.4, 10.0, 10.8, 11.2, & 12.0 GHz	8.8, 9.2, 10.8, 11.2 & 12.2 GHz	8.8, 9.8, 10.6, 11.4 & 12.0 GHz
Average Loss tangent	0.01880	0.0006847	0.005670	0.006243

Each marble is made up of different proportions of chemical compounds, which means each marble has its own unique electrical properties. There are studies about different marble's electrical properties in the literature [89–92]. Since it is not the main purpose of this study to simulate separately for each marble, it is discussed to examine the

differences by measurement and to observe the results of a marble with average value in the simulation environment. RFID tag antennas on the marbles can show different features in different environments due to the structure of the marble. The measurement results related to this were presented in the previous sections with the change of RSSI values. The relative magnetic permeability parameters and relative dielectric conductivity parameters of marble $\varepsilon_r = \varepsilon'_r - j\varepsilon''_r$, which is a dielectric material, will change when the ambient conditions change, the material property changes that occur will cause changes in the electromagnetic performance shown by the tag antenna. Both the electromagnetic (Equation 3.1) (wave equation – heat equation) and thermal (Equation 3.2) (heat equation) behavior of the RFID tag antenna should be examined together with the problems that may occur due to ambient conditions.

$$\nabla x \left(\mu_r^{-1} \nabla \mathrm{x} \tilde{E}\right) - \left[\varepsilon'_r - j\left(\varepsilon''_r + \frac{\sigma}{\omega\varepsilon_0}\right)\right] k_0^2 \tilde{E} = 0 \tag{3.1}$$

$$\rho C_p \frac{\delta T}{\delta t} - \nabla . (k_{th} \nabla \mathrm{T}) = \mathrm{Q} \tag{3.2}$$

In order to observe the electromagnetic performance changes caused by the ambient conditions, the wave and heat equations (Equation 3.1) and (Equation 3.2) are connected with the local electromagnetic heating source. As a result of the new equation (Equation 3.3), the electromagnetic performance that changes depending on the ambient temperature change has been investigated.

$$Q = \omega\varepsilon_0 \varepsilon''_r(T) \frac{|\widetilde{E}|^2}{2} \tag{3.3}$$

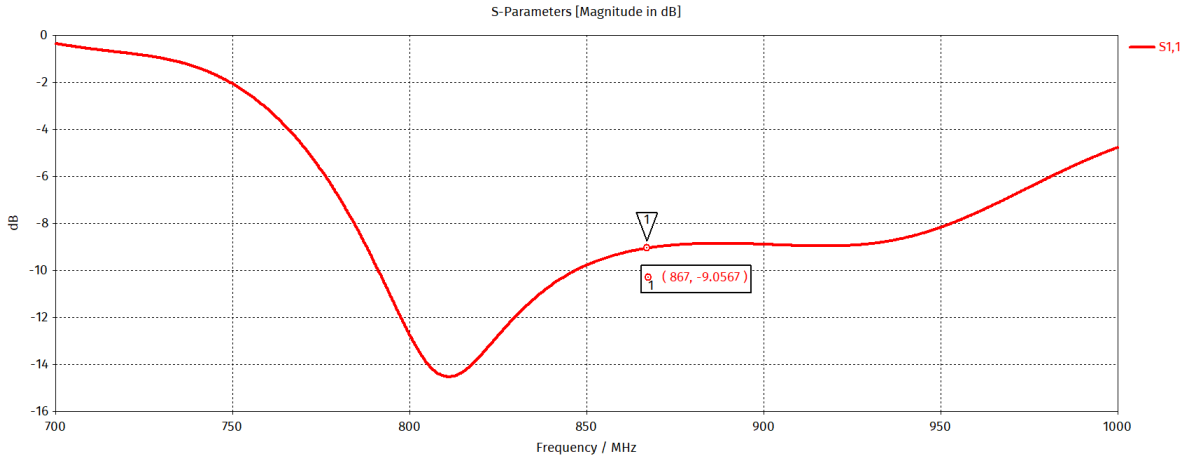

Figure 3.41 S_{11} results of Smartrac Dogbone R6 RFID Tag on marble.

After deciding on the choice of tags, the simulation of the tests carried out in the laboratory, as described in section 3.3, has been reproduced as many marbles were found. Consequently, as can be seen in the previous results, marbles and tags affect each other in environments with multiple marbles. There is a difference between the absence of any material in front of the tag when identifying the tag and the presence of marble in front of it. This difference is presented in section 3.3 with the transmission results.

3.5 RFID Network Planning

While planning the RFID network used when transforming a factory into a smart factory environment, different components are also needed apart from the RFID reader antenna, RFID tag, and RFID reader mentioned in the previous sections. It is crucial to design a system integrated with these components in order to make the factory smart. Apart from the components mentioned in an RFID system, the following components can be used. These are:

-Antenna Hub,

-Ethernet Hub,

-Wifi Bridge,

-GPIO

-Industrial PC.

While planning the system, it should be determined which component will be used for what purpose, and the system should be designed accordingly.

First of all, in order for the system to be monitored and controlled by the end-user, there is a need for a computer that can operate consistently under harsh environmental conditions. **Industrial PC** has been used to meet this requirement.

The number of antennas to be used in the factory varies according to the factory's size where the RFID system will be applied. Speedway R420 RFID reader of Impinj company have been used in the system planned in this study. Speedway R420 RFID reader has four antenna ports internally. However, four antennas are not enough to control a large factory. Because of that, for increasing the number of antenna ports on the RFID reader, one of the components mentioned above, **Antenna Hub (**Figure 3.42a**)**, has been used.

Besides, in some scenarios to be realized in the factory, more than one RFID reader must work on a single PC. The connection between the PC and the RFID reader is made via an ethernet cable. **Ethernet Hub (**Figure 3.42b**)** has been used to control multiple RFID readers on a single PC.

RFID readers to be used in the factory will have different tasks. Although the healthiest connection between the PC and the reader is made with a LAN cable, in some scenarios, it is necessary to access the reader wirelessly. To achieve this, a **Wi-Fi Bridge (**Figure 3.42c**)** has been used in the study.

For a system to help make a factory smart, the system must give feedback and inform the end-user. These notifications can be made by the software with the graphical user interface or by means of sound, light and, engine, as well as hardware. In this study, **GPIO (General Purpose Input Output) Box (**Figure 3.42d**)** has been used to enable RFID reader to interact with any hardware and to give general-purpose input and output.

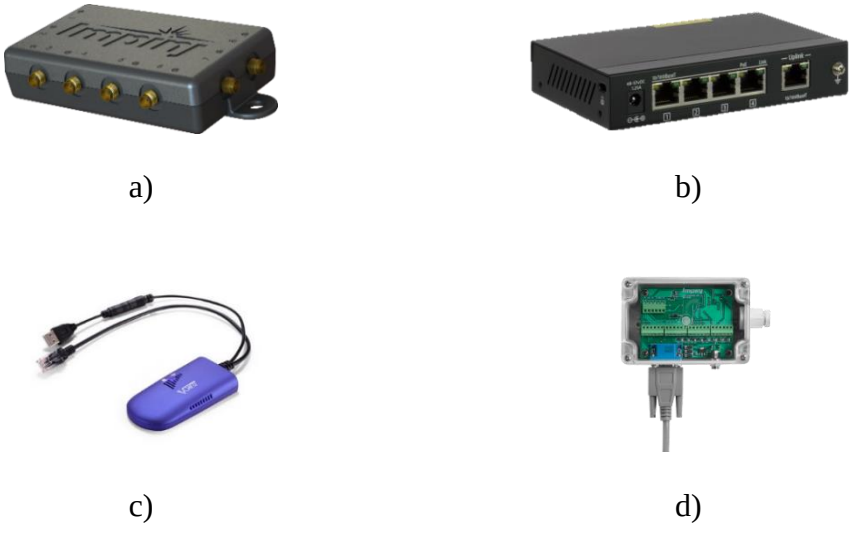

a) b)

c) d)

Figure 3.42 a) Impinj Speedway Antenna Hub, b) Ethernet Hub, c) Vonets VAP11G-300 Wi-Fi Bridge, d) Impinj GPIO Box.

IoT connectivity is one of the essential conditions for a factory to become smart. For this reason, the planned RFID network system must have IoT connectivity. To provide this connectivity and communication, the Wi-Fi bridge and GPIO Box have been used together. Wi-Fi bridge commands can be sent by connecting to the reader on the Wi-Fi. At the same time, the GPIO box can be triggered this way. The system's working principle can be changed according to the scenarios that may occur in the factory. Factors such as temperature, humidity, electromagnetic field density affect the system. Thus, it is vital to obtain information about the factory's environmental conditions and operate the system accordingly. This situation is made with two important components as mentioned.

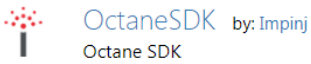

Figure 3.43 Impinj Octane Software Development Kit.

In addition to all these components, the software part is of great importance in RFID systems to provide control. A graphical user interface is required for the end-user to interact with and control the system. Before starting the user interface design, the software development kit and test software offered by Impinj company have been examined. The software used for measurement tests in the previous sections, called

ItemTest, can provide detailed RFID tag reports. However, the software to be used in the smart factory environment must be personalized software with a database, rather than a test software. The software development kit is the package that offers all the tools in a single installable package. Impinj firm offers a software development package called OctaneSDK (Figure 3.43) for .NET and Java platforms. As mentioned before, the system will be controlled by an Industrial PC, which is not affected by harsh environmental conditions, and the graphical user interface to be designed has been developed as a desktop application on a Windows-based PC. The software has been developed using C# programming language, WinForm application type, and MSSQL database infrastructure. Working with the marble factory, which is planned to make the graphical user interface smart from the development stage, screens and menus have been prepared accordingly. Detailed information about the graphical user interface and software has been given in Section 5.

In summary, RFID network planning consists of many components and stages. These components and stages differ according to the area of application of the system. The RFID network structure planned in this study has been shown in Figure 3.44 in detail.

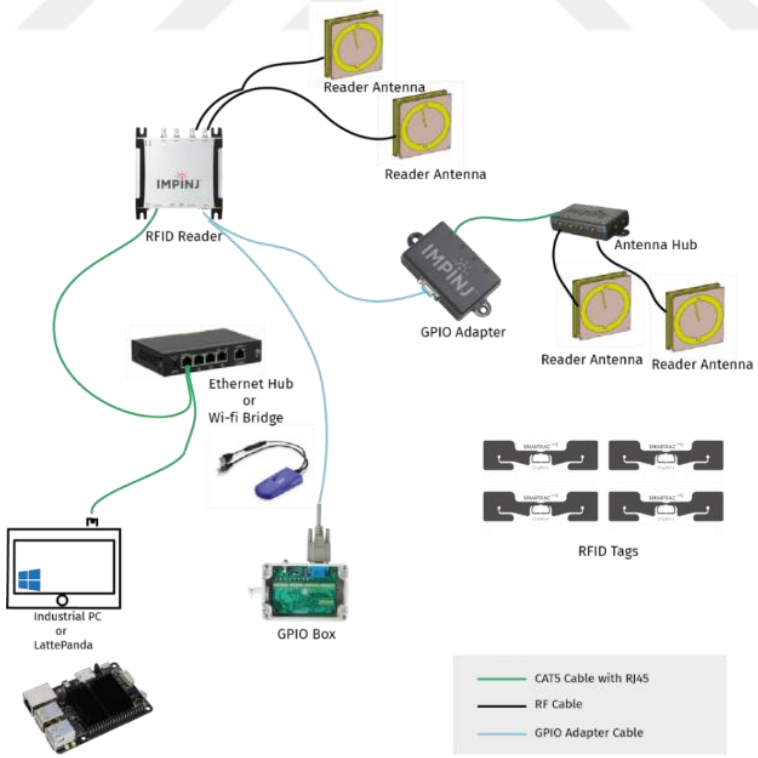

Figure 3.44 RFID Network Planning diagram.

3.6 Adding AI to the System with Machine Learning Antenna Design

With the advances in circuit technology, the dimensions and weight of wireless electronic systems have rapidly decreased. As mentioned before, in section 3.2, the RFID reader antenna is a crucial part of an RFID system. Antenna's dimensions, the geometric shape is also an important issue. Designing a compact antenna with high-gain is essential, but it is only possible with trade-offs. With simulation programs, the parametric study can determine the dimensions, but it is a long time-consuming process. For deciding these trade-offs, a machine learning model can be applied to RFID antennas. Machine learning is a technique that can be applied in different specialization areas such as engineering, science, medicine, and economics and provides accurate results and evaluations. For implementing a machine-learning algorithm to an RFID antenna, the input parameters are important. Because with more input parameters, more results can be obtained. For this reason, the E-shaped RFID antenna has been chosen mentioned in section 3.2 for implementing the machine learning model. Because it has a lot of components and has geometric parameters open to change. So the inputs of the model are the geometric parameters of the E-shaped antenna, and the output is the S-parameters of the antenna in linear and complex. In this section, the machine-learning model and the results of this model have been shown. The necessary parameters have been first determined on the CST Studio Suite program to apply machine learning algorithms to the antenna. The changed geometric parameters have been shown in the Figure 3.45.

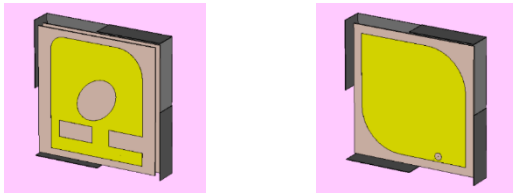

a) b)

Figure 3.45 Antenna design and geometric parameters; a) Antenna top layer, b) Antenna middle layer, c) Antenna top layer design parameters, d) Antenna middle layer design parameters, e) Antenna bottom layer, f) Antenna substrate and feed link design parameters.

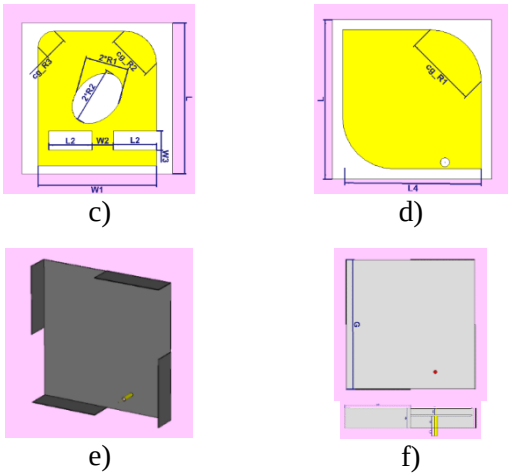

Figure 3.45 (cont.) Antenna design and geometric parameters; a) Antenna top layer, b) Antenna middle layer, c) Antenna top layer design parameters, d) Antenna middle layer design parameters, e) Antenna bottom layer, f) Antenna substrate and feed link design parameters.

Upper layer of antenna design (Figure 3.45a and Figure 3.45c), modified E-shaped patch (main beam patch), has one-sided 0.8mm thick FR-4 substrate material (dielectric constant = 4.4, loss tangent value = 0.02). The two corners of the E-shaped patch in the first layer are designed to create a curve with a special angle value to increase the circular polarization. The middle layer of the antenna design (Figure 3.45b and Figure 3.45d) is designed using a single-sided 0.8 mm thick FR-4 substrate material, with two corners curved at a special angle, the square patch with parasitic effect. This layer has no electrical contact with the upper and lower layers; It is designed to increase gain values, reduce return loss, and improve the circular polarization level. The lower layer of the antenna design (Figure 3.45e and Figure 3.45f) has been designed using 0.5 mm thick aluminum material. The ground structure produced in 2.5 dimensions is designed in 3 dimensions such that some of the edges are curved perpendicular to the interior due to some optimization studies that experience the antenna operation performance. Antenna design parameters are presented in detail in Table 3.21. The proposed antenna design is fed from the bottom perpendicular to the ground plane.

Table 3.21 Design parameters of the proposed antenna (mm).

G	L	L2	L4	Ln	Hn	R1	R2
150	140	40	122	75	25	27	19
cg_R1	**cg_R2**	**cg_R3**	**h1**	**h2**	**W1**	**W2**	**W3**
45	30	15	15	8	110	20	18

In order to apply machine learning algorithms, a data set have been created using geometric parameters. The results of scattering parameters according to different design parameters of the E-Shaped RFID antenna design have been calculated in the simulation program and the antenna design parameters data set is presented in Table 3.22.

Table 3.22 Antenna design parameters dataset.

Parameter	Change Rate (Unit)	Step Size	Number of Samples
cg_R1	[30 50] (degree)	10	3
cg_R2	[20 55] (degree)	7	6
G	[140 155] (mm)	5	4
L2	[34 43] (mm)	3	4
R2	[16 20] (mm)	2	3
W3	[9 19] (mm)	5	3
Total Data:	2592		

The design parameters changed in the antenna design have been determined as cg_R1, cg_R2, G, L2, and W3 (Table 3.21). The change and step intervals of the determined parameters and the number of patterns have been presented in Table 3.22 together with the design parameters. The data set consists of 2592 samples in total, and the training and test data set is divided into 34% and 66%. The simulation performance of the E-Shaped RFID antenna has been realized on 2592 data. As a result of these simulations,

the scattering parameter (S_{11}) of the antenna's input port has been obtained. Various scattering parameters have been obtained from the simulation program: The real (S_{11}_Real) and imaginary parts (S_{11}_Img) and linear form of the scattering parameters have been added to the output for use in the S_{11}_Linear machine learning model. When the data set have been examined, it has been determined that the input and output values have been suitable for the regression methods on machine learning.

Since different scattering parameters have been obtained from the simulation program, the Multi-Output Regression technique has been used in addition to the single-output regression types to compare performance. The first model in Figure 3.46 has been used to estimate the linear scattering parameter. The input parameters, i.e., independent variables, in this model belong to the antenna design and the output parameter, that is, the dependent variable consists of linear values normalized according to 50-ohm transmission line impedance data. Random Forest, Gradient Boosting, Bayesian Ridge, and Polynomial Regression algorithms have been applied to this single output data set. In addition to single regression performances, the Voting regression technique, which can run more than one regression algorithm together, has also been applied, and performance comparison has been made.

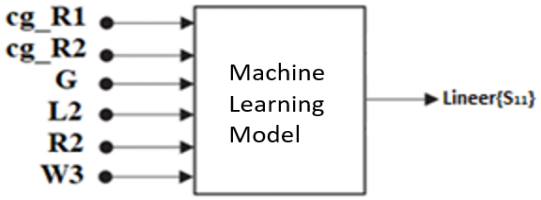

Figure 3.46 Machine-learning model; input(RFID antenna design parameters) and output(linear-resonance frequency scattering parameter) data.

In the second model, the scattering parameter values with real and imaginary parts have been evaluated as output data, and the model in Figure 3.47 has been applied to the data set. The input parameters in this model belong to the antenna design, and the output parameter consists of the real and imaginary parts of the scattering parameter normalized according to the 50-ohm transmission line impedance data. Since there are two outputs in the data set, a multi-output regression algorithm has been applied.

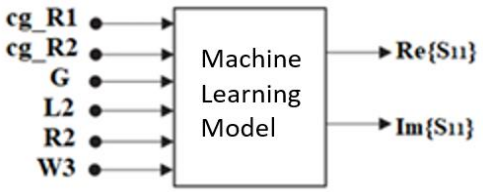

Figure 3.47 Machine learning model; input (RFID antenna design parameters) and output (real and imaginary - resonance frequency scattering parameter) data.

After the data set and models have been decided, different machine learning algorithms were applied using the Python programming language. For linear s-parameters, Polynomial (Figure 3.48), Random Forest (Figure 3.49), Bayesian Ridge (Figure 3.50), Gradient Boosting (Figure 3.51) and Voting (Polynomial + Random Forest + Gradient Boosting) (Figure 3.52) regression techniques have been applied, respectively. Using 20 test data, graphs of these techniques' actual and predicted values have been presented in figures. For complex s-parameters, Multi-Output (Figure 3.53) regression technique has been applied. The actual and estimated value graphs of this technique using 20 test data have been presented in the figure.

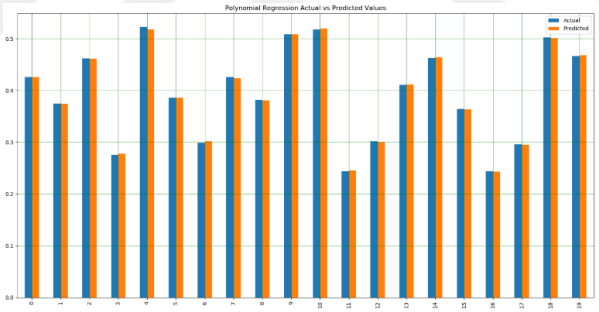

Figure 3.48 Polynomial Regression Actual/Predicted Data.

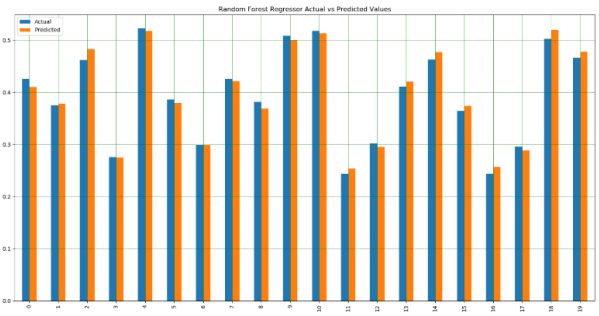

Figure 3.49 Random Forest Regression Actual/Predicted Data.

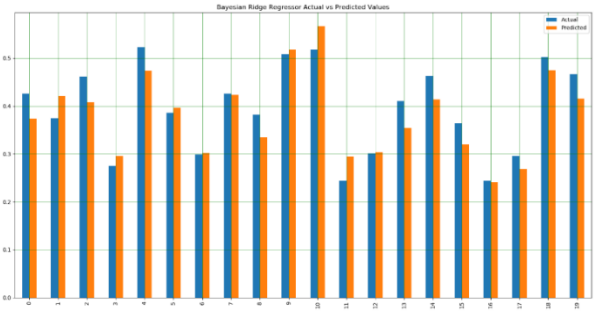

Figure 3.50 Bayesian Ridge Regression Actual/Predicted Data.

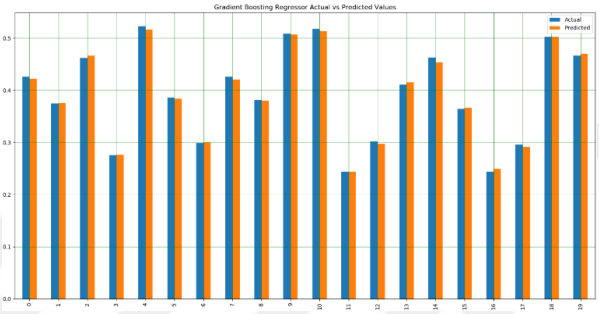

Figure 3.51 Gradient Boosting Regression Actual/Predicted Data.

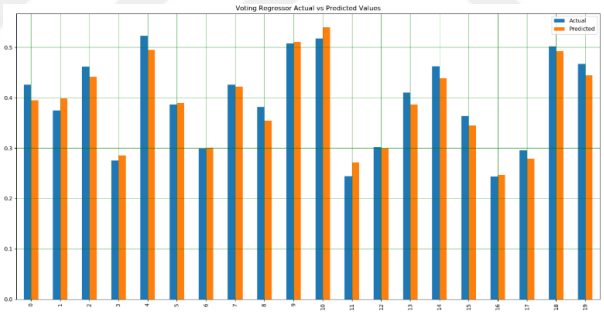

Figure 3.52 Voting Regression Actual/Predicted Data.

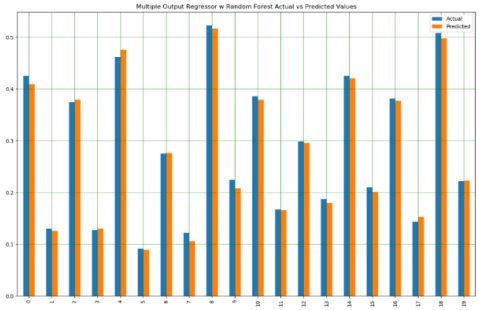

Figure 3.53 Multiple-Output Regression Actual/Predicted Data.

When the results of the test data have been examined, it has been observed that the best prediction performance has been obtained in the Polynomial regression technique. However, when Figure 10, where all performance data has been presented, is examined, the R^2 value is above 0.99 in most of the regression methods. Since the high-degree of polynomial regression may negatively affect the estimation performance, it may be more logical to use Random Forest regression or Gradient Boosting regression at this stage. At the same time, a value of 0.9866 R^2 has been obtained from the multiple output regression method. Figure 3.54 shows the comparison of test input data and predicted output data with actual output values for the multi-output regression method. By increasing the number of samples of the data set used in this study, much more accurate results can be obtained. Simultaneously, using the predictive performance of machine learning, the study can also be applied to different antenna designs, supported by different methods, and an antenna calculation tool can be created for future studies.

Results	Polynomial Regressor
R2 Score %	99.90662709397212
Mean Squared Error %	0.0010266886153524478
Root Mean Squared Error %	0.32041982075902353
Mean Absolute Error %	0.19226702979175123
Maximum Error %	2.2553053657385194
Results	**Random Forest Regressor**
R2 Score %	99.28562257840106
Mean Squared Error %	0.007854989172142429
Root Mean Squared Error %	0.8862837678837646
Mean Absolute Error %	0.6787669734511294
Maximum Error %	3.301863899999999
Results	**Gradient Boosting Regressor**
R2 Score %	99.68788354635682
Mean Squared Error %	0.003431899286972569
Root Mean Squared Error %	0.5858241448568478
Mean Absolute Error %	0.39535378127960735
Maximum Error %	2.707831120804452
Results	**Bayesian Ridge Regressor**
R2 Score %	83.63744676562939
Mean Squared Error %	0.17991565046514224
Root Mean Squared Error %	4.241646501833247
Mean Absolute Error %	3.32204528926926
Maximum Error %	18.862973633697962
Results	**Voting Regressor**
R2 Score %	95.65845152520089
Mean Squared Error %	0.047737813694543066
Root Mean Squared Error %	2.1848984803542493
Mean Absolute Error %	1.6977540653497412
Maximum Error %	9.326977240455097
Results	**Multi Output Regressor**
R2 Score %	98.66034026909941
Mean Squared Error %	0.007001640632340577
Root Mean Squared Error %	0.8367580673253516
Mean Absolute Error %	0.609230755779637
Maximum Error %	---

Figure 3.54 Comparison of Regression Methods Table Created with “plotly”.

Table 3.23 Multiple-Output regression method input test data and output results.

Input Parameters G,L2,R2,W3,cg_R1,cg_R2	**Predicted Output Values (S_{11_real}, S_{11_img})**	**Actual Output Values (S_{11_real}, S_{11_img})**
[145,37,20,14,40,55]	[0.409,0.126]	[0.426,0.130]
[150,43,18,9,30,55]	[0.516,0.155]	[0.506,0.140]
[150,43,20,14,30,34]	[0.340,0.099]	[0.337,0.095]
[145,34,18,9,40,55]	[0.405,0.210]	[0.407,0.219]
[145,40,20,14,50,41]	[0.376,0.057]	[0.342,0.059]

As a summary, in this section, different machine learning algorithms' performance data have been presented on the estimation of the scattering parameter in the ultra-high frequency band operating resonance frequency of the proposed E-Shaped RFID antenna. The design parameters of the antenna have been changed parametrically and concerning each other, and a data set consisting of 2592 samples has been created. The data set has been divided into test and training data set, and the performances of different machine learning algorithms have been compared. As a result of the simulations, two different data types (linear and complex) belonging to the scattering parameter have been obtained. Since the linear scattering parameter is uni-valued, it can make predictions with a single output data Polynomial, Random Forest, Bayesian Ridge, Gradient Boosting regression methods have been applied, and the Multi-Output regression method, which can estimate with double output data, has been used for the complex scattering parameter consisting of double output values. In the light of the information obtained in this section, the machine learning model can be developed and applied to different antennas presented and made specifically for the smart factory environment requirements, and original designs for the smart factory can be created with the machine learning model.

4. SMART MARBLE FACTORY SOFTWARE AND SYSTEM INTEGRATION

In communication systems, the software is essential in order to provide full control of the system. A user interface is required for the data obtained wirelessly to be processed and analyzed by the end-user or analyst. These data can be used for purposes such as supply chain management, stock and inventory control, and the data obtained can be used with machine learning methods to measure different performances. The user interface to be designed for the smart factory should be shaped according to the demands of the market. As every factory needs different issues, each common feature is to be able to make the parts of the products included in the stock management from the production/distribution processes to the customer, completely and accurately. In order for this process to work correctly, the products in the inventory must be accurately labeled according to their different characteristics and kept in a database. As mentioned in the previous sections, software development kit support is also important when choosing an RFID reader. Impinj Speedway R420 RFID reader, which is the RFID reader used, offers a software development kit called OctaneSDK for C#.NET. In this direction, an end-user interface has been prepared for the marble factory, integrated with the RFID system and smart factory. Also, in this section, a machine learning designed RFID antenna has been presented for integrating system with artifical intelligence. The details about machine learning antenna design technique will be explain in detail later.

4.1 Smart Factory System End-User Application Graphical User Interface

In this section, a graphical user interface of the RFID tracking system for smart factory applications in a marble factory will be introduced. There are sections such as version information and theme selection menu on the opening screen of the smart factory RFID

tracking application. The end-user can choose according to his preference. There is a "settings" button for the user to make the necessary adjustments in the upper-right part of the program. The main screen of graphicel user interface has been shown in Figure 4.1.

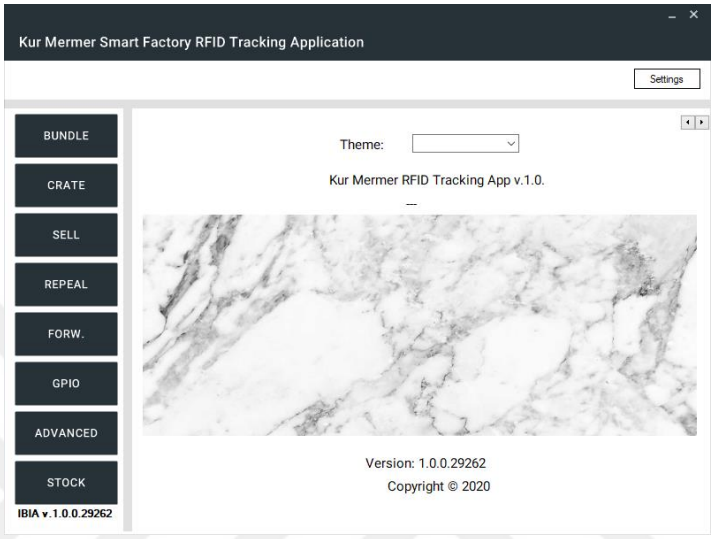

Figure 4.1 GUI main screen.

When entered in the Settings tab in Figure 4.2, the user makes the IP definitions of RFID readers used in warehouse entry and exit areas. All of the information is stored in a Microsoft SQL Server-based database. You can also choose between marble casings or marble bands. The "Pre-EPC" section in the menu can be changed according to the product. Each of the marbles tagged in the marble factory contains its unique electronic product code. Different parts of this electronic product code represent different features. The part shown as "Pre-EPC" represents that the RFID tag read is a marble belonging to that factory. This part can be changed upon request.

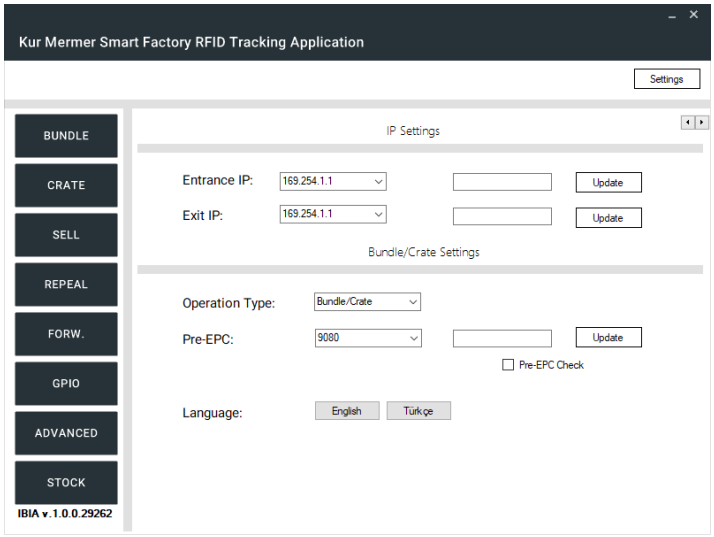

Figure 4.2 GUI settings screen.

In order to explain the operation of the graphical user interface, it would be more correct to describe the process of marble in the factory first. First of all, the marbles are transferred to the plate recording line by rail system, ready to be recorded on the plate - furnace line (FRNHAT) in Figure 4.3a.

a) b)

Figure 4.3 a) FRNHAT workstation, b) PLKSHT workstation.

Registration starts with the graphical user interface on the plate registration (PLKSHT) line in Figure 4.3b. The screen named "Bundle" in Figure 4.4a, contains the information of the marble to be defined. First of all, by connecting with the RFID reader, the RFID tag's electronic product code on the marble is read. During this reading, the information in the database is analyzed instantly, and if the same electronic product code is in the database, no action can be taken shown in Figure 4.4b.

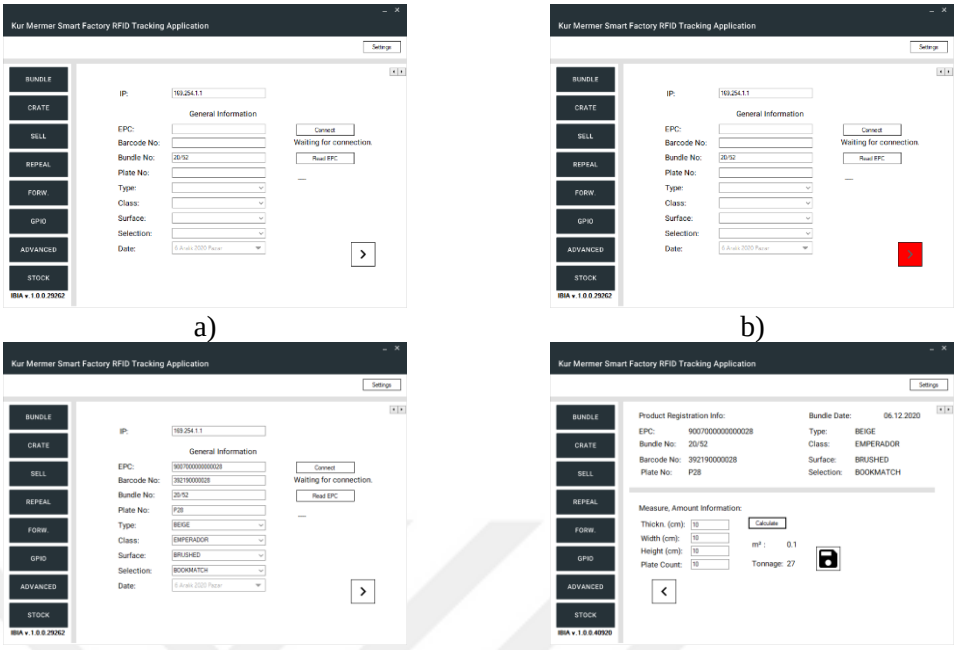

Figure 4.4 a) Bundle registration module, b) “EPC already registered.”, c) Bundle module with information, d) Bundle module screen – 2 with information.

Then, it is switched to the "Bundle-2" screen in Figure 4.4d. On this screen, information such as the size and quantity of the marble is available. Simultaneously, the information entered on the previous screen is displayed again, although there is an error. After all the necessary information is entered, tonnage and square meters are calculated with the calculate button, and the marble is matched with the electronic product code with all the features on the screens and saved in the database.

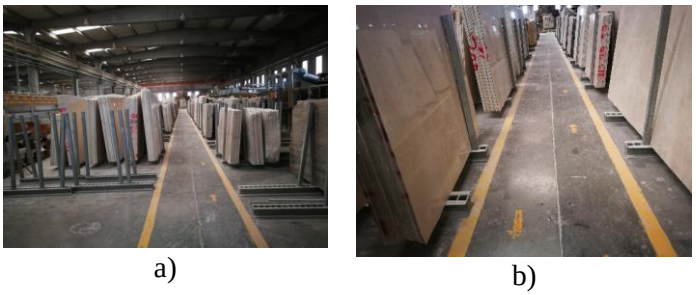

Figure 4.5 a) Finished product waiting line, b) Stock waiting station.

After the marbles are registered in the database, the finished products are transferred to the parking areas in the stock waiting stations in Figure 4.5a and Figure 4.5b where

the finished products and plate-sized products to be stocked are stored by a rail transfer system in the factory shown in Figure 4.8b. The collective stock control of the marbles here can also be done with the RFID system.

Figure 4.6 a) Registrated marble database, b) Product reservation/sell module, c) Product reservation with bundle number, d) Product reservation with EPC number.

After the registration phase, the marbles registered in the database can be viewed on the graphical user interface with their features which shown in Figure 4.6a also editing can be done manually with database module. At the same time, sales and reservation adjustments of the marbles can be made through the sales / reservation module in Figure 4.6b.

When making the sales / reservation process, the necessary information is taken from the database with the bundle number in Figure 4.6c or EPC in Figure 4.6d. Here, when the data is wanted to be taken with EPC, the EPC on the marble bundle is read with the RFID reader and all the features of that band are added to the reservation. At the same time, while making a reservation, more than one band can be reserved with the same code. Also, if different dimensions are to be entered while making a reservation, they can be edited on the registration screen of the module as shown in the Figure 4.7a.

Figure 4.7 a) Reservation module dimension edit, b) Shipment station, c) Shipment module, d) Shipment module with reservation number.

After the registration and reservation processes are made, the most important module in the graphical user interface, the shipping module, is activated. Marbles come to the shipment areas, in the storage areas. The reserved marbles with all their information are displayed on the screen in the shipment module. At the same time, Bundle numbers that are matched with the EPC are displayed on the screen so that the operator in the shipment area can choose the wrong operation easily. When the shipment is started, the RFID reader starts to read the products with the antennas located at the exit of the warehouse. All electronic product codes in the list of that reservation number are compared with the products leaving the warehouse. While the products are dropped from the stock in the right product output, in the case of a wrong product, the user is returned with the GPIO system. The shipping module does not complete the operation until all products that need to be released at the same time are checked out. If everything is correct and all products that need to exit exit the shipping area as required, the shipping module completes the reading and stops the RFID reader and notifies the end user as "transaction successful". Wrong and correct shipping products can be easily distinguished by bundle numbers on the marbles.

The process of marble from the beginning to registration and stocking and the above mentioned FRNHT and PLKSHF workstations are shown in Figure 4.8a.

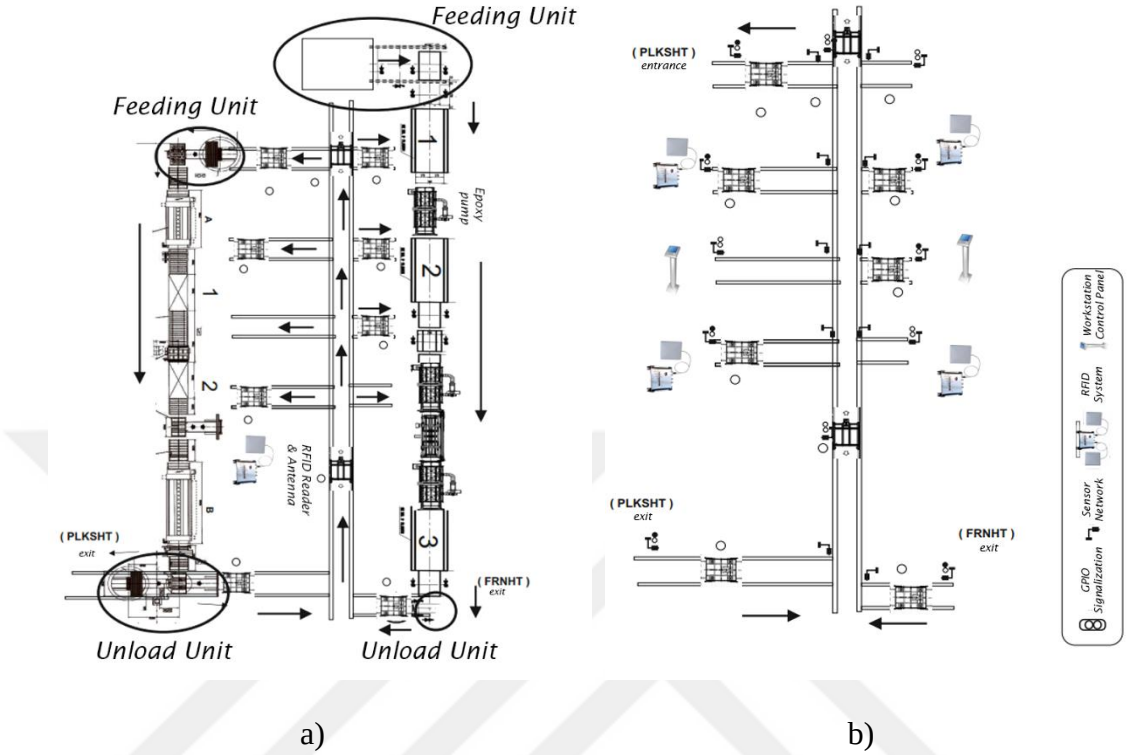

Figure 4.8 a) Workstation schematic of the marble factory, b) Rail transportation system in factory.

To summarize, RFID graphical user interface includes important modules such as recording, stock tracking, shipment control. The advantages of this graphical user interface, which works simultaneously with the RFID reader used, for the in-factory process can be listed as follows:

- ✓ With the use of the RFID system with an automated graphical user interface, manually made works in in-plant operations is reduced and human errors are prevented.
- ✓ Since manual processes are reduced, a large amount of time and labor is saved.
- ✓ Situations such as stock loss and product theft are prevented, the location of the products can be determined more quickly by keeping records of the stations where the products in the factory were last passed.

- ✓ Unnecessary stocks can be avoided by keeping only the stocks for the needs at the factory, and therefore stock holding costs can be minimized.
- ✓ By monitoring the process in the supply chain from production to customer service in and out of the factory, improvement can be achieved in customer service with rapid returns as well as production and shipment.

4.2 Industry 4.0 – Digital Traceability Systems in Marble Production and Service Processes

The cornerstone of digital traceability systems is RTLS (Real-time location tracking systems). In recent years, these systems have drawn attention to applications built with RFID (Radio Frequency Identification), GPS and Beacon technologies that enable traceability and monitoring in production and service processes. Details on the thorough integration of RFID systems, one of the digital traceability systems, the factory setting, and the application areas of the system and the added value it offers will be addressed within the framework of this section.

In Section 4.1, the operation of the marble factory and the working of the graphical user interface was explained. Parallel to this, in this section, real-time location tracking of the products at the stations within the factory mentioned earlier will be discussed. At the same time, the algorithms of the graphical user interface modules will be explained and the layers of the system will be presented. In the marble factory, the product that comes as a raw material is processed and goes through many stages until it is ready for sale. The product is subjected to different processes at different stations at each stage, and finally, it is labeled with an RFID tag that contains a unique electronic product code with its own characteristics, is recorded in the database and becomes ready for transactions such as sales, shipment, stock control. The production system in marble factories starts with the selection of raw blocks in the quarries. Blocks brought from the quarry are stocked in the factory stock area. The next step is to cut the blocks. The first process in the cutting step is to choose the cutting line. It is of great importance that the blocks are properly marked in the stock area and then transported under appropriate transportation conditions in the processing facility. The blocks coming from the quarry to the factory area are washed in the stock area and the suitability of the gang saw is checked by the technical personnel. While unsuitable blocks are stored in separate places to be cut in STs, suitable blocks are placed in the

gang saw after determining their direction. The 2 cm or 3 cm raw plates coming out of this machine, which cuts beige marble at a speed of 12-18 cm / min, are applied in the slab epoxy unit. The plates, whose epoxy process is finished, are fed to the plate polish machine the next day, depending on the order criteria, and pass through one of the polishing, honing or patina processes. Plates with the desired surface quality are packaged either in groups of plates using wood material (bundle) according to the quality of the order or shipped to sizing machines such as plate sizing and bridge cutting. Plates cut to various sizes in multiple sizing machines are sent to the finishing unit for control and other operations. Here, the products with the necessary repairs and quality controls are separated into their selections, crate and become suitable for shipment. This production process in the factory includes complex stages. After this meticulously carried out production and quality control process, the marbles are stocked and kept or sold according to the customer's request. During these processes, it is extremely important to be able to monitor and track the marbles, which have very different characteristics, within the factory, and to complete the stock record accurately and completely. Developing technology has made significant progress in delivering a good or service produced in one part of the world to consumers at the other end. As a result, the market for those who produce goods and services has become the whole world. This growth of the market has led to the growth of the competitive environment. The key to competition is to produce quality goods and / or services. In order to be successful in the age of high competition and communication, it is now necessary to produce quality products and services. Quality is what the customer demands. In other words, the definition of quality is made by the customer. Therefore, the concept of quality does not have a single definition, and these definitions are not fixed. For customer satisfaction, it is necessary to produce quality goods and services on the one hand, and to control quality costs in order to control production costs on the other. In today's conditions, for a good quality control system, it is necessary to ensure that every point of the chain of activities from the demands of the consumer to the product stock area and loading is traceable and controllable. A comprehensive digital conversion need of enterprises operating in the mining sector of our country has become obligatory due to 3 main factors. These are: customer, competition and cost. Customers now want to shop from companies that not only produce quality products,

but also have good services, respect the society and the environment, and show their commitment to doing the best for the customer. In addition, quality costs arising from faulty production and customer dissatisfaction are much more dramatic in the mining industry compared to other sectors. For this reason, the cost should be reduced by reducing errors and variations or targeting zero errors. For this, the digital conversion process should be handled comprehensively with all its elements. The quality of the marbles offered to the market, the flawlessness in the polishing, the smoothness of the chamfering, the homogeneity in the color and pattern, and the classification without physical defects are of great importance in natural stone trade and especially in exports. Achieving all these features is possible with the quality control stages carried out at certain stages from marble blocks produced in the quarry to the final product slabs and tiles. The need for qualified and experienced personnel is important, which leads to control and inspection standards. All over the world, certain standardization studies in natural stones and digital technological approaches have entered a rising trend in recent years. Unfortunately, it has not been possible for engineers and employees in the sector to keep up with these rapid developments at the same rate. These digital smart factory studies provide economic benefits in relation to a specific activity, revealing the features to be sought in the production of goods and services, but can also be used in other fields (law, method, etc.)

Following this detailed analysis, the importance of RFID systems will continue in digital traceability and tracking process.

4.2.1 RFID-enabled smart marble factory feasibility and integration process

The process in marble factories is presented in detail in section 4.2. In this section, detailed information about the implementation phases of RFID-enabled smart factory integration, algorithms, factory map and the process, which is the main purpose of the study, will be presented, and the improvement of the process and the developments in terms of added value will be discussed directly. The process from the aforementioned marble production to the preparation for sale is shown in Figure 4.9 and Figure 4.10 below with its transition through the workstations.

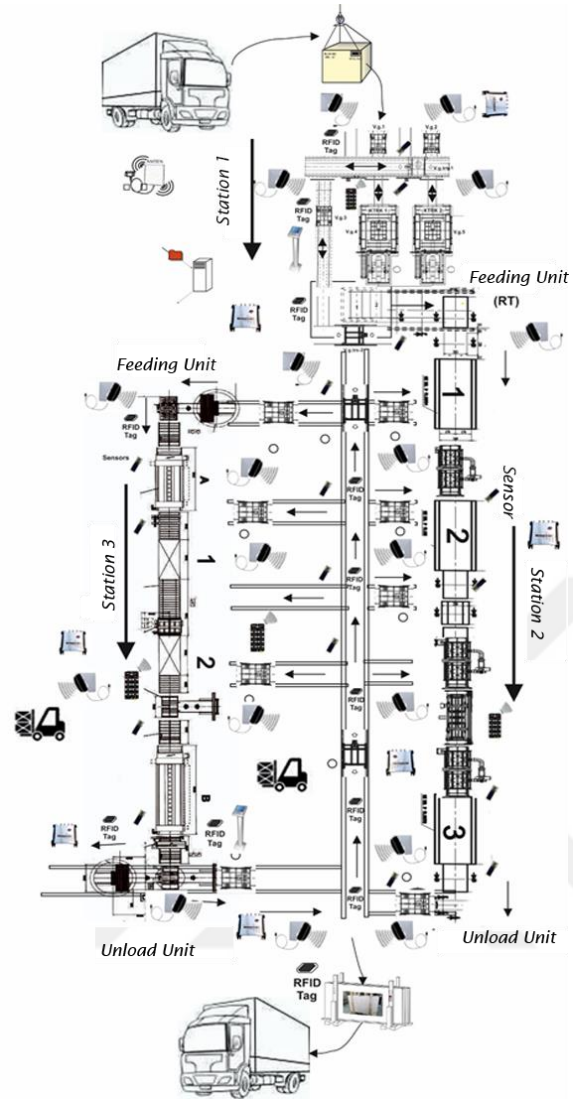

Figure 4.9 Workstation and factory schematic with its stages from raw material to the supply chain.

As explained in Section 4.2, all stages that the marble passed through on the sketch of the factory are summarized in the block diagram in Figure 4.10. Coming as a raw material, marble goes through many stages until it reaches the supply chain. It is extremely important to follow these stages and to manage them meticulously. Here, RFID systems come into play along with real-time location tracking on workstations. With the information on the stage of the product, the ready-made product is labeled and recorded in accordance with the stock record, and the preliminary preparation for the required shipment stages is completed. The shipping module, on the other hand,

provides all the controls at the last stage, as mentioned before, and prevents issues such as error and wrong delivery.

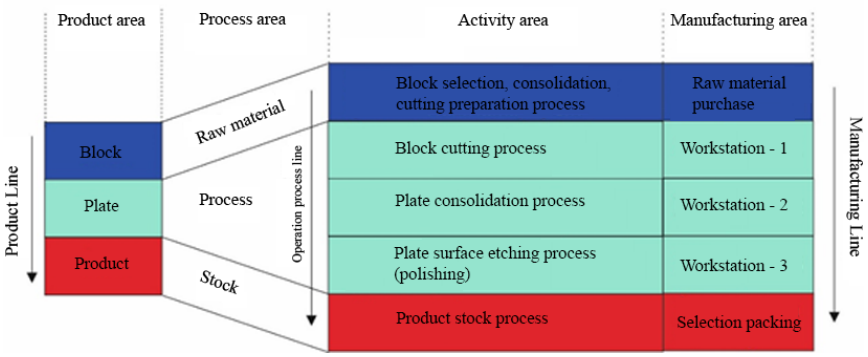

Figure 4.10 Workstation, processes block diagram.

In addition to all these, the different layers in the system and their importance are detailed in the Figure 4.11 below.

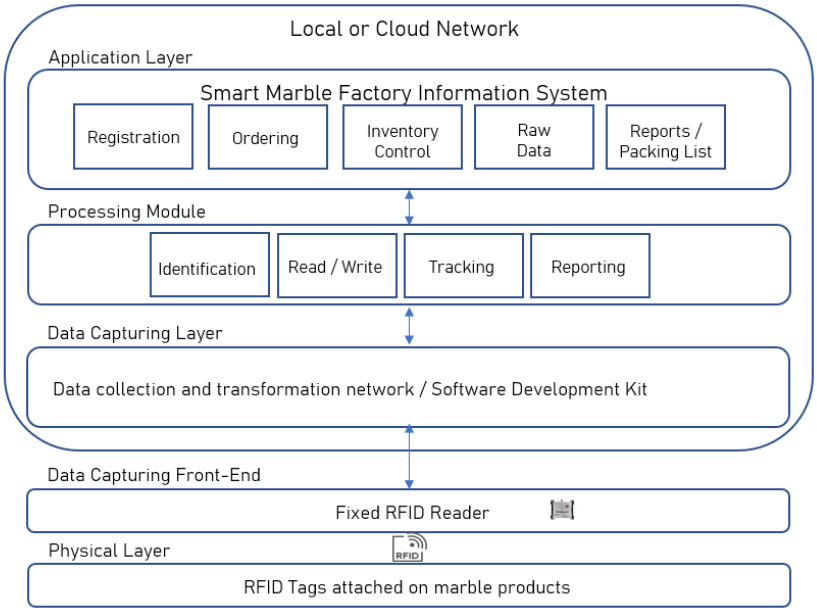

Figure 4.11 Framework of RFID-enabled smart factory and its layers.

With the graphical user interface in the Processing Module, necessary identification, reading / writing, monitoring and reporting operations are performed. In order to understand this stage better, "Bundle Recording Module" and "Shipping Module" algorithms are explained below.

Algorithm Register Product Bundle Module

Input: Marble Features (Type, Surface, Selection, Date, Number, Weight, Height, Width, EPC)
Output: Database variable which contains necessary inputs about marble.
Method:

1) *Connect the RFID reader wiht using its IP adress in database.*
2) *Read the Electronic Product Code with using nearest RSSI algorithm.*
3) *if EPC is already registered, don't allow go next step.*
4) *else:*
5) *Enter the necessary information about the marble.*
6) *Calculate the physical information about marble.*
7) *Match the information with EPC and save to MSSQL database.*
8) *end if*

Algorithm Shipment Module

Input: Reservation Number (List of reserved numbles with their electronic product codes and bundle numbers).
Output: Comparison of products in list and products that have been read by antennas from exit point.
Method:

1) *Connect the RFID reader wiht using its IP adress in database.*
2) *Select the reservation number from list.*
3) *Reserved products will be added to reserved list.*
4) *Start the shipment module.*
5) *Program will read the EPC from antennas on the exit.*
6) *Read EPC's will be added to read list.*
7) *Reserved and read lists will be comparised,*
8) *if list are matched, reading process will be done and GPIO1 will be triggered*
9) *else if the wrong products will be shown in GUI and GPIO2 will be triggered.*
10) *End if*

For the smart factory integration, which is the main goal of the project, these layers and algorithms were integrated with the operation of the marble factory, and the necessary procedures for digital transformation were carried out. In the final system, which was completed as a form, advantages were provided in matters such as the traceability and traceability of the products. Manpower is reduced, human errors are prevented, time is saved. In order to present them better, besides the smart factory integration, the benefits of the RFID system to the marble factory can be listed as follows:

- ✓ It helps to make production according to certain plans and programs,
- ✓ Provides appropriate quality and serial production,

- ✓ Loss and wastes are minimized,
- ✓ It facilitates storage and transportation, reduces stocks,
- ✓ It reduces the cost.
- ✓ By changing the organization, the duties, authorities and responsibilities of all employees are determined, ensuring that employees have performance, motivation and a comfortable working environment.
- ✓ Provides an easy management style to top management.
- ✓ It saves time.
- ✓ It helps to reduce the amount of scrap.
- ✓ It increases the productivity of the employees.
- ✓ It helps to reduce the amount of defective products.
- ✓ Provides optimum use of resources (human, time, machine, capital).
- ✓ Increases production and profit.
- ✓ It increases the chance of competition in the market.
- ✓ Facilitates the delivery of the product on schedule.
- ✓ Provides prestige in national and international markets.

In summary, in this section, issues related to the integration of RFID system into the marble production process and the creation of a smart factory are discussed. Starting from the process where the marble passes in the factory, it is explained by combining with the graphical user interface with the points where the RFID system plays an active role. While making the necessary integrations, the reader antennas and RFID tags that have been designed and simulated since the beginning of the study were used. At the same time, with the components described in the network planning section, the entire factory was installed. Along with operations such as stock registration and stock control, the shipping module has been developed and tested in real scenarios. As a result of all these, the advantages provided to the factory are also listed and presented. Figure 4.12 shows a summarized block diagram of the entire process in the factory, while Figure 4.13 contains various images from the factory.

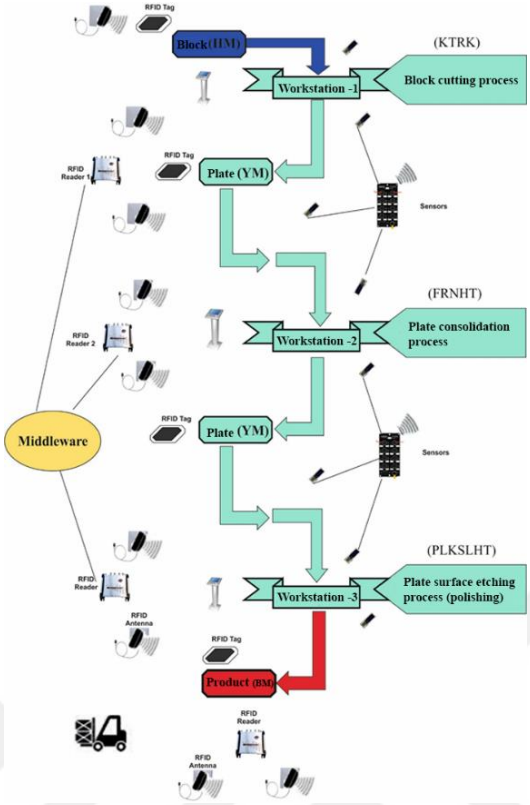

Figure 4.12 Detailed block diagram of all the processes in marble factory.

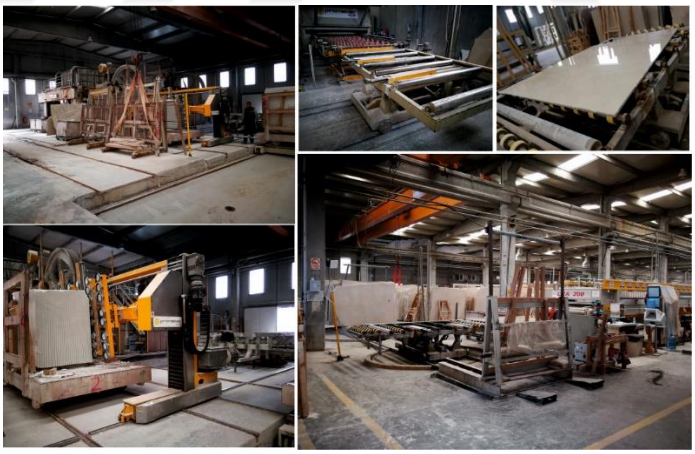

Figure 4.13 Various images from marble factory.

5. CONCLUSION

With the development of technology, new needs of manufacturing factories have emerged in subjects such as product stock tracking and supply chain management. In fact, the in-factory management process also addresses the operation, follow-up and traceability within the factory. To increase productivity in the factory, currently used cyber-physical systems and automatic identification technologies have begun to be replaced by technologies that can adapt to the smart factory and Industry 4.0 process. One of the important technologies that can adapt to this process is RFID technology. To adapt RFID technology to a manufacturing factory, the integration process must consider many stages. The RFID system, a component that will provide smart factory integration, contains many elements. In this study, research and development were made on the importance of these components both theoretically and experimentally, the RFID system and smart factory integration process for a sample marble factory, component selection, necessary antenna designs for the system and graphical user interface creation. After examining the literature studies, the problems in supply chain management and the smart factory integration processes, an antenna was designed for the RFID system to be used in the smart marble factory. The designed antenna gives similar performance to commercially available products and is compact, 7.2 dBi high gain, circular polarized. Simultaneously, considering the marble's electrical properties, different RFID tag benchmark tests were carried out, and the most suitable RFID tag was selected for use on the marbles.

Along with these, all the RFID system's different components have been selected, these choices and the reasons for the RFID network structure are explained. With all these choices, the entire network structure to be used in the factory has been designed, and a graphical user interface has been designed so that the end-user can use the RFID system effectively. Along with the hardware and software, the system was installed in the marble factory in an entire form, and different tests were carried out on subjects

such as sample inventory recording, stock tracking, shipment management, supply chain management, product stock/sales reports. With these tests, the feedback was received from the factory regarding the increase in productivity and the efficiency and other advantages obtained as a result of using the RFID system in the smart marble factory integration and testing were summarized. As a result of the measurement tests carried out in the factory, 287 of the 291 marbles in the stock area could be identified without any problems and the related features of these marbles matched with the EPC codes were verified in the database. As observed in laboratory tests, RFID tag reading performance also depends on the characteristic and electrical properties of marbles. The tests carried out in the factory confirm the laboratory studies, especially considering the higher rate of problems in the identification of "Travertine Denizli" marbles. With all these results, the system can be fully optimized and smart factory integration can be achieved with the RFID system, allowing the factory to get full efficiency from the system by keeping up with the Industry 4.0 requirements. As a conclusion, this study handles smart factory integration and testing studies of a marble factory with specific details and system performance optimizations.

REFERENCES

1. Dai Q, Zhong R, Huang GQ, Qu T, Zhang T, Luo TY. Radio frequency identification-enabled real-time manufacturing execution system: A case study in an automotive part manufacturer. Int J Comput Integr Manuf. 2012;25(1):51–65.

2. Lu S, Xu C, Zhong RY. An Active RFID Tag-Enabled Locating Approach with Multipath Effect Elimination in AGV. IEEE Trans Autom Sci Eng. 2016;13(3):1333–42.

3. Biswal AK, Jenamani M, Kumar SK. Warehouse efficiency improvement using RFID in a humanitarian supply chain: Implications for Indian food security system. Transp Res Part E Logist Transp Rev [Internet]. 2018;109(October 2017):205–24. Available from: https://doi.org/10.1016/j.tre.2017.11.010

4. Lu S, Xu C, Zhong RY, Wang L. A RFID-enabled positioning system in automated guided vehicle for smart factories. J Manuf Syst [Internet]. 2017;44:179–90. Available from: http://dx.doi.org/10.1016/j.jmsy.2017.03.009

5. Huang S, Gan OP, Hwang ZQ, Song H, Xie L. Passive UHF far-field RFID based localization in smart rack. IECON 2015 - 41st Annu Conf IEEE Ind Electron Soc. 2015;5026–31.

6. Li J, Liu H, Zhang S, Luo M, Zhang Y, He S. A wideband single-fed, circularly-polarized patch antenna with enhanced axial ratio bandwidth for UHF RFID reader applications. IEEE Access. 2018;6:55883–92.

7. Cao R, Yu SC. Wideband Compact CPW-Fed Circularly Polarized Antenna for Universal UHF RFID Reader. IEEE Trans Antennas Propag. 2015;63(9):4148–51.

8. Lu JH, Wang SF. Planar broadband circularly polarized antenna with square slot for UHF RFID reader. IEEE Trans Antennas Propag. 2013;61(1):45–53.

9. Wang Z, Fang S, Fu S, Jia S. Single-fed broadband circularly polarized stacked patch antenna with horizontally meandered strip for universal UHF RFID applications. IEEE Trans Microw Theory Tech. 2011;59(4 PART 2):1066–73.

10. Sim CYD, Hsu YW, Yang G. Slits loaded circularly polarized universal UHF RFID reader antenna. IEEE Antennas Wirel Propag Lett. 2015;14(c):827–30.

11. Sim CYD, Liang SY, Hsieh CK, Han TY. A circularly polarized slits loaded UHF RFID antenna with parasitic element. 2017 IEEE Int Conf Comput Electromagn ICCEM 2017. 2017;349–51.

12. Chen ZN, Qing X, Chung HL. A Universal UHF RFID Reader Antenna. IEEE Trans Microw Theory Tech. 2009 May;57(5):1275–82.

13. Nasimuddin N, Qing X, Chen ZN. A wideband circularly polarized stacked slotted microstrip patch antenna. IEEE Antennas Propag Mag. 2013;55(6):84–99.

14. Chung HL, Qing X, Chen ZN. A Broadband Circularly Polarized Stacked Probe-Fed Patch Antenna for UHF RFID Applications. Int J Antennas Propag. 2007;2007:1–8.

15. Sim CYD, Chi CJ. A slot loaded circularly polarized patch antenna for UHF RFID reader. IEEE Trans Antennas Propag. 2012;60(10):4516–21.

16. Nasimuddin, Chen ZN, Qing X. Asymmetric-circular shaped slotted microstrip

antennas for circular polarization and RFID applications. IEEE Trans Antennas Propag. 2010;

17. Yuan J, Wu S, Chen Z, Xu Z. A Compact Low-Profile Ring Antenna with Dual Circular Polarization and Unidirectional Radiation for Use in RFID Readers. IEEE Access. 2019;7:128948–55.

18. Yeh S, Chen H, Lin Y, Yang Z, Chen C. Circularly polarized crossed dipole antennas for handheld RFID reader. In: 2010 International Conference on Applications of Electromagnetism and Student Innovation Competition Awards (AEM2C). 2010. p. 134–8.

19. Jong ML, Nae SK, Cheol SP. A circular polarized metallic patch antenna for RFID reader. 2005 Asia-Pacific Conf Commun. 2005;2005(October):116–8.

20. Yeh SA, Lin YF, Chen HM, Chen J Sen. Slotline-fed circularly polarized annular-ring slot antenna for RFID reader. APMC 2009 - Asia Pacific Microw Conf 2009. 2009;618–21.

21. Saygin C, Sarangapani J, Grasman SE. A Systems Approach to Viable RFID Implementation in the Supply Chain. In: Jung H, Jeong B, Chen FF, editors. Trends in Supply Chain Design and Management: Technologies and Methodologies [Internet]. London: Springer London; 2007. p. 3–27. Available from: https://doi.org/10.1007/978-1-84628-607-0_1

22. Michael K, McCathie L. The pros and cons of RFID in supply chain management. In: International Conference on Mobile Business (ICMB'05). 2005. p. 623–9.

23. Suhong L, K. VJ, M. KB, Chen Z. Radio frequency identification technology: applications, technical challenges and strategies. Koschan A, editor. Sens Rev [Internet]. 2006 Jan 1;26(3):193–202. Available from: https://doi.org/10.1108/02602280610675474

24. Thonemann UW. Improving supply-chain performance by sharing advance demand information. Eur J Oper Res [Internet]. 2002;142(1):81–107. Available from: http://www.sciencedirect.com/science/article/pii/S0377221701002818

25. Jerry L, Barbara C. Shrouds of Time: The History of RFID. AIM Publ [Internet]. 2001;11. Available from: https://www.aimglobal.org/estore/ProductDetails.aspx?ProductID=529

26. Leung YT, Cheng F, Lee YM, Hennessy JJ. A Tool Set for Exploring the Value of RFID in a Supply Chain. In: Jung H, Jeong B, Chen FF, editors. Trends in Supply Chain Design and Management: Technologies and Methodologies [Internet]. London: Springer London; 2007. p. 49–70. Available from: https://doi.org/10.1007/978-1-84628-607-0_3

27. Sarac A, Absi N, Dauzère-Pérès S. A literature review on the impact of RFID technologies on supply chain management. Int J Prod Econ [Internet]. 2010;128(1):77–95. Available from: http://www.sciencedirect.com/science/article/pii/S0925527310002835

28. Atali A, Lee H, Özer Ö. If the Inventory Manager Knew: Value of Visibility and RFID under Imperfect Inventory Information. SSRN Electron J. 2009;

29. Kang Y, Gershwin SB. Information inaccuracy in inventory systems: stock loss and stockout. IIE Trans [Internet]. 2005;37(9):843–59. Available from:

https://doi.org/10.1080/07408170590969861

30. Fleisch E, Tellkamp C. Inventory Inaccuracy and Supply Chain Performance: A Simulation Study of a Retail Supply Chain. Int J Prod Econ. 2005;3:373–85.

31. Joshi Y V. Information Visibility And Its Effect On Supply Chain Dynamics. Mech Eng. 1998;

32. Lee YM, Cheng F, Leung YT. A Quantitative View on How RFID Will Improve a Supply Chain. In.

33. Kök G, Shang K. Inspection and Replenishment Policies for Systems With Inventory Record Inaccuracy. Manuf Serv Oper Manag. 2007;9:185–205.

34. Iglehart DL, Morey RC. Inventory Systems with Imperfect Asset Information. Manage Sci [Internet]. 1972;18(8):B388--B394. Available from: http://www.jstor.org/stable/2629009

35. Lee H, Özer Ö. Unlocking the value of RFID. Prod Oper Manag. 2007;16:40–64.

36. de Kok AG, van Donselaar KH, van Woensel T. A break-even analysis of RFID technology for inventory sensitive to shrinkage. Int J Prod Econ [Internet]. 2008;112(2):521–31. Available from: http://www.sciencedirect.com/science/article/pii/S0925527307001946

37. Sahin E. A qualitative and quantitative analysis of the impact of the Auto ID technology on supply chains. 2004;

38. Sahin E, Buzacott J, Dallery Y. Analysis of a newsvendor which has errors in inventory data records. Eur J Oper Res. 2008;188:370–89.

39. Rekik Y. The Impact of the RFID Technology in Improving Performance of Inventory Systems subject to Inaccuracies. 2006;

40. Rekik Y, Jemai Z, Sahin E, Dallery Y. Improving the performance of retail stores subject to execution errors: coordination versus RFID technology. OR Spectr [Internet]. 2007;29(4):597–626. Available from: https://doi.org/10.1007/s00291-007-0087-2

41. Rekik Y, Sahin E, Dallery Y. Analysis of the impact of the RFID technology on reducing product misplacement errors at retail stores. Int J Prod Econ [Internet]. 2008;112(1):264–78. Available from: http://www.sciencedirect.com/science/article/pii/S0925527307001454

42. Rekik Y, Sahin E, Dallery Y. A Comprehensive Analysis of the Newsvendor Model with Unreliable Supply. OR Spectr. 2007;29.

43. Gaukler G, Seifert R, Hausman W. Item-level RFID in the retail supply chain. Prod Oper Manag. 2007;16:65–76.

44. Sounderpandian J, Boppana R, Chalasani S, Madni A. Models for Cost-Benefit Analysis of RFID Implementations in Retail Stores. Syst Journal, IEEE. 2008;1:105–14.

45. Szmerekovsky JG, Zhang J. Coordination and adoption of item-level RFID with vendor managed inventory. Int J Prod Econ [Internet]. 2008;114(1):388–98. Available from: http://www.sciencedirect.com/science/article/pii/S0925527308000893

46. Uckun C, Karaesmen F, Savas S. Optimal Investment Levels to Eliminate Inventory Inaccuracy in a Two-Level Supply Chain. In: 2007 1st Annual RFID Eurasia. 2007. p. 1–6.

47. Brown K, Inman R, Calloway J. Measuring the Effects of Inventory Inaccuracy in MRP Inventory and Delivery Performance. Prod Plan Control. 2001;12.

48. Krajewski LJ, King BE, Ritzman LP, Wong DS. Kanban, MRP, and Shaping the Manufacturing Environment. Manage Sci [Internet]. 1987;33(1):39–57. Available from: http://www.jstor.org/stable/2631610

49. Kim J, Tang K, Kumara S, Yee S-T, Tew J. Value analysis of location-enabled radio-frequency identification information on delivery chain performance. Int J Prod Econ [Internet]. 2008;112(1):403–15. Available from: http://www.sciencedirect.com/science/article/pii/S0925527307001764

50. Sarac A, Absi N, Dauzère-Pérès S. A simulation approach to evaluate the impact of introducing RFID technologies in a three-level supply chain. In: Proceedings - Winter Simulation Conference. 2008. p. 2741–9.

51. Saygin C. Adaptive inventory management using RFID data. Int J Adv Manuf Technol [Internet]. 2007;32(9):1045–51. Available from: https://doi.org/10.1007/s00170-006-0405-x

52. Vrba P, Macůrek F, Mařík V. USING RADIO FREQUENCY IDENTIFICATION IN AGENT-BASED CONTROL SYSTEMS FOR INDUSTRIAL APPLICATIONS. IFAC Proc Vol [Internet]. 2006;39(3):459–64. Available from: http://www.sciencedirect.com/science/article/pii/S1474667015359619

53. Wang S-J, Liu S-F, Wang W-L. The simulated impact of RFID-enabled supply chain on pull-based inventory replenishment in TFT-LCD industry. Int J Prod Econ [Internet]. 2008;112(2):570–86. Available from: http://www.sciencedirect.com/science/article/pii/S0925527307001971

54. Yoo JS, Hong SR, Kim CO. Service level management of nonstationary supply chain using direct neural network controller. Expert Syst Appl [Internet]. 2009;36(2, Part 2):3574–86. Available from: http://www.sciencedirect.com/science/article/pii/S0957417408001231

55. Lefebvre LA, Lefebvre E, Bendavid Y, Fosso Wamba S, Boeck H. RFID as an Enabler of B-to-B e-Commerce and Its Impact on Business Processes: A Pilot Study of a Supply Chain in the Retail Industry. In 2006. p. 104a-104a.

56. Fosso Wamba S, Lefebvre LA, Bendavid Y, Lefebvre É. Exploring the impact of RFID technology and the EPC network on mobile B2B eCommerce: A case study in the retail industry. Int J Prod Econ [Internet]. 2008;112(2):614–29. Available from: http://www.sciencedirect.com/science/article/pii/S0925527307002009

57. Tzeng S-F, Chen W-H, Pai F-Y. Evaluating the business value of RFID: Evidence from five case studies. Int J Prod Econ [Internet]. 2008;112(2):601–13. Available from: http://www.sciencedirect.com/science/article/pii/S0925527307001995

58. Wang L-C, Lin Y-C, Lin PH. Dynamic mobile RFID-based supply chain control and management system in construction. Adv Eng Informatics [Internet]. 2007;21(4):377–90. Available from: http://www.sciencedirect.com/science/article/pii/S1474034606000528

59. Chuang M-L, Shaw W. RFID: Integration Stages in Supply Chain Management. Eng Manag Rev IEEE. 2007;35:80–7.

60. Huber N, Michael K, McCathie L. Barriers to RFID Adoption in the Supply Chain. In 2007. p. 1–6.

61. Toth L, Dobrossy P, Manik D. RFId application in production process of an automotive industry supplier. In: 2006 International Conference on Intelligent Engineering Systems. 2006. p. 45–8.

62. Kim EY, Ko E, Kim H, Koh CE. Comparison of benefits of radio frequency identification: Implications for business strategic performance in the U.S. and Korean retailers. Ind Mark Manag [Internet]. 2008;37(7):797–806. Available from: http://www.sciencedirect.com/science/article/pii/S001985010800028X

63. Toaha A, Islam MT, Misr N. RFID Technology: Perspectives and Technical Considerations of Microstrip Antennas for Multi-Band RFID Reader Operation. Curr Trends Challenges RFID. 2011;(July).

64. Nekoogar F, Dowla F. Ultra-Wideband Radio Frequency Identification Systems. Springer Publishing Company, Incorporated; 2011.

65. Dobkin DM. The RF in RFID. 3th ed. The RF in RFID. Elsevier; 2008.

66. Committee AS. IEEE Standard Test Procedures for Antennas. Vol. 23, IEEE Antennas and Propagation Society Newsletter. 1981. 28 p.

67. Toh BY, Cahill R, Fusco VF. Understanding and measuring circular polarization. IEEE Trans Educ. 2003;46(3):313–8.

68. Schrank H, Milligan T. Link Budget When Using olarization Gains. IEEE Antennas Propag Mag. 1996;38(1):56–9.

69. Preradovic S, Karmakar C. Modern RFID Readers [Internet]. Microwave Journal. 2007 [cited 2020 Oct 28]. Available from: https://www.microwavejournal.com/articles/5271-modern-rfid-readers

70. Wang L, Norman BA, Rajgopal J. Placement of multiple RFID reader antennas to maximise portal read accuracy. Int J Radio Freq Identif Technol Appl. 2007;1(3):260–77.

71. Nikitin P V., Rao KVS. Antennas and propagation in UHF RFID systems. 2008 IEEE Int Conf RFID (Frequency Identification), IEEE RFID 2008. 2008;277–88.

72. Ukkonen L, Sydänheimo L, Kivikoski M. Read range performance comparison of compact reader antennas for a handheld UHF RFID reader. 2007 IEEE Int Conf RFID, IEEE RFID 2007. 2007;63–70.

73. Tseng JD, Ko RJ, Wang W De. Switched beam antenna array for UHF band RFID system. 2007 IEEE Int Work Anti-counterfeiting, Secur Identification, ASID. 2007;(35):92–5.

74. Buffi A, Michel A, Nepa P, Tellini B. RSSI Measurements for RFID Tag Classification in Smart Storage Systems. IEEE Trans Instrum Meas. 2018;67(4):894–904.

75. P.V. Nikitin, K.V.S Rao, R.D. M. Differential RCS of RFID. Electron Lett. 2005;41(2):40–1.

76. Kim D, Ingram MA, Smith WW. Measurements of small-scale fading and path loss for long range RF tags. IEEE Trans Antennas Propag. 2003;51(8):1740–9.

77. Mayer LW, Wrulich M, Caban S. Measurements and channel modeling for short range indoor UHF applications. Eur Sp Agency, (Special Publ ESA SP. 2006;626 SP(October).

78. Aroor SR, Deavours DD. Evaluation of the State of Passive UHF RFID: An Experimental Approach. IEEE Syst J. 2007;1(2):168–76.

79. Nikitin P V., Rao KVS. Performance Limitations of Passive UHF RFID Systems Pavel. 2006;1–21.

80. Blanchi CH, Sivaprasad K. A channel model for multipath interference on terrestrial line-of-sight digital radio. IEEE Trans Antennas Propag. 1998;46(6):891–901.

81. Nikitinj P V., Stancil DD, Cepni AG, Tonguz OK, Xhafa AE, Brodtkorb D. Propagation model for the HVAC duct as a communication channel. IEEE Trans Antennas Propag. 2003;51(5):945–51.

82. Arumugam DD, Engels DW. Characterisation of RF propagation in metal pipes for passive RFID systems. Int J Radio Freq Identif Technol Appl. 2007;1(3):303–43.

83. White MO. Radar cross-section: measurement, prediction and control. October. 1998;(August):169–80.

84. Rappaport TS. Characterization of UHF Multipath Radio Channels in Factory Buildings. IEEE Trans Antennas Propag. 1989;37(8).

85. Foster PR, Burberry RA. Antenna problems in RFID systems. IEE Colloq. 1999;(123):13–7.

86. Turner L, Mickle MH. Overview primer on near-field UHF versus near-field HF RFID tags. Int J Radio Freq Identif Technol Appl. 2007;1(3):291–302.

87. Karmakar C. Readers - a review. 2006;(December):19–21.

88. Litum RFID. Litum 7.5 dBiC UHF RFID Antenna [Internet]. [cited 2020 Nov 10]. Available from: https://litumrfid.com/rfid-products/uhf-rfid-antenna-8-db/

89. Scott AH. Dielectric constant, power factor, and resistivity of marble. J Res Natl Bur Stand (1934). 1940;24(3):235.

90. MALIK SI, KHAN KM, SHAMIM A, SULEMAN M, MATEEN A. Determination of dielectric constant of marble by the application of Looyenga's equation. J Mater Sci Lett. 1988;7:368–70.

91. Bapna PC, Joshi S. Measurement of Dielectric Properties of various Marble Stones of Mewar Region of Rajasthan at X-band Microwave Frequencies. Int J Eng Innotavite Technol. 2013;2(7):180–6.

92. K.Dhoot MV. Measurement of Dielectric Properties of Marble Stone Samples in The Frequency Range 0.2GHz – 20GHz. Int J Sci Res Phys Appl Sci [Internet]. 2019;7(4):1–7. Available from: https://www.isroset.org/journal/IJSRPAS/full_paper_view.php?paper_id=1419

APPENDIX

In the appendix section, RFID tag reading tests in marble factory, and the improvements that can be made in the system with the smart model factory are mentioned. Many tests have been carried out with marbles in a laboratory environment to examine the reading performance of the RFID system. As a result of these tests, it was observed that many factors affect reading performance. In addition to the performance parameters of the antenna and RFID tags, the type of marble on which the tag is placed is among the factors that affect the reading performance. These tests were also applied in the marble factory in sample scenarios. For the tests, many marble records of different types were made, and the tag reading performance scores were measured with the antennas fixed in certain parts of the warehouse. In the measurements, the tags read with the database were compared, and erroneous readings were evaluated.

In the tables below, the marbles of different qualities, types and types and their numbers are given. Each of these marbles has RFID tags and the information of the marbles are matched with each other in the EPC database. As a result of the tests carried out, it is seen that 4 of 291 tags in total are missing. One of the unreadable RFID tags belongs to "Noble Beige Burdur" marble, 1 to "Emperador Konya" marble, and 2 to "Travertine Denizli" marble. Angel White, Gray and Ice type marbles can all be identified in accordance with the records. When the test environment was examined, it was observed that this faulty reading situation was independent of the distance. The ambient conditions and the different types of marbles are thought to cause this result.

Table A.1 and Table A.2 contain information such as total number of tags, square meter, kind, type, quality, and surface treatment, while Table A.3 contains the test results. Also, Figure A.1 contains the schematic of the factory test environment.

Table A.1 Bundle Module Registration Data

Bundle Registration Module (BM)							
Registered EPC Count	**Kind**	**Type**		**Quality**	**Surface**	**Total m2**	**Registered Bundle Count**
15	NOBLE	BEIGE	BURDUR	**A**	**POLISHED**	522.31	15
334	NOBLE	BEIGE	BURDUR	**B**	**POLISHED**	12574.21	334
1	NOBLE	BEIGE	BURDUR	**C**	**POLISHED**	38.92	1
2	ANGEL WHITE	BEIGE	KEÇİBORLU	**A**	**HONED**	**68**	2
50	ANGEL WHITE	BEIGE	KEÇİBORLU	**B**	**HONED**	**1696**	50
21	ANGEL WHITE	BEIGE	KEÇİBORLU	**C**	**HONED**	**764**	21
13	EMPERADOR	BEIGE	KONYA	**B**	**HONED**	**535**	13
18	GRAY	MARBLE	MERSİN	**B**	**HONED**	**632.25**	18
1	GRAY	MARBLE	MERSİN	**A**	**HONED**	**23.52**	1
3	TRAVERTINE	TRV	DENİZLİ	**A**	**POLISHED**	**101.67**	3
10	TRAVERTINE	TRV	DENİZLİ	**B**	**POLISHED**	**360.15**	10
9	ICE MARBLE	MARBLE	UŞAK	**B**	**POLISHED**	**357**	9
477						17672.74	**477**

Table A.2 Shipment Module Registration Data

Shipment Module (BM)			Expected Stock Count	
SM EPC QTY	**SM Bundle Count**	**Total Shipment m2**	**Bundle QTY**	**Stock m2**
15	15	522.31	0	0.00
120	120	4518.68	214	8055.53
1	1	38.92	0	0.00
2	2	**68**	0	0.00
22	22	**678**	28	1017.12
10	10	**354**	11	410.18
		0	13	534.98
6	6	210.75	12	421.50
1	1	23.52	0	0.00
3	3	101.67	0	0.00
6	6	270.12	4	90.03
			9	357.06
186		6786.34	**291**	10886.40

Table A.3 RFID Tag Reading Test Scores

RFID TAG Reading Test Scores (Total Score)

Date:	28.12.2020	**Event:**	RFID Stock Count
Test time:	08:30-08:42	**Total Tags**	287
Read time:	12 min.	**Total Lost Tags**	4

Bundle Module Stock (BM)								
Read Tag Count	**Kind**	**Type**		**Quality**	**Surface**	**Total m²**	**Reg. Bund. Count**	**Lost Tags**
213	NOBLE	BEIGE	BURDUR	B	POLISHED	8020.42	214	1
28	ANGEL WHITE	BEIGE	KEÇİBORLU	B	HONED	1017	28	N
11	ANGEL WHITE	BEIGE	KEÇİBORLU	C	HONED	410	11	N
12	EMPERADOR	BEIGE	KONYA	B	POLISHED	500	13	1
12	GRAY	MARBLE	MERSİN	B	POLISHED	421.50	12	N
2	TRAVERTINE	TRV	DENİZLİ	B	POLISHED	42.20	4	2
9	ICE MARBLE	MARBLE	UŞAK	B	POLISHED	357	9	N
287						10768.48	291	4

The test was carried out on a total of 291 products, with a reading time of 12 minutes. The necessary verifications were made with the data obtained from the database of the graphical user interface, and the number of matching products and the number of unreadable products are indicated in Table A.3. These data can be easily verified from the database provided with Microsoft SQL Server in the graphical user interface. The EPC of the RFID tag on each product and the characteristics paired with that product are available in the database. As a matter of fact, the RFID system is not just a simple inventory counting process, but a complex inventory counting task in a very short time. The factory measurement environment where reading tests are performed is presented in detail in Figure A.1. The marbles marked with red in the stock area are successfully identified, while the marbles marked with green show unidentified / lost RFID tags.

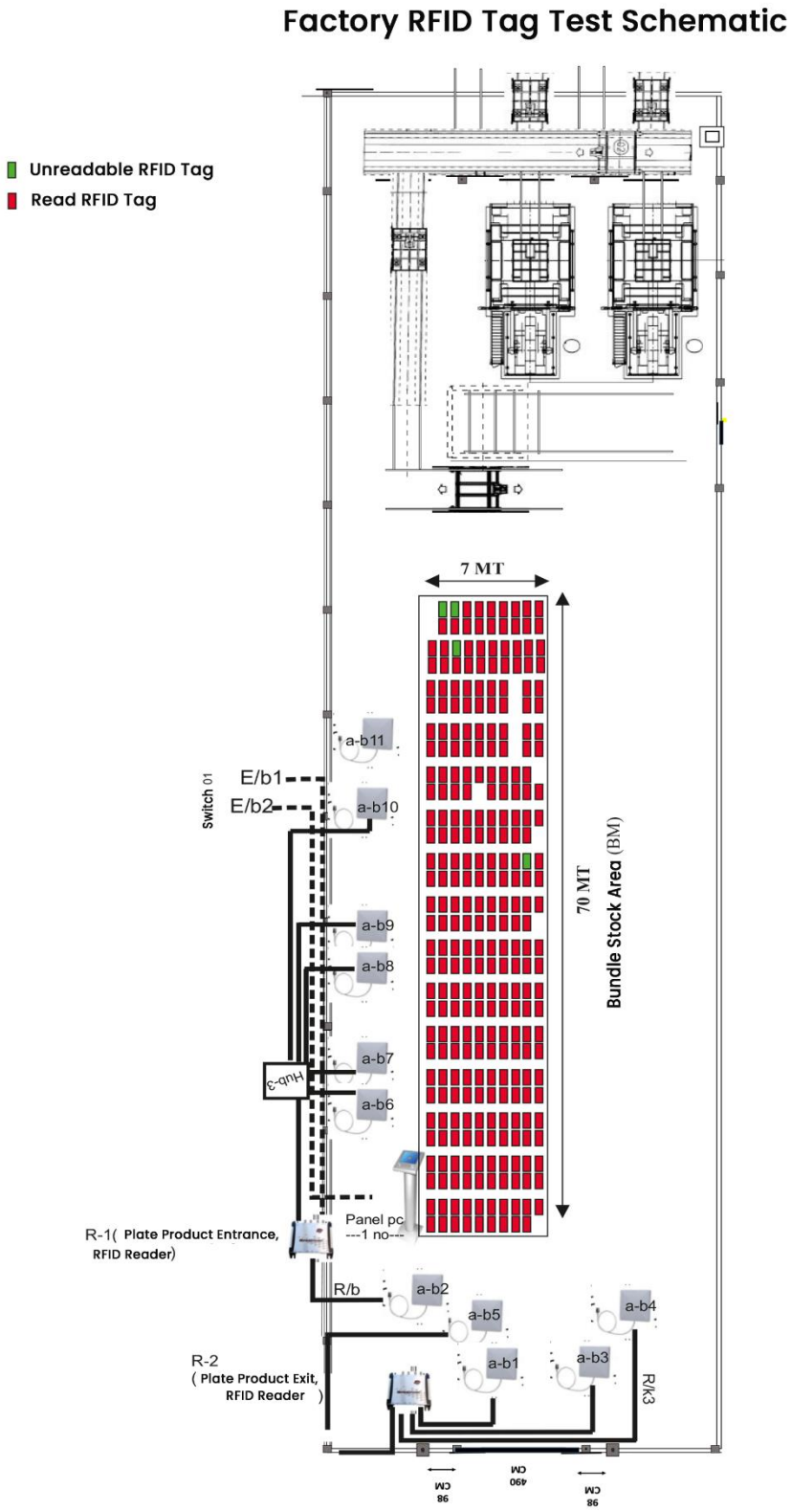

Figure A.1 Schematic of RFID Tag Reading Test Area in Marble Factory

In the future stages of this study, a whole system will be established in which the components of the RFID system applied in sample scenarios for the marble factory, such as the conveyor belt, robot arm, control stations in the factory, are modeled and a smaller sample model factory is created. With this smart model factory infrastructure created, RFID system tests can be easily applied for different samples and different scenarios. In addition, IoT components and automation systems required for compatibility with Industry 4.0 can be integrated into the entire system. The aim of the smart model factory is to provide the integration of the smart factory with all processes in a factory with problem-specific solutions, regardless of product. At the same time, this smart model factory assembly, designed in a modular structure, will be planned in a laboratory environment that every user can contribute, and with 3-dimensional printing methods and printed circuit machines, new components and expansion kits for existing components can be designed and tested directly on the model. The block diagram of smart model factory innovation and transformation center has been shown in Figure A.1 and the image of its built base has been shown in Figure A.2.

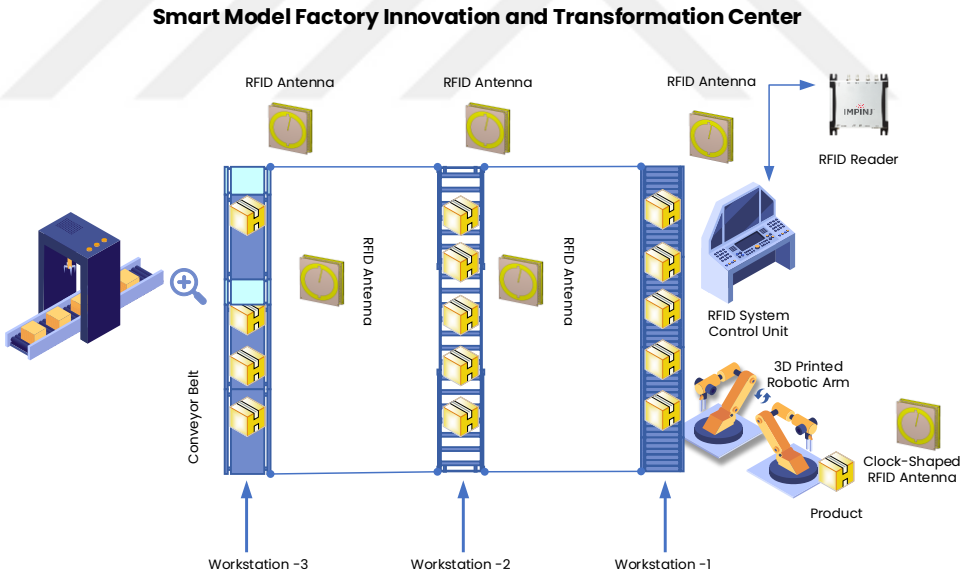

Figure A.2 Smart Model Factory Innovation and Transformation Center.

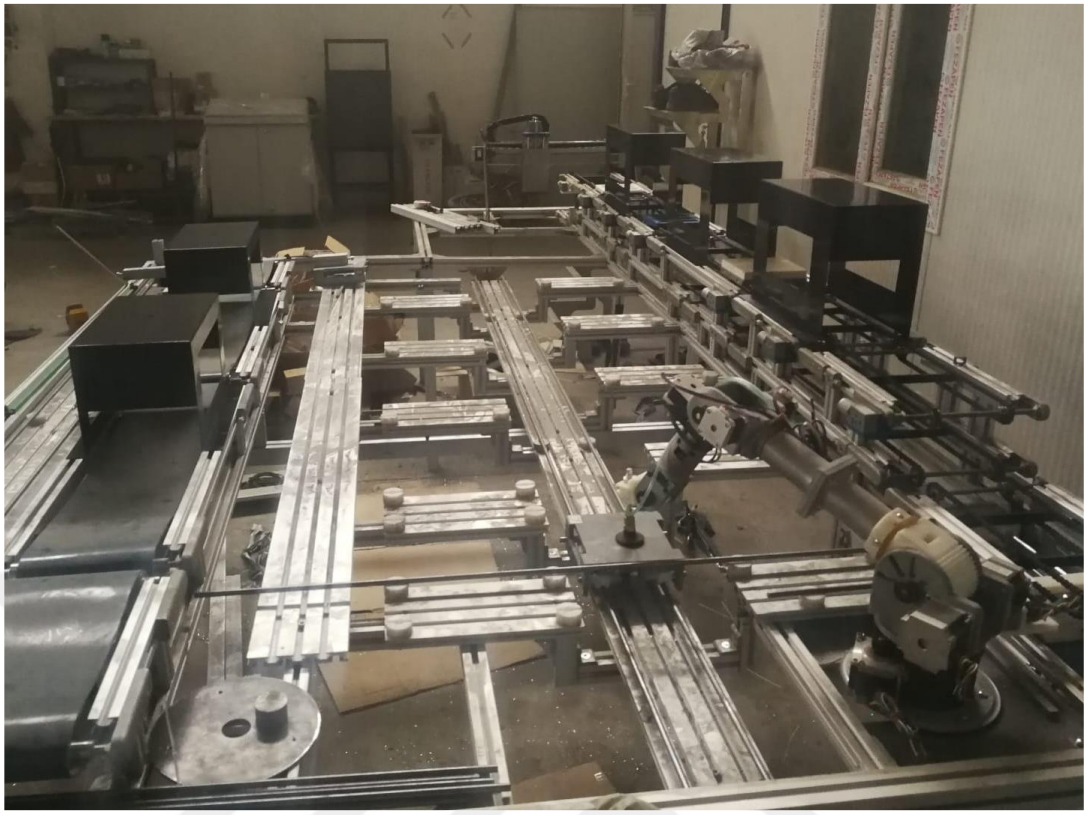

Figure A.3 Image of Smart Model Factory Innovation and Transformation Center Base.